Ionic strength sensitivity of complex coacervation between ß-lactoglobulin & lactoferrin : From protein-protein interactions to the characterization of the coacervates

Rima Hachfi Soussi

DOCTORAT ECOLOGIE BRETAGNE GEOSCIENCES LOIRE AGRONOMIE ALIMENTATION

L'INSTITUT agro Rennes Angers

THESE DE DOCTORAT DE

L'Institut Agro Rennes-Angers
ECOLE DOCTORALE N°600
Ecole doctorale Ecologie, Géosciences, Agronomie et alimentation
Spécialité: *Science de l'aliment*

Par

Rima Hachfi Soussi

Ionic strength sensitivity of complex coacervation between β-lactoglobulin & lactoferrin: From protein-protein interactions to the characterization of the coacervates

Thèse présentée et soutenue à Rennes, le 16 mars 2023

Unité de recherche : INRAE, L'institut Agro Rennes-Angers, UMR 1253 Science & Technologie du Lait & de l'Œuf

Thèse N° : B-369_2023-6

Rapporteurs avant soutenance

Rémi **Saurel** Professeur, L'Institut Agro Dijon, UMR PAM, Dijon

Marie-Hélène **Morel** Directrice de Recherche, INRAE, UMR IATE, Montpellier

Composition du Jury

Président :	Thomas **Croguennec**	Professeur, L'Institut Agro Rennes-Angers, UMR STLO, Rennes
Examinateurs :	Delphine **Salvatore**	Senior R&D Project Manager, Laïta, entreprise coopérative laitière, Pouldreuzic
	Mónica **Bravo Anaya**	Chargée de Recherche, CNRS, ISCR, Rennes
Dir. de thèse	Saïd **Bouhallab**	Directeur de Recherche, INRAE, UMR STLO, Rennes
Co-dir. de thèse	Marie-Hélène **Famelart**	Chargée de Recherche, INRAE, UMR STLO, Rennes
Invité:	Mikael **Lund**	Professeur, University of Lund, Theoretical Chemistry, Lund, Suède,

This page was intentionally left blank

Remerciements

C’est avec une profonde reconnaissance que je souhaiterais exprimer mes sincères remerciements à toutes les personnes ayant contribué à la réalisation de cette thèse. Sans leur soutien, leurs encouragements et leurs précieux conseils, ce travail n'aurait pas été possible.

Je tiens tout d'abord à remercier mes deux directeurs de thèse, Saïd et Marie-Hélène pour votre confiance, votre patience et les conseils avisés tout au long de ces années de recherche. Votre disponibilité et votre bienveillance m'ont permis de progresser et de m'épanouir dans mes travaux de recherche. Je vous remercie également pour votre implication, votre rigueur et votre expertise qui ont été des atouts majeurs dans la réussite de ce travail.

Je souhaite également exprimer ma gratitude à l'ensemble des membres de mon jury, le président du jury Thomas Croguennec, mes deux rapporteurs, Marie-Hélène Morel et Rémi Saurel, ainsi que mes examinatrices, Delphine Salvatore et Mónica Bravo Anaya pour leurs temps, leurs expertises et leurs soutiens lors de la soutenance de ma thèse. Leur regard critique et leurs remarques pertinentes ont été d'une aide précieuse dans l'amélioration de ma thèse.

Je remercie aussi les membres de mon CSI, Dénis Renard et Véronique le Tully et Thomas Croguennec de m’avoir accompagnée et aidée tout au long de ces trois années de thèse.

Ce travail a été réalisé à l’INRAE STLO ainsi je remercie Yves Le Loir pour son accueil et le soin qu’il prend à diriger l’UMR. Je remercie également mes collègues et amis du labo pour leur soutien moral tout au long de cette aventure. Leur présence a été une source de motivation et de réconfort dans les moments difficiles. Je remercie Stephan, Luca, Valérie G, Fabienne, Aurélie, Ghazi, Thomas et Fanny pour nos discussions très intéressantes qui ont grandement enrichi mon travail de recherche et ont contribué à son succès.

Je tiens aussi à remercier l'INRAE et région Bretagne d'avoir financé ce projet de thèse.

Un grand merci à Pascaline et Florence qui m'ont accompagnée pendant ces trois années de thèse. Votre présence rassurante et vos conseils avisés m'ont permis d'acquérir de nouvelles compétences et ont facilité mes travaux. Merci pour votre disponibilité et votre bonne humeur qui ont rendu les moments passés au laboratoire plus agréables et motivants.

Je tiens également à remercier les personnes qui veillent à la bonne gestion du laboratoire Jessica, Sébastien, Sylvie, Anne G., Nathalie L., Laurence et Danielle.

Je suis également reconnaissante à la team de Mikael Lund pour votre accueil et pour l'atmosphère de travail conviviale que vous avez contribué à créer et qui m'a rendu vite à l'aise pendant mon séjour à Lund. Merci aussi pour votre patience, votre précision et votre volonté de partager vos connaissances sur la modélisation moléculaire.

Je remercie aussi tous les collègues avec qui j'ai eu la chance de partager mon bureau au fil de ces trois années : Fanny, Julien, Jun, Stefano, Céline, Margot, Salima, Kandi et Ibra. Je vous remercie pour l'atmosphère conviviale et chaleureuse que nous avons créée ensemble. Vos sourires, votre bonne humeur et votre disponibilité (surtout pour les pause-café) ont fait du bureau un espace de travail accueillant où il était agréable de venir chaque jour.

Merci à tous les non permanents, doctorants, post-doctorants et stagiaires que j'ai rencontrés pendant ma thèse, qui sont vite devenus des amis (la liste risque d'être longue mais j'espère n'oublier personne) : François, Fanny, Maellis, Manon, Julien, Stefano, Linda, Brenda, Ines, Nolwenn, Charles, Marie, Félicie, Margot, Alizé, Ralph, Elise, Erik, Julia, Ligia, Yasmin, Lucas, Marina, Mathilde, Tales. Merci pour toutes les pauses, les sorties, les soirées, les blagues, les jeux et les moments de folie qui ont été une véritable bouffée d'air frais pour maintenir notre équilibre et notre bien-être au travail.

Mes mots ne pourront jamais exprimer pleinement l'immense gratitude que je ressens envers mes parents pour leur amour et leur soutien émotionnel constant. Merci d’avoir toujours été là pour m'écouter, me réconforter et me donner la force de persévérer. C'est grâce à vous que je suis parvenue à franchir les obstacles avec confiance et à atteindre la ligne d'arrivée de cette thèse. Je ne saurais jamais vous remercier assez pour tout ce que vous avez fait pour moi.

Je remercie aussi mon frère Amine pour son soutien, sa bienveillance et ses blagues qui ont toujours réussi à détendre l’atmosphère dans les moments les plus stressants.

Je dédie cette thèse à la mémoire de mon grand-père, Baba Fatéh, merci d’avoir été une source inépuisable d'amour, de sagesse et d'inspiration. Tu nous manques énormément, mais je suis reconnaissante et fière pour chaque instant passé à tes côtés.

Finalement je remercie toutes les personnes, famille, amis et collègues qui ont contribué à la réalisation de cette thèse. Sans votre soutien ce travail aurait été impossible.

Table of contents

Abstract

Complex coacervation is a liquid-liquid phase separation that leads to the formation of a highly concentrated phase or coacervates. The formed coacervates are proposed as carriers for bioactives thanks to their high encapsulation efficiency under defined optimal processing conditions. In this thesis, we investigated the specific case of heteroprotein complex coacervation of two globular milk proteins; lactoferrin (LF) and β-lactoglobulin (βLG) under specific physicochemical conditions. We aimed to determine how the ionic strength affects i- the LF/βLG complex coacervation process and ii- the rheological properties of formed coacervates. We showed that low ionic strengths, below 5 mM of added NaCl, promoted the coacervation process. Above 20 mM of added salt, the complex coacervation was abolished even if the interaction between the two proteins was still detected. Monte Carlo simulations demonstrated that the interaction free energy between the two proteins remarkably decreases with increasing ionic strength. In addition to that, a complete rheological characterization illustrated that coacervates exhibited a viscoelastic liquid-like behavior and showed exceptional viscosity, which was 2500 times higher than that found for individual proteins at equivalent total protein concentration. A decrease of the temperature or a small increase of the ionic strength enhanced the rigidity and the viscosity of the coacervates. These results allow better understanding of the involved interactions in concentrated protein solutions and open new avenues for the use of coacervates as texturizing agents in food matrices.

Key words: Complex coacervation, Ionic strength, Rheology, β-Lactoglobulin, Lactoferrin.

Résumé

La coacervation complexe est une séparation de phase liquide-liquide (SPLL) qui conduit à la formation d'une phase concentrée appelée coacervats. Ces coacervats permettent entre autres applications l'encapsulation efficace de molécules bioactives. Des travaux précédents focalisés sur le cas spécifique de la coacervation hétéroprotéique entre deux protéines globulaires du lait, la lactoferrine (LF) et la β-lactoglobuline (βLG), ont établi les conditions optimales du processus de coacervation. L'objectif de ce projet de thèse était de déterminer l'influence de la force ionique sur le processus d'interactions et d'assemblage des protéines ainsi que sur l'état final des coacervats en combinant des approches expérimentales et de la modélisation moléculaire. Ce travail a montré que la coacervation complexe entre LF et βLG est hautement sensible à la force ionique dans une gamme allant de 0 à 20 mM de NaCl ajouté. Au-delà de 20 mM NaCl, le processus de coacervation était aboli mais pas l'interaction au niveau moléculaire entre les deux protéines. La Simulation par méthode de Monte Carlo a permis de montrer que l'énergie libre d'interaction a fortement diminué avec l'augmentation de la force ionique du milieu. La caractérisation rhéologique a mis en évidence des propriétés exceptionnelle des coacervats avec notamment une viscosité 2500 fois supérieure à celle des protéines individuelles utilisées à une concentration protéique équivalente. Une diminution de la température ou une légère augmentation de la force ionique entraine une augmentation de la rigidité et la viscosité des coacervats. Ces résultats contribuent à mieux comprendre les interactions impliquées dans les solutions fortement concentrées en protéines en vue de leurs applications dans des matrices alimentaires comme substituts au additifs texturants.

Mots clés : Coacervation complexe, Force ionique, Rhéologie, β-Lactoglobuline, Lactoferrine.

Thesis outputs

❖ **Published or submitted research paper**

- Soussi Hachfi, R., Famelart, M.-H., Rousseau, F., Hamon, P., & Bouhallab, S. (2022). Rheological characterization of β-lactoglobulin/lactoferrin complex coacervates. *LWT- Food Science and Technology*. https://doi.org/10.1016/j.lwt.2022.113577
- Soussi Hachfi, R., Hamon, P., Rousseau, F., Famelart, M.-H., & Bouhallab, S. (2022). Ionic strength dependence of the complex coacervation between Lactoferrin and β-lactoglobulin. *Foods*. https://doi.org/10.3390/foods12051040

❖ **Paper in preparation**

- Soussi Hachfi, R., Famelart, M.-H., Rousseau, F., Hamon, P., & Bouhallab, S. (2023). Rheological properties of lactoferrin/β-lactoglobulin coacervates: ionic strength and temperature effects. Submitted.
- Lund, M., Soussi Hachfi, R., & Bouhallab, S. (2023). Ionic strength effect on lactoferrin - β-lactoglobulin interactions: Monte-Carlo simulation. In preparation.

❖ **Oral communications**

- Soussi Hachfi, R., Famelart, M.-H., Rousseau, F., Hamon, P., & Bouhallab, S. Rheological characterization of β-lactoglobulin/lactoferrin complex coacervates. 17th Journées de la Matière Condensée (JMC). August 2021 France.
- Soussi Hachfi, R., Famelart M.H., Rousseau F., Hamon, P., Bouhallab S. Lactoferrin/ β -lactoglobulin complex coacervates: rheological properties- 35th EFFoST International Conference. November 2021 Lausanne, Switzerland.

- Soussi Hachfi, R., Hamon, P., Rousseau, F., Famelart, M.-H., & Bouhallab, S. Insights into ionic strength-modulated complex coacervation between Lactoferrin/β-lactoglobulin. 9th **R**encontres **B**iologie~**P**hysique du **G**rand-**O**uest (RPBGO). Juin 2022, Brest, France.
- Soussi Hachfi, R., Famelart, M.-H., Rousseau, F., Hamon, P., & Bouhallab, S. Ionic strength and temperature effects on the rheological properties of Lactoferrin/β-lactoglobulin coacervates. 56ème Congrès du **G**roupe **F**rançais de **R**heologie (GFR). October 2022, Rennes, France.

❖ **Poster presentation**

- Soussi Hachfi, R., Famelart M.H., Rousseau F., Hamon, P., Bouhallab, S. Lactoferrin/β-lactoglobulin complex coacervates: rheological properties. Tweeter poster in Geneva Colloid 2021. Online conference.

Tables of Figures

Tables of tables

Abbreviation

α -Lac: α-lactalbumin

βCG: β-conglycinin

βLG: β-lactoglobulin

βLG A: β-lactoglobulin variant A

βLG B: β-lactoglobulin variant B

ΔH: The enthalpy

BSA: Bovine Serum Albumin

CC: Complex Coacervation

Cp: Protein Concentrations

HPCC: Heteroprotein complex coacervation

IS: Ionic strength

ITC: Isothermal Titration Calorimetry

Ka: The binding constant

KDa: Kilodalton

LF: Lactoferrin

LLPS: Liquid Liquid Phase Separation

Lys: Lysozyme

MC: Monte-Carlo

MES: 2-(N-morpholino) ethanesulfonic acid hydrate

Ova: Ovalbumin

pI: Isoelectric point

Rh: hydrodynamic radius

WPI: Whey protein isolate

1 General introduction

The electrostatically driven interactions between oppositely charged polymers in aqueous solution can lead to a spontaneous liquid−liquid phase separation (LLPS) into polymer rich phase called coacervates phase and a much less concentrated phase called the dilute phase. This LLPS also known as complex coacervation (CC) has been widely studied one century ago (Bungenberg De Jong & Kruyt, 1929) and until nowadays. The coacervation processes is rigorously investigated. Several theoretical models were put forward to understand the mechanism and the main steps of the coacervation (Overbeek & Voorn, 1957; Tainaka, 1967; Veis, 2011; 1967). The influence of the medium conditions i.e. pH, ionic strength (IS), temperature, polymers concentration (Cp) and molecular weight (Mw) was also studied (Kaushik et al., 2016; Schmitt et al., 1998; Timilsena et al., 2017, 2019; Timilsena, Wang, et al., 2016; B. Wang et al., 2014; Zheng, Tang, et al., 2020a; Zhou et al., 2020). Furthermore, a detailed characterization of the formed coacervates was conducted as well as their potential application in several field (Anal & Singh, 2007; Arfin et al., 2014; Banani et al., 2017; Chapeau et al., 2016; Mi et al., 2020; Timilsena et al., 2019). LLPS is an active field of research where the three communities, i.e. physics, chemistry and biology meet with complementary approaches of soft matter, thermodynamic and molecular and cell biology. Combining efforts from physicists, chemists and biologists were required to answer the multiple questions rising around the chemical structure, the organization and the thermodynamic stability of the coacervates but also to understand how do coacervates interact with soft interfaces such as biological membranes and affect biomolecular processes such as enzyme activity or biopolymer folding. CC is regaining such a strong interest and flourishing in research fields. Coacervates microdroplets are successfully incorporated into diverse applications in many areas such as agri-food processing technologies (Chapeau et al., 2016), cosmetic industries (Kalantar et al., 2007), biomedicine (Blocher & Perry, 2017), synthetic biology and cytomimetic engineering (Crowe & Keating, 2018) depending on the used polymer system in the coacervates formation. In biology, polyelectrolytes-based coacervates were used in the construction of membrane-less protocells to mimic the living cell function. In fact, conventional membrane-bounded protocells such as polymersomes, colloidosomes and

proteinosomes, although proved effective, did not resemble the cytoplasmic matrix of living cells as closely as the membrane-less coacervates-based protocells as membrane-bounded protocells are mainly water-filled while the coacervates are considered as a molecularly crowded medium (Gao & Mann, 2023). On the other hand, biopolymers-based coacervates were widely used in food industry and it included a great number of biopolymers systems. These studies included a great number of biopolymers systems; the most used are proteins (notably gelatin) and polysaccharides (mainly gum Arabic). However, the use of gelatin is highly discouraged by consumers due to environmental and animal production issues. Providing other proteins source is required to answer to the high demand for protein-based clean label food products. The current thesis is focused on the protein-based coacervates. Proteins are essential for the human's health thanks to their rich diversity of functional, physico-chemical and biodegradable properties. In addition to that, the ability of proteins to modify food's color, flavor, physicochemical and textural properties made them of a great interest to the food industry (Damodaran & Paraf, 1997). Therefore, the number of studies on the interaction between proteins and their ability to form complex was raising (Adal et al., 2017; Chapeau et al., 2016; Pathak et al., 2015; Zheng et al., 2020). Heteroprotein complex coacervation (HPCC), involving only proteins, is rather a recent research area and there is still a lot to study in this subject. This thesis project focuses on the specific case of β-lactoglobulin (βLG) /lactoferrin (LF) complex coacervation. In fact, previous work, especially from our research group, reported the efficiently of βLG/LF coacervation as encapsulating agent for vitamins (Chapeau et al., 2016). An in-depth study of the effect of the pH, proteins total concentration and stoichiometry on the βLG/LF coacervation was also conducted (Tavares et al., 2015). However, little was reported on the salt effect on coacervation process between these proteins. As HPCC is governed by electrostatic interactions, the ionic strength plays a major role on the coacervation process as well as the final state of the formed coacervates. Moreover, salt concentration is an important factor to be considered for many applications in food industry.

Two main objectives were assigned to this thesis:

- Studying the influence of the ionic strength on the interaction between two proteins in order to better understand the effect of salt concentration on the involved interactions and subsequent process of HPCC.

- Characterizing the structural properties of the βLG/LF coacervates by investigating their rheological properties first under the optimal conditions of formation and with increasing ionic strengths and changes in temperature.

The present document is divided in three main sections:

1. **Literature review** in which a detailed description of previous works on complex coacervation is presented. Starting from a historical overview then the suggested theoretical models that explained the mechanism of complex coacervation are developed, followed by the effect of the most important parameters affecting the complex coacervation and finally, the most common potential application. The second part of the literature review focused on the HPCC; the optimum condition and the characterization of protein-based coacervates are reported. In the last part of this section, previous works on the specific case of βLG/LF CC are mentioned and finally the objectives and the chosen strategy of this present work are given.
2. **Results and Discussion,** this section includes two chapters, and each chapter is divided into two parts.
   - The first chapter covers the effect of ionic strength on the interaction between the two proteins using an experimental approach (part 1: submitted for publication) and a simulation method (part 2 manuscript in preparation)
   - The second chapter aimed to characterize the formed complex coacervates. An in-depth study of the rheological properties of the coacervate network formed under reported optimal

conditions (Part1: Soussi-Hachfi et al.: *10.1016/j.lwt.2022.113577*) then while varying the ionic strength and temperature (Part 2: manuscript submitted)

All the chapters are represented as book chapters rather than published research papers and all the references are sorted at the end of the manuscript.

3. The last section includes a **General Discussion** of the presented results followed by a **Conclusion and perspectives section.**

2 Literature Review

2.1 Complex coacervation: liquid-liquid phase separation

2.1.1 Historical overview

Biopolymers such as proteins, polysaccharides and nucleic acids are abundantly present in the living organisms. These biopolymers spontaneous self-assembly can undergo an associative liquid-liquid phase separation (LLPS) into two distinct phases; a diluted supernatant phase and a biopolymer-concentrated phase called coacervates. The LLPS, also called complex coacervation (CC), is driven mainly by electrostatic attractions between two oppositely charged biopolymers. However, a combined effect of other weak attractive interactions such as Van Der Waals intermolecular forces, hydrophobic interactions and hydrogen bonding also come into play in the coacervation process. Around 1920, Oparin (1924) suggested that life could have originated inside phase-separated droplets formed by coacervation as shown in the Figure 2-1. In other words, LLPS between biopolymers is reported to be the precursor to the origin of cells. In fact, coacervates are membrane-free droplets formed between relevant molecules such as peptides, RNA, and nucleotides which lead to the idea of presenting them as protocell models.

The coacervation process was described for the very first time by F.W.Z. Tiebackx in 1911 (Tiebackx, 1911). Later during the 1920s and 1930's, an in-depth investigation was conducted by Bungenberg de Jong and Kruyt using gelatin and gum Arabic as model biopolymers (Bungenberg De Jong & Kruyt, 1929). Since then, numerous works aimed to study the complex coacervation between different macromolecules and polyelectrolytes but also bio macromolecules such as proteins and polysaccharides.

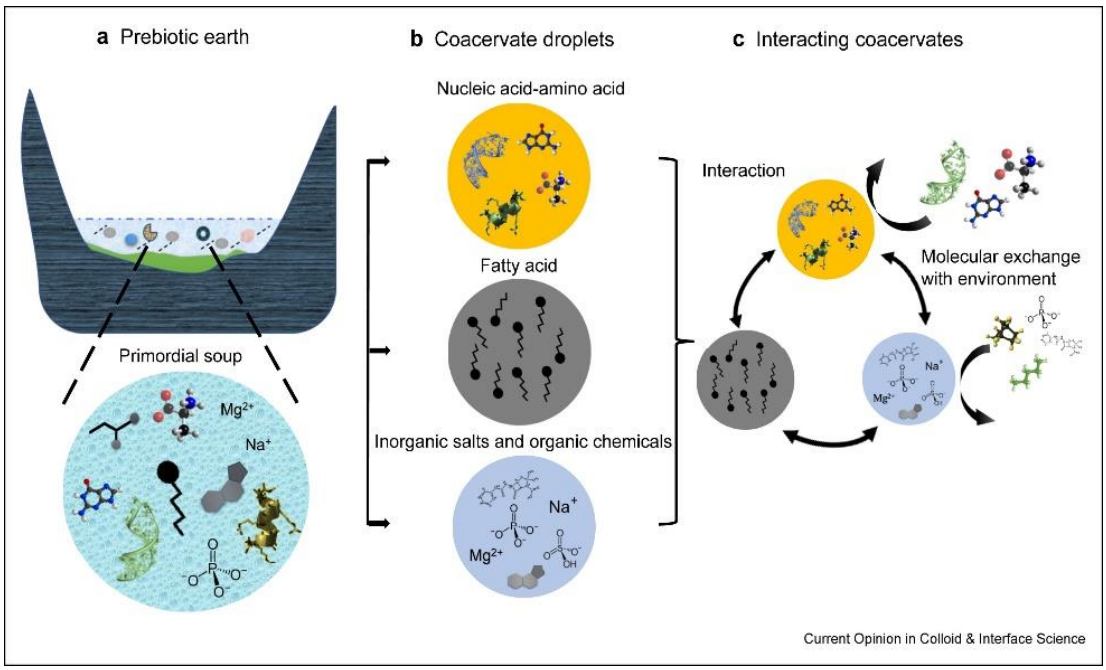

Figure 2-1: Coacervates formation on prebiotic Earth. (a) A primordial soup on prebiotic Earth may have been contained biomolecular precursors. (b) Coacervation, a phase separation process, could have enriched the biomolecular precursors into membrane-free coacervates droplets to facilitate reactions by up concentration (c) Coacervates can concentrate reactants, support enzyme reactions and allow the exchange of ions and small molecules with surrounding media and other compartments (B. Ghosh et al., 2021).

From 1980 till 2000, the majority of the works focused on the coacervation of gelatin with different polysaccharides such as acacia gum and *κ*-carrageenan (Antonov & Goncalves, 1999; Burgess & Carless, 1984; Elgindy & Elegakey, 1981; Peters et al., 1992). However, the animal gelatin was tending to be highly discouraged by consumers due to its environmental problems associated with animal production systems. For this reason, coacervates systems other than gelatin/polysaccharides were studied. During the early 2000's, the coacervation of milk proteins/polysaccharides was starting to gain interest (Bryant, 2000; Eleya & Turgeon, 2000; Kazmierski et al., 2003; Laneuville, 2000; Schmitt et al., 2001; Weinbreck et al., 2003). Starting from the mid 2000's, works on plant proteins based coacervates, in particular pea, chia and lentil proteins were published (Archut et al., 2023; Aryee &

Nickerson, 2012; Ducel et al., 2005; G.-Y. Li et al., 2021; S. Liu et al., 2009; Muhoza et al., 2022; Rios-Mera et al., 2019; Timilsena, Wang, et al., 2016; Q. Zhang et al., 2020). Around the same period, the interest in heteroprotein complex coacervation (HPCC) started to rise (Ainis et al., 2019; Archut et al., 2023; Croguennec et al., 2017; Desfougères et al., 2010; Diarrassouba et al., 2015; Muhoza et al., 2022; Nigen et al., 2007; Salvatore et al., 2011; Zheng, Tang, et al., 2020).

2.1.2 Theoretical description of complex coacervation

The complex coacervation is driven by electrostatic interactions between two oppositely charged polymers that lead to phase separation. Generally, the coacervation results from a two-step process as seen in Figure 2-2:

- First, the formation of neutral charged macromolecules by electrostatic interactions by the release of the counter ions to create larger micrometric spherical droplets with a high density leading to an entropy driven phase separation (microphase separation).
- A second step is the rearrangement and coalescence of the formed droplets forming the highly concentrated liquid phase (macrophase separation)

Various theories have been put forward to adequately describe the coacervation mechanisms. De Jong, Voorn, Veis, Tainaka and co-workers (Bungenberg De Jong & Kruyt, 1929; Overbeek & Voorn, 1957, 1957; Veis, 2011; Veis et al., 1967) proposed models in which the coacervation conditions, the driving forces, the formation process and phase separation kinetics have been discussed.

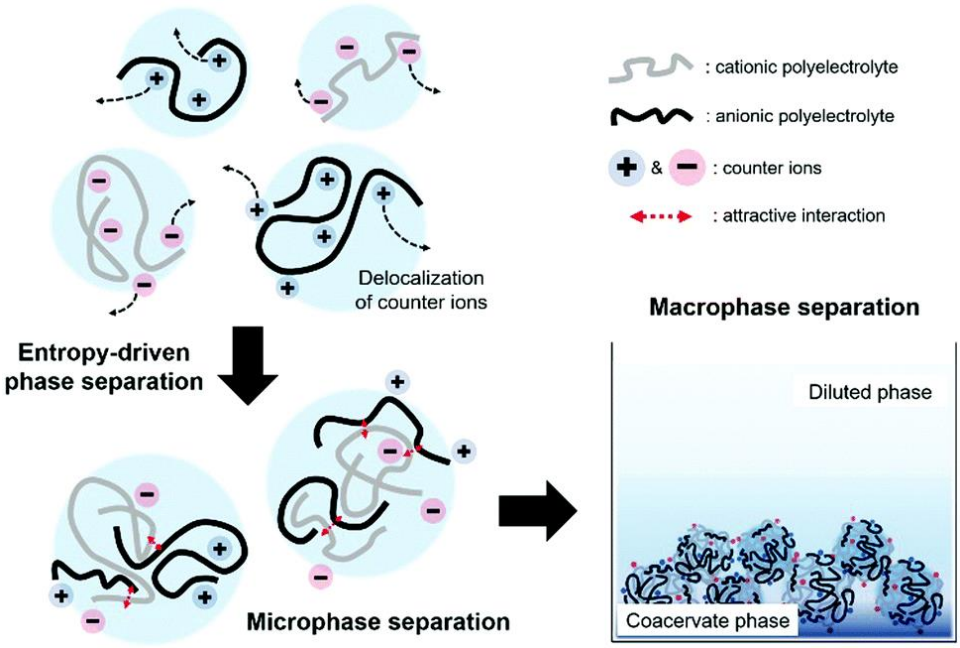

Figure 2-2: Schematic drawing of complex coacervation (Curk et al., 2016).

2.1.2.1 Voorn's model

One of the first models aiming to explain the mechanism behind the complex coacervation was the Voorn-Overbeek's model (1957). According to these authors, the coacervation is a spontaneous phenomenon resulting from a competition between electrostatic attraction between the oppositely charged biopolymers and entropy effects that tend to disperse those biopolymers. Voorn-Overbeek adapted Bungenberg de Jong's experimental data of gelatin/gum Arabic complex coacervation (Bungenberg De Jong & Kruyt, 1929) to propose a theory that describes the process of the coacervation. These authors assume that the coacervation system should have a low charge density otherwise the polymers will be in an unfolded state rather than in a random coil configuration and so a precipitation rather than coacervation would most likely occur (P. Dubin et al., 1994). Several parameters affecting complex coacervation were also discussed in this theory such as the effect of charge densities and molecular weights of polymers, dielectric constant of the solvent and Huggins interaction parameters on

coacervation phenomenon (Timilsena et al., 2019). According to Voorn-Overbeek's model, the critical condition for coacervation is when the interaction between solvent and solute is neglected and the equation 2 is satisfied. However, it was proved that complex coacervation could occur even when the equation 2 was not respected.

$$\sigma^3 r \geq 0.53 \qquad \textit{2-1}$$

σ is the charge density and r is the polymer molecular weight.

2.1.2.2 Veis's model

In order to correct the Voorn-Overbeek theory, Veis et al. (Veis, 1967; 2011) included the effects of non-electrostatic interactions in their study of a practical case of coacervation between two oppositely charged gelatin molecules. Unlike Voorn-Overbeek, Veis et al. (1967) reported that the Huggins interaction parameter is not negligible, on the contrary, it is the driving force for coacervation. These latter authors stated that LLPS into a randomly mixed coacervates phase and dilute phase is driven by the gain in configurational entropy. Veis et al. (1967, 2011) were the first to describe the coacervation as a two-step process; the first step is the spontaneous aggregation of gelatin by electrostatic interactions to form complexes of low configurational entropy, and then, coacervation of these complexes leads to the phase separation.

2.1.2.3 Tainaka's model

Tainaka's theory (1967) is considered as the most relevant theory as it is applicable for a large number of both high and low charge density polymer systems. The novelty of this model is that it considers that polymer complexes became charge-neutralized prior to coacervation and are present in both the dilute and the coacervates phase. This means that the complexation of polymers is ensured by electrostatic interactions but that macro-phase separation is driven by attractive forces among the formed complexes without specific ion pairing. Another important reporting of this model is that the complexes can be symmetrical or asymmetric depending on the polyion symmetry. According to Tainaka,(1967) both the

charge density and the polymer molecular weight should be within a specific reasonable range. Surpassing this range, strong long-range attractive forces will take place among the polymer complexes leading to a concentrated gel or a precipitate rather than to a coacervate. However, if charge density as well as molecular weight is not high enough, the dilute solution will be stabilized by short range repulsive forces and coacervation will not occur. The suppression of coacervation at high salt concentration is explained according to this model, by non-symmetrical mixing of polyions i.e., an excess of negative or positive charges.

2.1.2.4 Comparison of the theoretical models

Those models raised some contradictory points regarding the nature of interactions leading to coacervation, the entropy role and the significance of Huggins interactions (Timilsena et al., 2019). In order to find a common ground between coacervation theories to understand the coacervation process, Burgess (1990) analyzed various complex coacervation systems to study the complex coacervation process as well as the effects of pH, ionic strength, and the presence of ions. The latter author reported that Voorn-Overbeek's theory was able to describe coacervation only under very specific conditions. On the other hand, according to Tainaka and Veis's theories, coacervation still occurs even outside these conditions. However, none of the theories adequately describes all cases of complex coacervation.

Even though a great deal of efforts has been devoted to demonstrate the complex coacervation process, the exact mechanism of formation of complex coacervates is very intricate and complex and still not yet sufficiently understood. However, several works were put together to try and find a generic process of complex coacervation. These studies have agreed that the complex coacervation occurs into four main steps:

- Initially, spontaneous attractive interactions between macromolecules of opposite charges lead to the formation of primary units whose stoichiometry is system dependent (Croguennec et al., 2017).

- Then, soluble complexes form from these primary building blocks according to a not completely elucidated mechanism.
- The third step is the growth of complexes with the formation of micrometric droplets characteristic of complex coacervation (X. Wang et al., 2021).
- Finally, the coalescence of these droplets leads to the LLPS (Jho et al., 2017).

2.1.3 Factors influencing the coacervation process

As mentioned above, complex coacervation results from a subtle balance between electrostatic interactions, hydrophobic associations, van der Waals forces, hydrogen bonds and other weak interactions. Any change in the coacervation process parameters such as pH, temperature, and ionic strength affects this balance leading to the suppression of the coacervation or the formation of a precipitate rather than a coacervate. In addition, the properties of the used polymers such as their concentration, mixing ratio, molecular weight and charge density also play a great role in the coacervation. These optimum conditions for complex coacervation not only depend on the properties of the medium but also on the physical properties of the studied polymer system. The most common way to set optimum conditions is to measure the turbidity of the solution, as well as the coacervates yield as a function of different conditions.

Setting the favorable conditions for coacervation is crucial to control the structure, texture, and stability of coacervates for more efficient applications especially in the food industry as the food matrix is often affected by the same factors during processing, storage, transportation and digestion. (Kaushik et al., 2016; Schmitt et al., 1998; Timilsena, Wang, et al., 2016; Timilsena et al., 2017, 2019; B. Wang et al., 2014; Zheng et al., 2020; Zhou et al., 2020).

2.1.3.1 Effect of pH

It is well established that the pH has a key role in the coacervation. Its adjustment is crucial in order to initiate the formation of the complex coacervates between biopolymer pairs as any change in the pH

affects the charge density of the polymers by changing the degrees of ionization of acidic or basic chemical groups, hence impacts electrostatic interactions that take place between them. For the majority of coacervate systems, the optimum pH range for coacervation is between the two isoelectric points (pI) of polymers. The range of pH where coacervation is stable is very narrow and it varies from a biopolymer system to another. For protein-based coacervates, when the pH is set below the pI of the protein, the protein becomes positively charged due to the protonation of its amino groups. Therefore, when a negatively charged polymer is mixed with it, the two biopolymers carry almost opposite net charges, resulting in a maximum electrostatic attraction hence a high coacervates yield. Any modification in this pH value provokes a change in the overall charge of biopolymers thus they begin to repel each other (Pathak et al., 2017; Schmitt et al., 1998; Timilsena et al., 2019; Zhou et al., 2020).

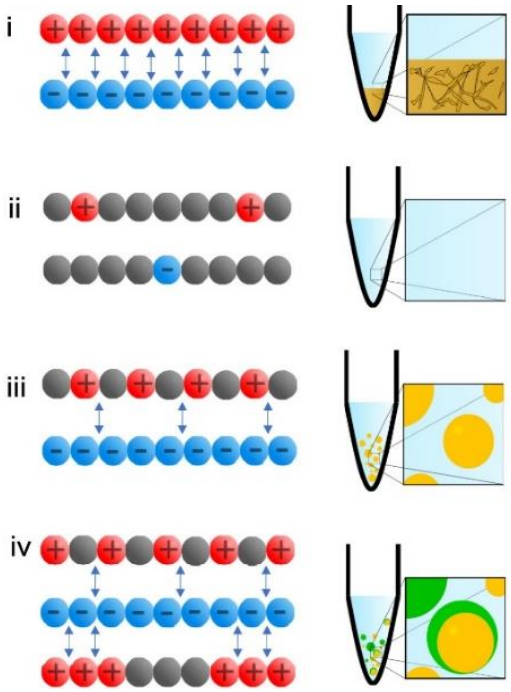

Figure 2-3: The strength of electrostatic interactions between the oppositely charged polyelectrolytes governs whether coacervates can be formed or not. (i) If there is a very strong attraction, precipitates will form. (ii) If the interactions are too weak, the polyelectrolytes will not phase-separate. (iii) Coacervates are formed when the strength of their interactions is optimal. (iv) When there are multiple polyelectrolyte species present in the solution, it is possible to form multiphasic coacervates depending on the critical salt concentrations of the coacervates forming pairs (Ghosh et al., 2021).

The prominent role of the oppositely charges of the polymers on the coacervation is seen in Figure 2-3. In fact, strong attractive forces between the biopolymers lead to a solid – liquid phase separation rather than LLPS and the formation of precipitates rather than coacervates. However, if the attraction is very weak the polymers do not interact hence no phase separation can take place. The complex coacervation occurs in a specific balance between the positive and the negative charges i.e. an optimal strength of interaction (Ghosh et al., 2021).

The influence of pH on the LLPS was widely studied by several authors (Knoerdel et al., 2021; S. Liu et al., 2010; Neirynck et al., 2004; Tavares et al., 2015; Tomé Constantino & Garcia-Rojas, 2022; Weinbreck et al., 2003; Xia et al., 1993; Yan et al., 2013). In some of these works, two important pH values were discussed as seen in Figure 2-4:

- A critical pH (pH_c) where soluble complexes are formed by electrostatic interactions
- A phase separation pH (pH_φ) where soluble complexes undergo Ostwald ripening and coalesce to form microscopic coacervates droplets leading to LLPS.

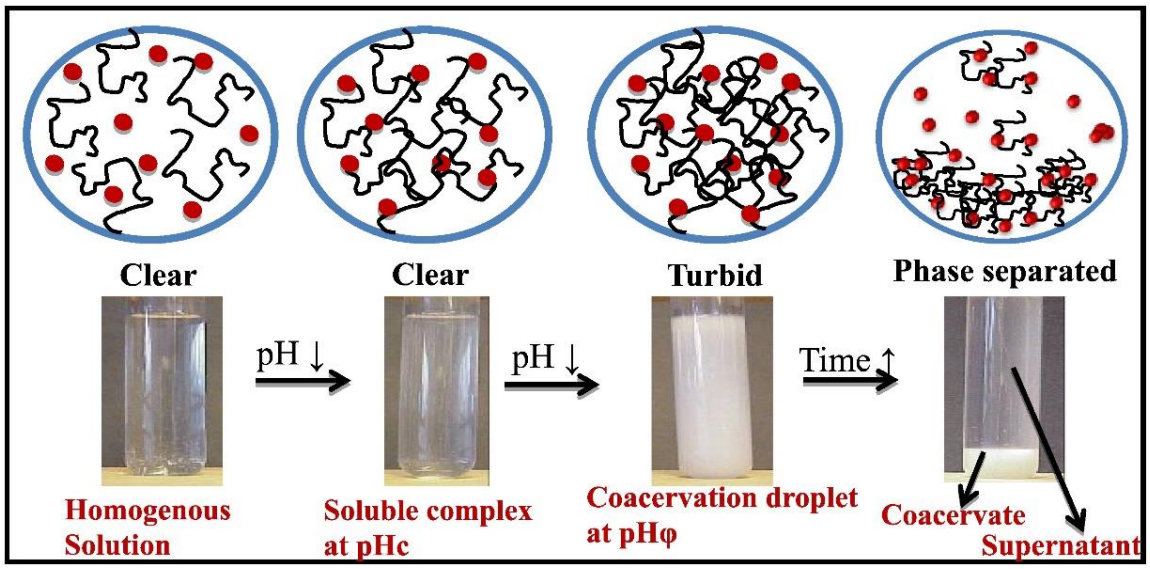

Figure 2-4: Schematic of interaction and complex coacervation of a globular protein with flexible polyelectrolyte driven by a decrease in pH (Pathak et al., 2017).

2.1.3.2 Effect of ionic strength

Another equally important factor that affects the complex coacervation is the ionic strength (IS), i.e. the total number of micro and mobile ions present in the biopolymer solution. In fact, microions can provoke charge neutralization of polymers, which prevents the electrostatic interactions to take place. Since electrostatic interactions play the most important role in complex coacervation as showed in Figure 2-3, the effect of salts on the coacervation is always the research focus. A high number of salt microions can form a dense atmosphere around polymers, which causes the screening of the net charge and as a result, prevents electrostatic interactions between polymers hence a suppression of coacervation. Besides, the LLPS is ensured by an entropic gain due to the release of the counter ions, but at a high salt concentration, these counter ions cannot be liberated in the medium. De kruif (2004) emphasized the high sensitivity of the coacervation to ionic strength by proving that even a small amount of salt weakens the electrostatic binding between polymers and prevents the coacervation. The presence of ions can cause higher charged macromolecules that will be in the extended molecular conformation which does not favor coacervation (P. Dubin et al., 1994). In addition to that, the presence of salt modifies the dielectric constant of the solvent which is another important factor in electrostatic interactions (Pathak et al., 2017). On the contrary, other authors reported that a small amount of salt enhances electrostatic interactions between the polymers, thus promotes the coacervates formation, but a further increase in the salt content suppresses coacervation (Burgess, 1990; X. Wang et al., 2021; Xiong et al., 2016). This behavior is called “salting-in” and was explained by Burgess (1990) as a consequence of the effect of added salt on the extent of coiling and charge densities of the involved macromolecules. It is also worth mentioning that after formation, the coacervates might dissolve at high ionic strength due to loss of the entropic release of bound counterions. As reported by Fares et al. (2018), polyelectrolyte complexes go from solids to coacervates to a single phase solution with increasing KBr concentration (Figure 2-5).

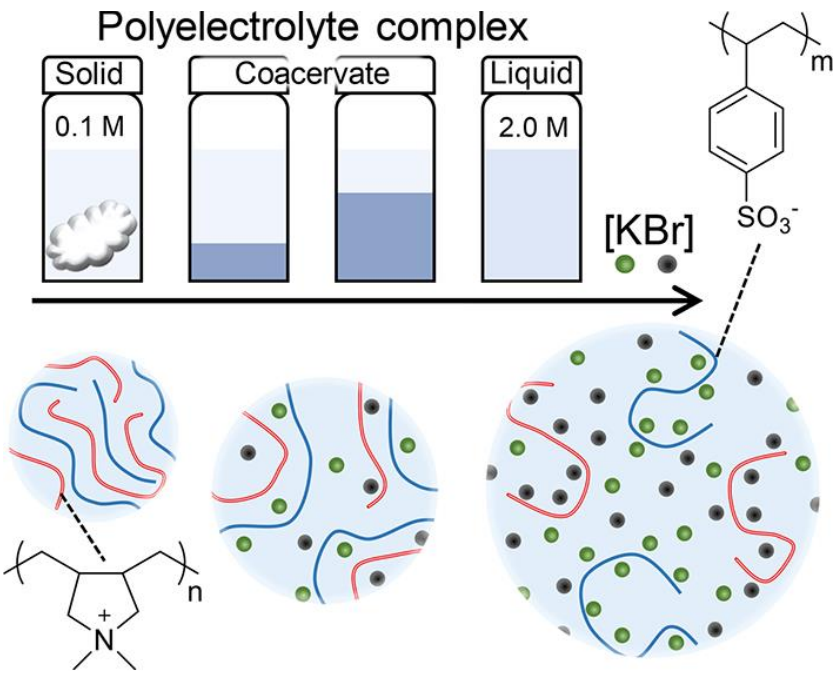

Figure 2-5: Schematic representation of phase transition of polyelectrolytes complex with increasing KBr concentration Fares et al. (2018)

2.1.3.3 Mixing Ratio

The coacervation process is highly dependent on the mixing ratio between the two biopolymers, their final concentration as well as the charge stoichiometry between the positive and negative biopolymers in the system since the electro-neutrality needs to be achieved for the coacervates to form. The maximum yield of coacervation is reached at a specific ratio between polymers at a given combination of pH and ionic strength. As a matter of fact, the coacervation cannot occur if one of the polymers is in excess because of the low energetic interest of concentrating the polymers into coacervates if the concentration in solution is already high (Schmitt et al., 1998). To predict the best mixing ratio for coacervation, charge stoichiometry should be investigated. However, since proteins contain both positively and negatively charged groups, the exact charge stoichiometry is hard to investigate. Therefore, for protein based coacervates, the driving force may come from specific charge patches on the molecular surface but not from the overall charge. It was also proved that the mixing ratio not only influence the formation of

coacervates but also their morphology, size, rigidity as well as the formation kinetics (Bartolini et al., 2019; Schmitt et al., 2001; Y. Wang et al., 2000).

2.1.3.4 Temperature

Temperature during the mixing of biopolymers significantly influences coacervation phenomenon by effecting biopolymers interactions. Several works claimed that the coacervation process is promoted at low temperature because of increased solvent-solvent, solvent-solute and solute-solute interactions. Beside its effect on the Flory-Huggins interactional parameters, temperature has an evident effect on the non-Coulombic interactions that could take place during the coacervation. In fact, low temperatures promote the hydrogen bond but reduces hydrophobic interactions. Moreover, for the protein-based coacervates, the structure of protein is often affected by temperature, which affects the binding of protein with other biopolymers, sometimes by exposing more active binding sites, and hence promotes the formation of complex coacervates (Tiebackx, 1911). On the other hand, heating biopolymer solution increases its solubility resulting in a decrease in the complex formation efficiency. For some polyelectrolyte system, the temperature effect is more important. In fact, the LLPS can only occur either over heating or cooling depending on the studied polymers. This phenomenon is called temperature-induced phase separation (Kelly et al., 1994).

As seen in Figure 2-6 that increasing ionic strength or the temperature had the same effect on all interaction types except hydrogen bonding that get weaker with increasing the temperature but is unaffected by ionic strength increase.

Although the influence of temperature on the complex coacervation of different systems seems obvious for several authors, others think that coacervation tends to have a relatively weak temperature dependence and others even think that the complex coacervation process is independent of the temperature (de Kruif et al., 2004; Kaibara et al., 2000; Weinbreck et al., 2004).

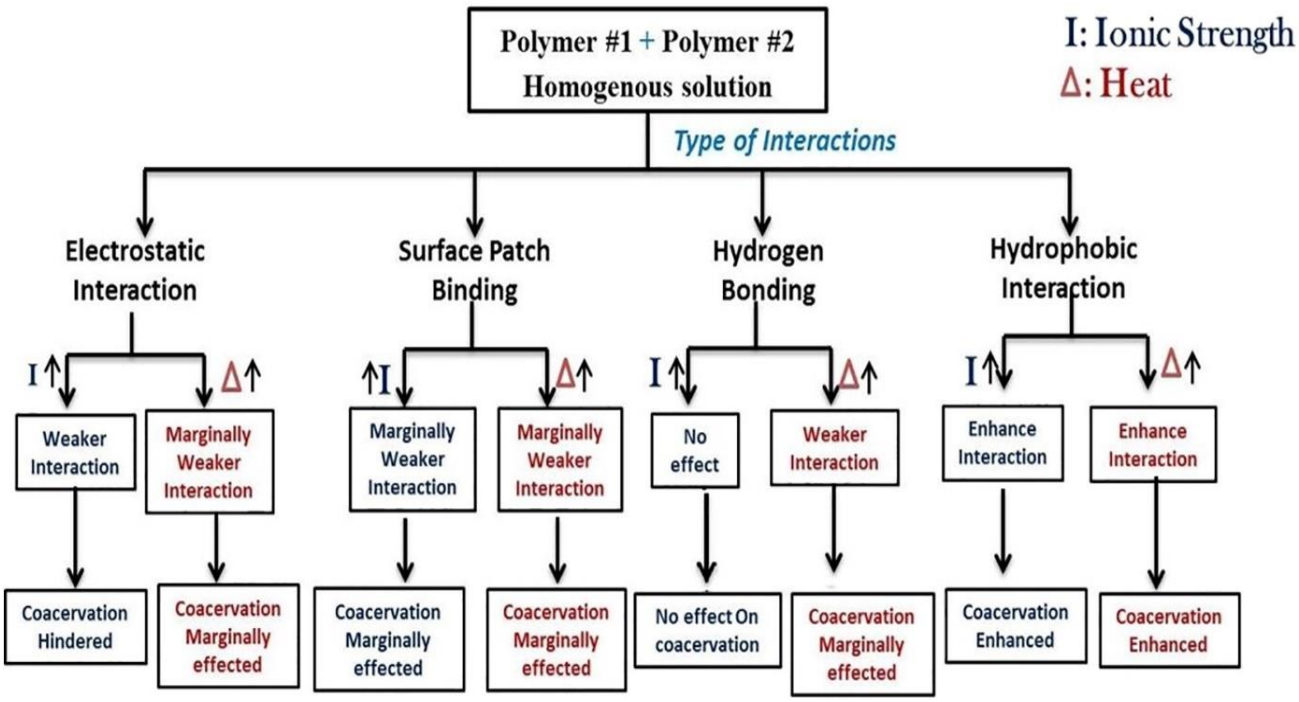

Figure 2-6: Schematic of intermediate complexation and coacervation based on temperature and ionic strength (Pathak et al., 2017).

2.1.3.5 Molecular weight

Another important factor influencing complex coacervation is the molecular weight (Mw) of the biopolymers. Just like pH, the molecular weight of polymers should fall into a specific range. Outside of this range, materials will form gels or precipitates rather than coacervates for high Mw and end up interacting by ion pairing rather than coacervation for low molecular weights (P. Dubin et al., 1994). Theoretically, increasing the molecular weight of the polyelectrolyte lowers the thermodynamic compatibility of the solution by lowering the combinatorial entropy of mixing. However, Voorn and Ovebeek's (1957) predicted the opposite. According to these authors, increasing Mw of polyelectrolyte increases the complex coacervation. In fact, polymers with low Mw have fewer binding sites available thus bind with less affinity. Therefore, polymers with a high Mw are able to form larger complexes that later coalesce into larger micro-coacervates droplets (Girard et al., 2002; Pathak et al., 2017; Y. Wang et al., 1999; Xia et al., 1993). On the other hand, for protein-polyelectrolyte pairs with strong electrostatic interactions, no effect of molecular weight was observed (Schmitt et al., 1998).

2.1.4 Potential applications

Numerous studies have highlighted the potential applications of complex coacervation for different coacervates systems. Complex coacervates-based materials have been widely used for a variety of applications across a range of disciplines of industry and biology, such as food, pharmaceutical and biomedicine. Complex coacervates are proved very useful in drug delivery, in cosmetic formulation for body and skincare products for instance, or as additives and microcapsules in food processing, viscosity modifiers and cartilage mimics.

2.1.4.1 Encapsulation

The first evident targeted application for coacervation is encapsulation. This technique is highly investigated in several fields such as food, biomedical, cosmetic and agriculture. Probiotic bacteria are encapsulated to improve their viability during food manufacturing processes and also to better control their release (Anal & Singh, 2007; Annan et al., 2008). On the other hand, carotenoids such as lutein and lycopene are encapsulated in order to protect them from light, humidity and temperature changes. As for oils, they are encapsulated in order to increase the stability of their fatty acids against oxidation (Zhang, 2012; Wang et al., 2014). Encapsulation is used mainly to protect sensitive compounds or to mask an unpleasant smell or taste. Two types of encapsulations are to be distinguished: nano-encapsulation for particles with sizes between 1 and 1000 nm and micro-encapsulation for larger micrometric particles in the range of size between 1 and 1000 µm. Since oppositely charged proteins or polysaccharides are known by their nontoxicity and biocompatibility, their coacervates are often used as shell materials to encapsulate different bioactives such as vitamins (Chapeau et al., 2016), essential oil (Tavares & Noreña, 2020), flavour (Xiao et al., 2014), proteins (McTigue & Perry, 2020), virus (Mi et al., 2020) and cells (Bhatia et al., 2005). Using this technique, the release of encapsulated agent can be controlled. The efficiency of the microencapsulation depends on the shape and size of the formed capsules. The encapsulation procedure consists, first, in mixing the bioactives with the first polymer. Then, the second polymer is added, with an optimum opposite charge density, to instantly initiate the

coacervation. The coacervates ,or the capsules in this case, tend to form layers around the encapsulated material. Figure 2-7 shows that mixing the virus with the oppositely charged polymers in their optimum coacervation conditions lead to the formation of virus/coacervates complex.

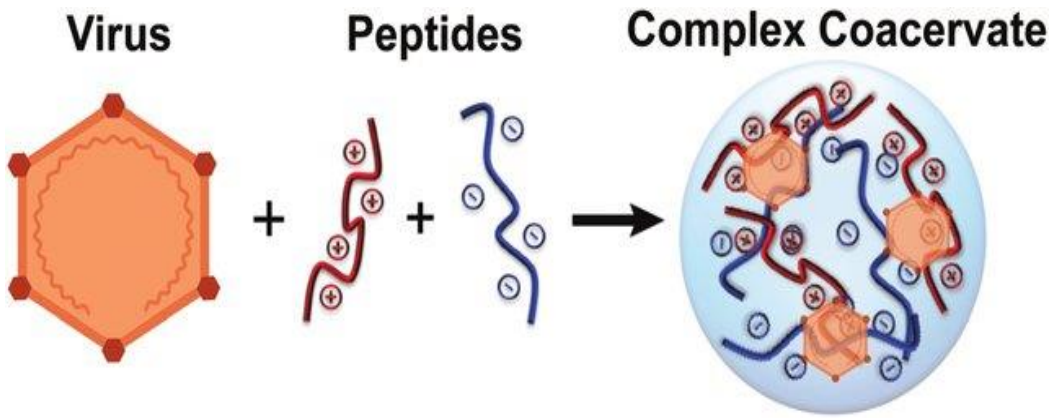

Figure 2-7: Schematic depiction of virus encapsulation via complex coacervation with two oppositely charged polypeptides (Mi et al., 2020).

The controlled release of encapsulated bioactive can be achieved by subtitle dissolution of formed complexes using a variety of chemical or physical parameters such as pH, temperature and ionic strength.

To further protect and store the microcapsules, these coacervates can be converted by freeze-drying or spray drying into powders (Zhou et al., 2020). Because complex coacervates-based microcapsules are surrounded by double layers of shell materials, their microcapsule powders are significantly less porous, more robust, more efficient and have longer storage life than the solid microcapsules produced using either individual proteins or gums as shell material (Timilsena et al., 2016). The applications of encapsulation by complex coacervation mainly concerned protein/polysaccharide interactions. However, in the recent years, encapsulation by heteroprotein complex coacervation was starting to draw attention (Chapeau et al., 2016; Diarrassouba et al., 2015; Zhao et al., 2020).

2.1.4.2 Platforms delivery

One of the most important applications for coacervates-based encapsulation technique is building delivery platforms. The most common materials used as platform for the delivery are drugs(Kataoka et al., 2001), proteins (Johnson et al., 2014), RNA (Frankel et al., 2016) and DNA (Arfin et al., 2014).

Complex coacervation is considered one of the most effective way for drug delivery thanks to the coacervates unique structure. In fact, the formed coacervates have a hydrophilic interface and a hydrophobic micro zone that can encapsulate a wide range of solutes and stabilize them from possible environmental stress such as pH, ionic strength, and temperature. Coacervates platform delivery can enhance protein stability and elevate transfection efficiency for genes. In addition to that, the coacervation was demonstrated as an efficient basis for drug delivery platform. As a huge number of drugs suffers from poor water solubility, the coacervates help to increase their solubility to facilitate delivery at therapeutically relevant concentrations. Coacervates drug delivery is gaining much attention thanks to its ability to release drugs in a controlled manner either being sustained release in long period or responsive release (Awada et al., 2016; Blocher & Perry, 2017; Moulik et al., 2022; Plummer et al., 2011).

2.1.4.3 Protein purification

The increasing demand for proteins as well as protein products such as insulins, monoclonal antibodies, cytokines, and subunit vaccines, has increased the requirement for more efficient and low-cost purification techniques. Despite being widely used, protein purification techniques such as chromatographic purification (Kelley, 2007) and membrane separation techniques (R. Ghosh, 2002) are still considered as high-cost and time-consuming processes. In addition, those techniques are still limited by several drawbacks, for example a large consumption of solvent for liquid chromatography, and a low binding capacity and a poor membrane quality for membrane separation (Xu et al., 2017; Zhou et al., 2020). Therefore, it becomes necessary to find highly selective and large-scale separation techniques. The selective characteristic of phase separation holds a great potential for protein purification without

influencing the protein stability. Several authors have presented complex coacervation as a suitable and promising method for large-scale purification of biomolecules due to its low cost and extremely high throughput (Pathak et al., 2015; Wang et al., 1996; Xu et al., 2011; Zhang et al., 2005). As complex coacervation is based on non-specific electrostatic interactions, the effectiveness of its selectivity compared to that of affinity chromatography has been widely discussed. However, a recent progress has demonstrated that non-specific electrostatic interactions can be properly applied to achieve a high protein selectivity (Xu et al., 2017). During complex coacervation, oppositely charged biopolymers interact to form coacervates i.e. positively charged biopolymers interact with negatively charged ones. Besides the net charge of biopolymers, charge density and charge distribution play an important role that explains the selectivity in the complex coacervation. In fact, in mixed solutions of three or more biopolymer, pH can be adjusted in order to promote the coacervation of two biopolymers and separate the third one in the supernatant. Pathak et al. (2015) prepared a mixed protein solution of gelatin B, β-lactoglobulin (βLG) and bovine serum albumin (BSA). Later, the pH of the mixed solution was adjusted to 5.0. At this pH, a selective coacervation and phase separation between BSA and gelatin B occurred and βLG was collected in the supernatant. Then, in order to separate gelatin B from BSA, ethanol was added to the BSA/ gelatin B coacervates to precipitate gelatin B and recover BSA in the supernatant.

2.1.4.4 Artificial cells development

As mentioned in the historical overview (section 2.1.1), Oparin (1924) reported that complex coacervation could have formed the basis for the evolution of life. In fact, coacervates play the role of phase-separated compartments that serve as a type of protocell. Several studies since then discussed phase-separated and coacervates-like materials in the context of cellular compartmentalization. Liquid–liquid phase separation might play an essential role in subcellular membrane-less compartments which may be reproduced in vitro and can bring insights into the mechanism of cell function, related prebiotic evolution and disease mechanisms (Alberti et al., 2019; Brangwynne et al., 2009; P. Li et al., 2012; Maharana et al., 2018; Zhou et al., 2020). The benefits of compartmentalization to intracellular processes are plentiful. To name a few: increasing interior reaction rates and specificity, reacting to the subtle

environmental changes and inhibiting exterior reactions (Banani et al., 2017; Crowe & Keating, 2018; Deng & Huck, 2017). Drobot et al. (2018) tried to mimic cellular processes by creating a protocell based on carboxymethyl dextran sodium salt and poly-L-lysine to support RNA catalysis. The latter authors proved that RNA was strongly partitioned into coacervates. They also demonstrated that coacervates support the RNA catalysis and up-concentrate oligonucleotides within their interiors. Moreover, complex coacervation exhibits selective retention and release of RNA without additional energy input (Drobot et al., 2018).

2.1.4.5 Other applications

Besides the applications mentioned above, complex coacervation still offers several other useful and practical applications. Among which, we can cite wastewater treatment, underwater adhesives and emulsion stabilization. Coacervates, especially protein-based ones, play an important role in texturing and improving the sensory quality, nutritional quality and antibacterial ability of food, thanks to the rich functional properties of proteins (Benkhedja et al., 2017; Moulik et al., 2022; Wang et al., 2015; Xu et al., 2017; Zheng et al., 2020; Zhou et al., 2020).

2.2 Heteroprotein complex coacervation

Proteins are natural biopolymers essential for human tissue and organ growth, maintenance and metabolism. In addition to that, they are also one of the most important food groups and are major nutrients for a balanced diet. Thanks to their multiple functional properties, proteins are able to modify food's color, flavor, physicochemical and textural properties. As proteins exhibit a rich diversity of functional, physicochemical and biodegradable properties, various works focus on their ability to form a large diversity of nano- and micro-structures throughout diverse interactions between them. Some of these works studied the heteroprotein complex coacervation (HPCC). The process of HPCC involves the complexation of two or more proteins that leads to a liquid-liquid phase separation. Even though complex coacervation has been sufficiently studied in a wide range of biopolymer systems, HPCC is still comparatively understudied. Heteroprotein coacervates are observed in very specific range of pH,

ionic strength, protein concentration and protein stoichiometry depending on the coacervates-based protein system. Gelatin (from pigs, bovine, chicken or fish), milk proteins and some plant proteins are the major source of proteins used during complex coacervation. (Adal et al., 2017; Croguennec et al., 2017; Muhoza et al., 2022; Zheng, Tang, et al., 2020). The field of heteroprotein coacervation has developed rapidly during the last ten years thanks to its diverse applications in both food and non-food industries such as protein purification (Pathak et al., 2015), drug and nutraceutical encapsulation (Chapeau et al., 2016), emulsion stabilization (Teo et al., 2016) and hydrogels construction (Bourbon et al., 2015).

2.2.1 Protein–protein systems

HPCC has attracted a rapid attention lately and many heteroprotein-based coacervates have been studied. Favored conditions for coacervation depend on the protein system. In order to induce HPCC, each system should respect specific conditions of the medium. The most studied protein couples are mentioned in the Table 2-1.

Table 2-1: Optimum conditions and coacervation properties of different heteroprotein complex coacervates.

Acidic proteins (pI)	**Basic proteins (pI)**	**Optimum conditions**	**Coacervates properties**	**References**
Pigskin gelatin B (4.5-5)	Pigskin gelatin A (9)	➢ pH = 6.3 ➢ GelatinA/Gelatin B stoichiometry =3/2	• Viscoelastic liquid-like dominant behavior. • Suitable for drug (salbutamol sulfate) encapsulation. • The coacervates matrix is softened in the presence of encapsulated drug.	(Tiwari et al., 2009)
Bovine Serum Albumin (BSA) (5)	Bovine gelatin (6)	➢ pH = 5 ➢ Gelatin/BSA stoichiometry ≤ 1	• mixing ratio < 1 • The surface patch binding governs the coacervation while hydrogen binding leads to gelation.	(Pathak et al., 2014)

Bovine gelatin (6)	Lysozyme (Lys) (10.7)	➢ pH = 7 ➢ IS = 0.01 mM ➢ Lys/gelatin weight ratio: 1.47 w/w	• Viscoelastic behavior solid-like • Complexation decreases sharply after increasing IS. • Lys and gelatin molecules within the complex have heterogeneous character. • No significant changes in tertiary structure of Lys after binding.	(Antonov et al., 2017)
β-lactoglobulin (βLG) (5.2)	Lys (10.7)	➢ pH = 7.5 ➢ IS = 10 mM ➢ β LG/Lys stoichiometry= 0.67	• βLG interacts with Lys molecules to form complexes that condensed to form coacervates. • Coacervates diameter = 7.1 ± 2.5 µm. • Encapsulation efficiency = 90.8 ± 4.8 %.	(Ainis et al., 2019; Diarrassouba et al., 2015)
Ovalbumin (Ova) (4.5)	Lys (10.7)	➢ pH = 7.5 – 8 ➢ Ova/Lys stoichiometry= 0.55 – 1	• Low NaCl concentrations disfavor the coacervation and suppress it at 300 mM. • The coacervates are microspheres with a mean size of 2-8 µm • The interaction is exothermic and spontaneous and is dominate by electrostatic interactions. • The interaction occurs in two steps with an enthalpically favorable and entropically unfavorable contribution. • 15 mM is the critical IS value.	(Desfougères et al., 2010; Santos et al., 2018)
α-lactalbumin (α-lac) (4.3–4.7)	Lys (10.7)	➢ pH = 7.5 ➢ α-lac /Lys stoichiometry = 1	• The coacervation is suppressed at IS = 100 mM. • $CaCl_2$ has the greatest coacervates destabilising effect because of the presence of a specific calcium binding site on α-lac. • The free energy of interaction minima ranges between -9 kT at 1 mM salt to -2 kT at 100 mM.	(Nigen et al., 2007, 2009, 2010; Persson & Lund, 2009; Salvatore et al., 2011)

			• Calculated second virial cross coefficients indicate that attractive interactions dominate in the pH range 6–10, whereas proteins dissociate at lower or higher pH due to electrostatic repulsions. • Lys and apo α-lac interact via electrostatic forces to form heterodimers at molecular level, then their self-assembly evolves toward clusters nano-spheres. Finally, reorganization of these clusters into spherical particles (size : 3-4 µm). • Hydrophobic interactions play a major role in the coacervates formation.	
BSA (5)	Lys (10.7)	➢ pH = 8.9 - 9.0 ➢ BSA /Lys stoichiometry = 0.3 - 0.5	• addition of NaCl decreases the interaction; no particles detected at IS > 20 mM. • coacervates have a globular structure with average size ~1.7 µm. • For pH > 9, aggregates of undefined shapes are observed. • Electrostatic interactions predominate for the coacervation but hydrogen bonds also participate. • Coacervates can be used for encapsulated food bioactive.	(Desfougères et al., 2010; Santos et al., 2018)
β-conglycinin (β-CG) (4.8)	Lys (10.7)	➢ pH = 6 ➢ β-CG /Lys mass ratio = 0.86	• β-CG/Lys coacervates are more thermodynamically stable then β-CG/Lys amorphous precipitates. • Coacervates size = 1−2 µm. • Curcumin encapsulation efficiency and loading capacity = 95%. • Coacervates significantly improve curcumin stability when exposed to light and heat treatment.	(Zheng et al., 2021; Zheng, Gao, Ge, Sun, et al., 2022; Zheng, Gao, Ge, Wu, et al., 2022)

OVA (4.5)	Avidin (AVI) (9.5)	➢ pH = 6.8 ➢ AVI /Lys stoichiometry = 1.5	• Size of formed spheres = 5-10 µm. • Coacervation is favored at low IS and completely hampered at IS> 15 mM.	(Desfougères et al., 2010)
Pea Protein Isolate (PPI) (4.3)	Lactoferrin (LF) (8.7)	➢ pH = 5.4 ➢ PPI/LF stoichiometry= 0.6	• Coacervates sizes = 40−80 nm with a predominance of elliptical over spherical shapes.	(Adal et al., 2017)
Soy Protein Isolate (SPI) (4.6)	LF (8.7)	➢ pH = 6.25 ➢ SPI/LF stoichiometry = 0.3	• All individual SPI fractions participated in HPCC. • Electrostatic interactions, as well as hydrogen bonds participate in the complexation. • Coacervation improves the heat-stability of the heat-sensitive lobe in LF. • Coacervates diameter = 50–150 nm	(Zheng, Gao, et al., 2020)

Heteroprotein complex coacervation is a specific case given the structural complexity of protein molecules. Constrained structural feature and surface charge anisotropy (surface charge density, charge patchiness, size and shape of the patches) orient the interactions to specific domains on the surface of the proteins. This constitutes specificities compared to complex coacervation involving polyelectrolytes and explain in a part that opposite charge stoichiometry is not a sufficient criterion for optimal heteroprotein coacervation. From combined protein systems described in the literature, evidences were drawn showing that complex coacervation in heteroprotein systems is a generic process that can occur in all oppositely charged mixtures, provided that the experimental conditions were relevant, considering the physico-chemical and structural properties of the involved proteins (Croguennec et al., 2017).

2.2.2 Computational simulation methods

In addition to the experimental techniques used to investigate HPCC, numerical simulation was conducted using different molecular modeling techniques in order to simulate proteins-proteins

interaction, predict their behavior and to get insights about their molecular structures. The three frequently used molecular modeling algorithms are : molecular dynamic (MD), Monte Carlo (MC) and Langevin dynamics (LD) simulations (Paquet & Viktor, 2015). In MD simulations, all atoms are taken into accounts and are represented as spherical beads. In this technique, the molecules are represented as a binding of these spheres with springs to mimic the covalent bonds. The force calculation is obtained by calculating the forces acting on one individual atom (n) by all others then the atom position is update (n+1) and the process is repeated until calculating all the forces exerted on all the atoms (Hospital et al., 2015; Polimeni, 2021). As for MC simulations, the smallest unit of molecules are not atoms but a bigger sub-unites such amino acids are used instead. The objective of the MC simulation is to generate representative configurations by applying random rotations and translation trail moves to the system then calculate the energy. A set of parameters is used to either accept or reject this configuration by comparing the value of the new configuration energy to the old one (Paquet & Viktor, 2015; Polimeni, 2021). On the other hand, LD is based on the assumption that N particles of a system are in thermal equilibrium and obey N-coupled Langevin equations. LD Implicitly simulates the effect of molecular collisions in real solvents and calculate the trajectories of these collisions.(Paquet & Viktor, 2015; Suresh & Gopalakrishnan, 2021; Trullàs et al., 1989). Those numerical simulations were employed to investigate the protein-proteins interaction that leads to the HPCC in order to understand the mechanism behind the formation of the heteroprotein coacervates. Table 2-2 summarized the different molecular modeling techniques used to study heteroprotein complex coacervates.

Table 2-2: Molecular modelling contribution to HPCC

Acidic proteins (PI)	Basque proteins (PI)	Molecular modelling technique	Molecular modelling contribution	References
α-lac (4.3–4.7)	Lys (10.7)	Monte Carlo simulations (MC)	• The proteins strongly align according to their charge distribution in the coacervates as well as the dilute phase. • The charge distribution plays a major role in the proteins assembly: the mutation of a single amino acid leads to the suppression of the LLPS. • The binding of heterodimers of α-lac and Lys via electrostatic interaction ensures the formation of the building blocks of the coacervates. • When most of the electrostatic charge patches of the protein surfaces are shielded, the hydrophobic interactions become dominant which leads to the formation of larger oligomers.	(Kurut et al., 2012; Salvatore et al., 2011)
βLG (5.2)	Lys (10.7)	Langevin Dynamics (Brownian Dynamics) (LD)	• heteroprotein assembly occurred after 2 μs. After 20 μs multimeric assemblies were formed • the number of the clusters reached 50 monomers.	(Ainis et al., 2019)
Whey protein Isolate (WPI) βLG, BSA, α-lac	Lys (10.7)	Molecular dynamics (MD)	Whey protein and Lys was proved effective for Fucoxanthin (FX) encapsulation. MD was used to understand the conformation transition and interaction of WPI and FX before the coacervation with Lys and proved that: • non-covalent whey protein−FX complexes became stable from 12 ns. However, pure WPI systems were equilibrated over a time of 20 ns.	(Zhu et al., 2019)

			• Hydrogen bonds between the three whey proteins and FX were formed. • WPI amino acids with hydrophobic side chain constituted the hydrophobic pockets to envelop the FX. • After binding with FX, the major secondary structure components of the whey proteins were reduced hence the protein tightness decreased and the structure transformed into a loose and unfolded state exposing more hydrophobic areas. • PI of WPI was reduced after binding.	
caseinate (Cas) (~ 5.3)	Lys (10.7)	Molecular dynamics (MD)	• The amino acids involved in the hydrophobic and/or the hydrogen bonding varies depending on the temperature. • Changing the temperature effected the interaction interface between Cas and Lys. • The strongest hydrophobic interactions as well as hydrogen bonding were reported for T = 318 K.	(J. Wang et al., 2022)
α-lac (4.3–4.7)	LF (8.7)	Monte Carlo (MC)	• It was virtually proved that no association is expected at a relatively high salt concentration (150 mM). • The attraction between α-lac and LF is relatively weak compered to other complexes e.g. βLG/LF • The complexation is driven by an association of electrostatic interactions i.e. charge-charge, charge-dipole.	(Delboni & Barroso da Silva, 2016)

2.2.3 Specific case of β-lactoglobulin/lactoferrin coacervates

2.2.3.1 Whey proteins

The principal constituents of milk are water, fat, proteins, lactose and minerals as salts. Aa summarized in Figure 2-8. Some other substances are also found in milk such as enzymes, vitamins and gases. In

recent years, milk constituents have become recognized as functional foods. milk composition depends on the animal's species, breed, feed and the stage of lactation.

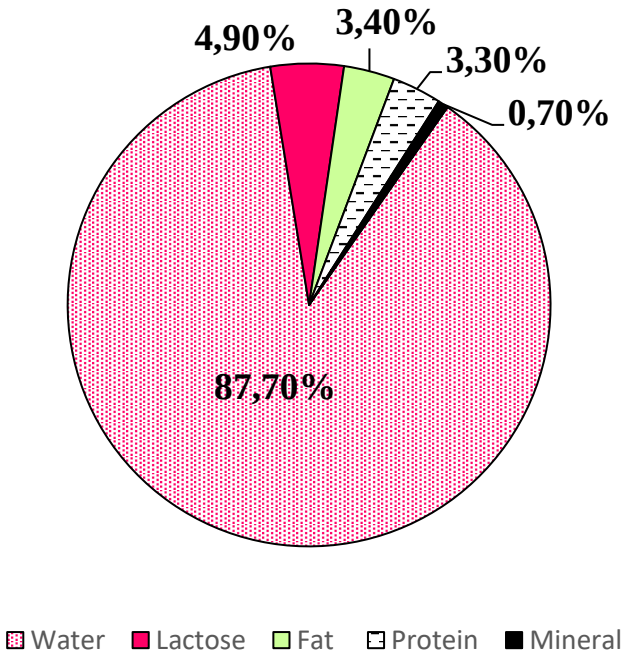

Figure 2-8: Milk composition

Milk contains two main sources of proteins: the caseins and the whey proteins. Whey proteins represent 20% of the total milk protein fraction and are mainly globular proteins. Whey are still soluble after acidification of raw skim milk at pH 4.6 unlike caseins.

Whey proteins have several health benefits such as providing antimicrobial activity, immune modulation, improved muscle strength and body composition. In addition to that, clinical trials have demonstrated that whey proteins play a role in the treatment of cancer, HIV, hepatitis B, cardiovascular diseases and osteoporosis (Marshall, 2004). Properties of whey proteins are summarized in Table 2-3.

Table 2-3: Main physico-chemical properties of bovine whey proteins

Protein	Concentration in milk (g/kg)	Molecular weight (kDa)	Isoelectric point (pI)	number of residues
β-lactoglobulin (βLG)	3.2	18.3	5.1	162
α-lactalbumin (α-lac)	1.2	14.2	4.3	123
Bovine serum albumin (BSA)	0.4	66.3	5.0	607
Lactoferrin (LF)	0.1	83	8.7	689

A- <u>β-lactoglobulin:</u>

βLG (shown in Figure 2-9) is a weakly acidic protein belonging to the lipocalin family which is the major whey protein i.e. that amounts to 50% of the total whey protein mass of ruminants such as cow or sheep. It is also found in the milk of monogastric, i.e. pigs, horse, dogs, cats, but is absent from human milk.

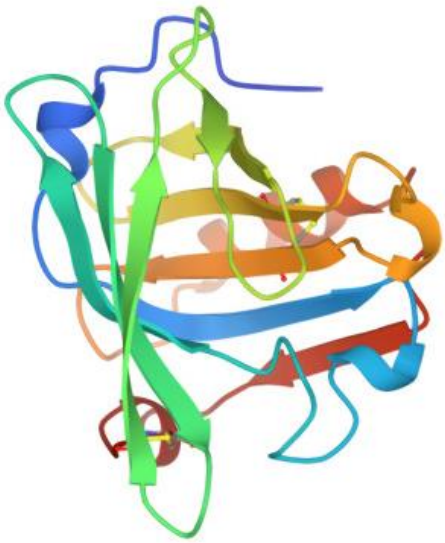

Figure 2-9: β-lactoglobulin structure from protein database (1BEB)

The isolation of βLG from milk was described in various protocols and involves four stages: removal of fat, removal of the caseins, fractionation of whey proteins and finally, purification of βLG. This proteins

known for its ability to bind a variety of small ligands or hydrophobic molecules such as fatty acids or retinol. B-lactoglobulin as most proteins is very sensitive to pH and undergoes several conformational changes between pH 2 and pH 9. In fact, βLG is present as monomers at pH < 3.5 and at pH > 7.5. Octamers form at pH 3.5 – 5.5 and dimers at pH 5.5 – 7.5 as shown in the Figure 2-10.

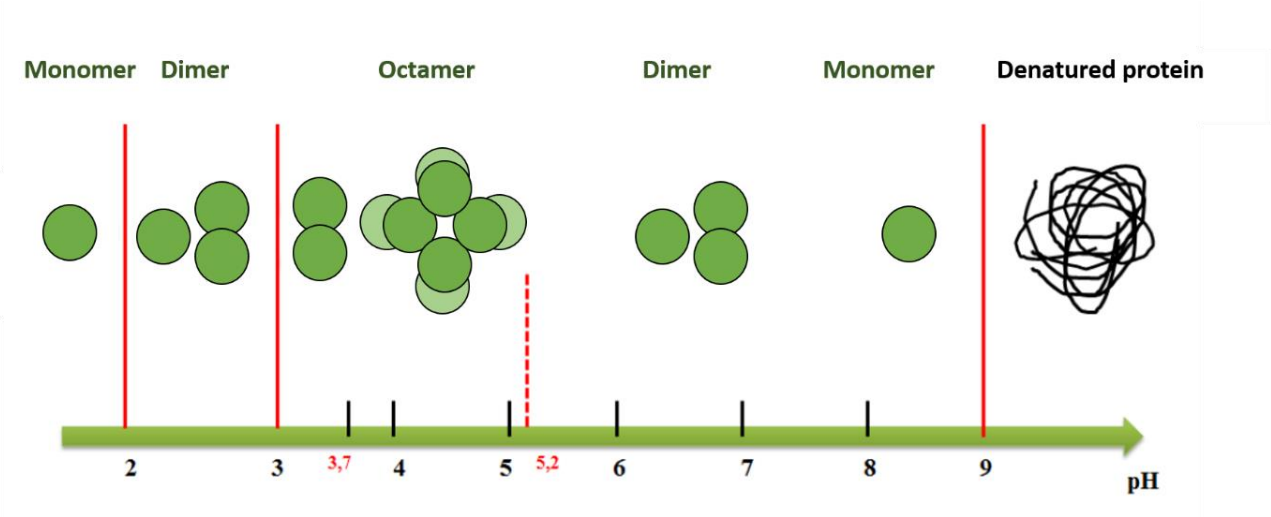

Figure 2-10: pH effect on the oligomerization state of β-lactoglobulin

The most commonly used variant of βLG are A and B, but more than ten genetic variants have been identified. The main difference between βLG are A and B is summarized in Table 2-4.

Table 2-4: Difference between β-lactoglobulin A and β-lactoglobulin B.

	Amino Acid 64	**Amino Acid 118**	**Isoelectric point**
β-lactoglobulin A	Aspartic	Valine	5.1
β-lactoglobulin B	Glycine	Alanine	5.2

B- Lactoferrin:

Lactoferrin (LF) was first identified in bovine milk in 1939. It is a strongly basic, red-colored protein and is recognized as an iron-binding protein with biochemical characteristics similar to those of transferrin. Like all milk proteins, the concentration of LF in milk depends on the species. Human milk is rich in LF. However, LF concentration is very low in cow milk and completely absent in the rat milk. LF has 689 amino acids for a total molecular weight of 83 kDa and is organized into two homologous lobes: N-terminal lobe and C-terminal lobe (Figure 2-11). Each lobe contains one iron-binding site and one glycan. The conformation of the two lobs as well as their affinity for iron is slightly different.

Figure 2-11: Lactoferrin structure from protein database (1BLF)

Three different forms of LF exist according to the level of iron saturation: apo-LF with saturation < 5 %, native LF with 15-20 % of saturation and holo-LF fully saturated in iron.

Thanks to its iron-binding property, lactoferrin was proposed to be involved in the regulation of iron uptake by the mucosa. In addition to that, during an inflammatory response, lactoferrin is released into blood by activated neutrophils. This increased level of circulating lactoferrin is responsible for the regulation of the anti-inflammatory response. Moreover, LF is a good anti-oxidant and anti-carcinogenic molecule (Corredig, 2009; Van Snick & Masson, 1976).

LF has a high isoelectric point i.e. pH 8.7 which allows it to associate with other molecules due to charge differences. Its electric charges are unevenly distributed on its surface and large positive patches are located on the N lobe and in the inter-lobe region. Ionic strength had a great influence on the LF. In fact, it is monomeric at low ionic strengths and tends to form dimers and aggregates at higher ionic strength.

2.2.3.2 Optimum conditions for β-lactoglobulin/lactoferrin complex coacervation

The two whey proteins, LF and βLG are able to form coacervates. Three research groups within the scientific community have been focusing on these two protein complex coacervation: Dubin et al. (Desfougères et al., 2010; Flanagan et al., 2015; Kizilay et al., 2014; Yan et al., 2013), Anema and De Kruif (Anema & de Kruif, 2014) and Bouhallab et al. (Chapeau et al., 2016; Peixoto et al., 2016; G. M. Tavares et al., 2015). These groups have studied the highly limited conditions of pH, IS, total protein concentration, and βLG: LF stoichiometry under which the LF/βLG complex coacervation can occur. During these studies, a multiscale characterization of the LF/βLG formed coacervates were conducted using biophysical tools such as SAXS measurements and solid-state NMR.

A- Effect of pH

Yan et al. (2013) studied the effect of pH on LF/βLG complex coacervation using turbidity as an indicator for the complexation and dynamic light scattering to investigate the size of the formed coacervates. These authors noticed an increase in the turbidity of βLG in a pH range of [3.5, 5.7] due to the self-aggregation of βLG. On a much smaller scale, LF also was observed to aggregate at pH 8−10. Interestingly, for pH 5.7−6.2, the mixing of the two proteins gave a higher turbidity than the sum of both individual protein turbidity which means that the interaction of βLG – LF causes a greater association or aggregation (Figure 2-12). Indeed Yan et al. (2013) reported that protein self-aggregation competes with complexation. However, pure coacervates yields was detected at 5.5 < pH < 6.5. at this pH range hydrodynamic radius (Rh) of LF/βLG complexes was around 7−12 µm (Yan et al., 2013).

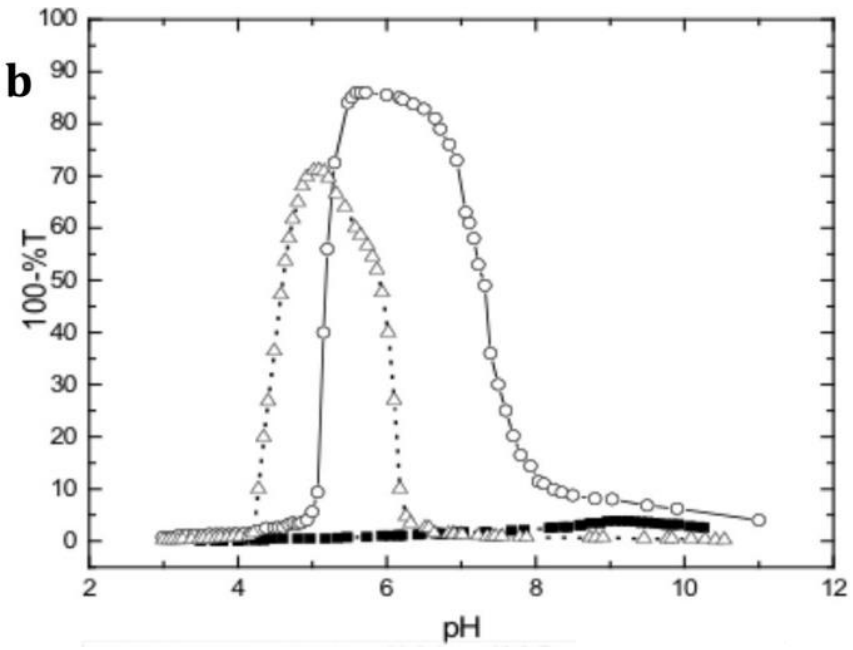

Figure 2-12: Turbidimetric titration of 20 g/L βLG −LF mixture (○), 10 g/L βLG (△), and 10 g/L LF (■) in pure water with 0.1 N NaOH (adapted from Yan et al., 2013).

For their part, Anema & de Kruif (2014), noticed that LF/βLG coacervates were formed in pH region of 5.0 - 7.3 with a maximum of turbidity at pH = 6.3 (Anema & de Kruif, 2014). Tavares et al (2015) conducted a comparative study on the coacervation of LF with the two βLG isoforms. They noticed that microspheres were formed throughout coacervation under a narrow pH range of 5.4 to 6.0. Moreover, βLG and LF mixture showed a maximum turbidity value at pH 5.50 and pH 5.75 respectively for βLG A and βLG B. The size of coacervates reported for those two turbidity maximum at pH 5.50 and 5.75 varied from 2.5 to 7.5 µm (Tavares et al., 2015). This difference in the optimum value of pH between these three studies can be explained by the characteristics of the whey proteins such as iron saturation for LF or denaturation or aggregation of βLG, but also by the proportions of isoforms of βLG A and βLG B.

B- <u>Effect of protein concentrations and molar ratios:</u>

Proteins concentration as well as the ratio between the two proteins are important factors to set in order for the coacervation to occur. From the previous studies, the total protein concentration was set in the

range from 10 to 50 g/L and the ratio between the two proteins varies according to the studies. Yan et al. (2013) demonstrated that the protein ratio r = LF/βLG (w/w) for an maximum coacervation between LF and βLG is = 1 ± 0.3, corresponding to a molar ratio of 0.24, i.e. to LF(βLG $_2$)$_2$. As seen in the Figure 2-13, the maximum yield of coacervation is indeed obtained at r = 1. Yan et al. (2013) confirmed those results with turbidity measurements. A maximum of turbidity was reported at r = 1. With increasing r values, a transition from LF(βLG$_2$)$_2$ to LF(βLG$_2$) or LF(βLG)$_2$ happens that hinders coacervation. The increase of r value till 2 leads to a suppression of the coacervation whereas an excess of βLG (r < 0.5) leads to the formation of fewer and smaller coacervates (Yan et al., 2013).

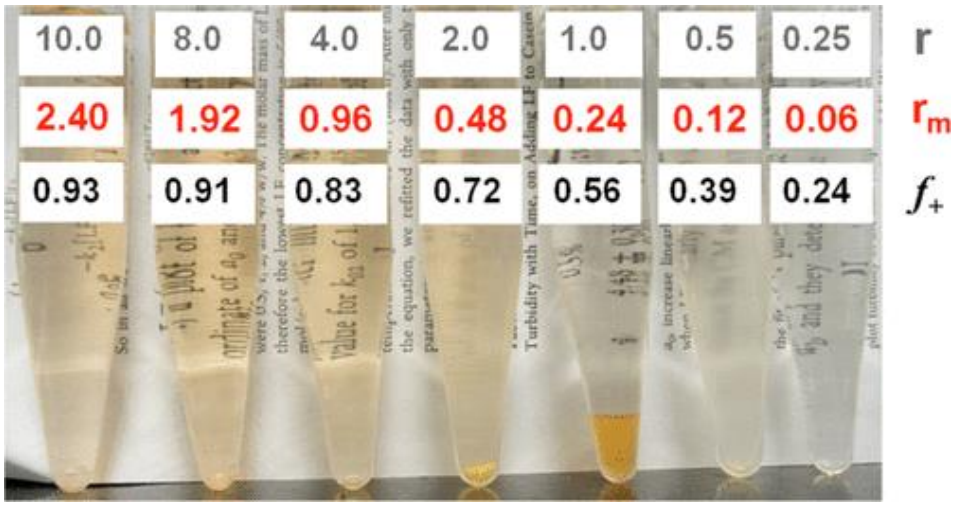

Figure 2-13: Effect of LF to BLG ratio, r, on βLG-LF mixture (pH 6.0, 0 mM NaCl, Cp = 20 g/L). The molar ratio and ratio of positive charge to total charge of LF/ Blg (f+) are indicated on the tubes (Yan et al., 2013).

Tavares et al. (2015) found that for both pH 5.5 and 5.75, the best molar ratio between LF and the two isoforms of βLG A and B LF:βLG is 1:10 as shown in Figure 2-14.

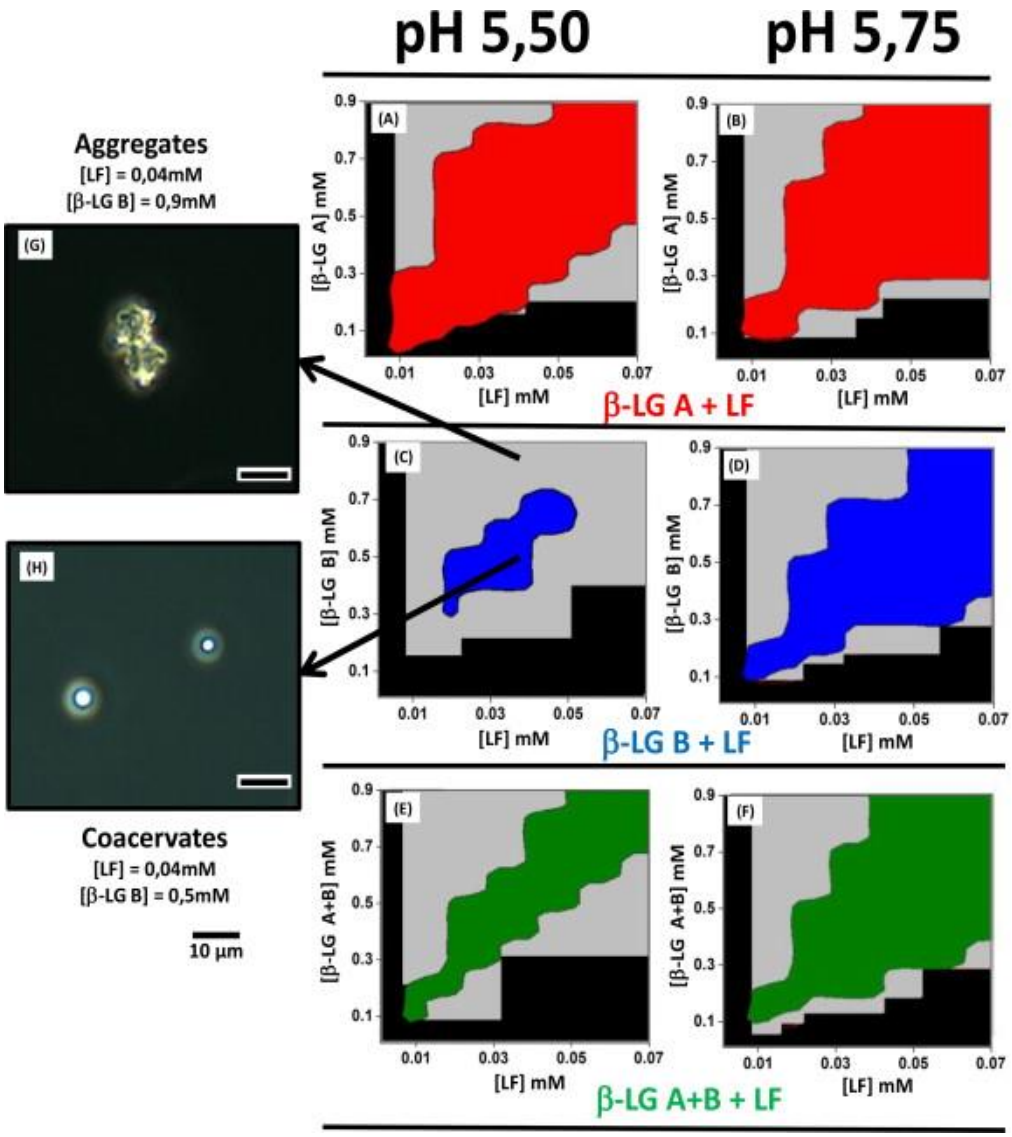

Figure 2-14: Phase boundaries of co-assembly of LF with βLG isoforms at pH 5.50 and pH 5.75. (A,B): LF/βLG A; (C,D): LF/βLG B; (E,F) LF/βLG A+B. Black zones: domains without detectable supramolecular structures; Grey zones: aggregation domains. Red, blue and green zones: coacervation domains. Optical microscopy of aggregates (G) formed by mixing for example 40 mM LF and 900 mM βLG B at pH 5.50 versus coacervates (H) formed by mixing for example LF 40 mM and βLG B 500 mM at pH 5.50 (Tavares et al., 2015)

Tavares et al. (2015) observed a selective coacervation in the mixture of LF and two isomeric forms of βLG, A and B. By varying the protein ratios, the coacervation domain between LF and βLG A was

found to be very larger than that found for LF and βLG B even though βLG A and βLG B only differ by the substitution of two amino acids as shown in Table 2-4 (Tavares et al., 2015).

C- Effect of ionic strength

Despite being a very important factor for the coacervation, the ionic strength was not sufficiently studied for the LF/βLG case. However, all the studies agreed that LF/βLG coacervation could only occur under a low salt concentration. Yan et al. (2013) found that for ionic strengths higher than 25 mM the liquid-liquid phase separation was suppressed. As for Anema and De Kruif (2014), the ionic strength was set for a value lower than 100 mM.

2.2.3.3 The mechanism of coacervates formation

The mechanism of LF/βLG coacervates formation is still not very well established. However, some attempts to describe this mechanism was conducted by Anema et al. (2014) and Tavares et al. (2015) and are illustrated in the Figure 2-15.

After mixing, the formation of the coacervates starts with the interaction of a βLG or a dimer of βLG with a LF to form the primary units of the coacervates LF$(\beta LG)_2$ or LF(βLG_2). Docking simulations showed that each LF molecule is able to bind two or more βLG_2. The first βLG_2 is most likely to bind to LF surface with higher affinity site, called S site, whereas, the second βLG_2 binds on lower affinity sites, called M sites (Peixoto et al., 2016).

The excess of LF would prevent the coacervation, while the addition of the βLG dimer leads to the formation of the building blocks LF$(\beta LG_2)_2$. These complexes would reassemble to form the final LF/βLG coacervates.

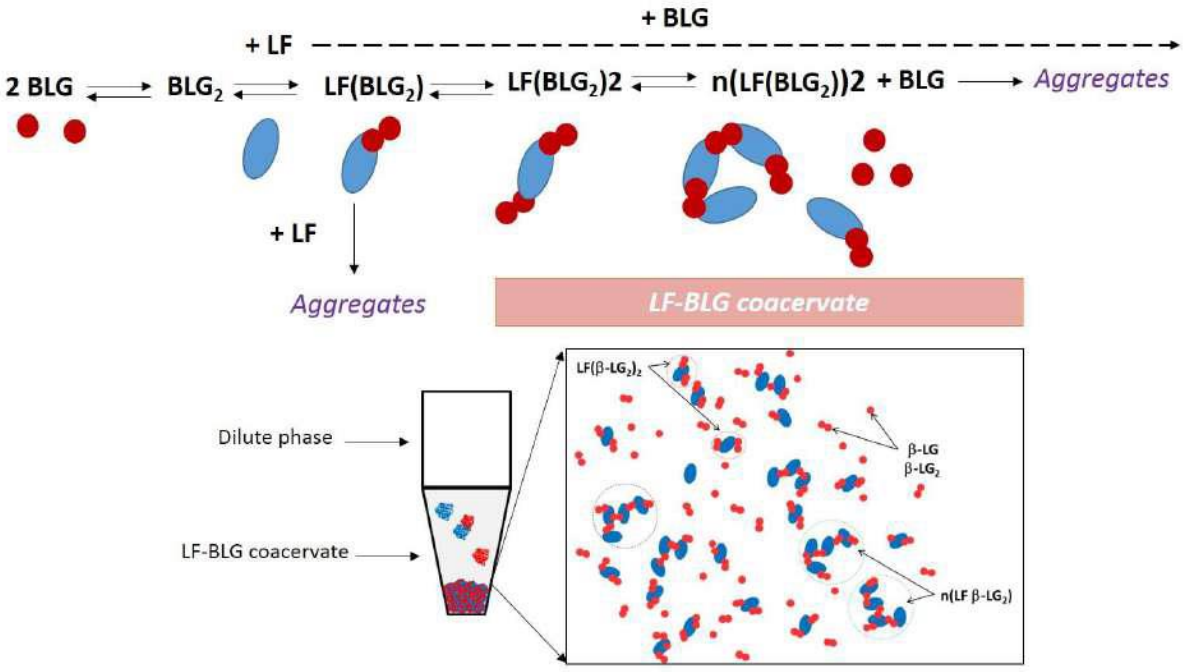

Figure 2-15: Proposed mechanism for the formation of LF- βLG coacervates (Chapeau, 2017).

2.2.3.4 Coacervates characterization

Different experimental methods could help characterizing the formed coacervates. Rheology measurements, confocal microscopy and small angle neutron scattering were conducted to better understand the structure of LF/βLG coacervates. The coacervates showed a viscoelastic liquid-like dominant behavior and that the interconnected structures responsible for the viscoelastic properties have relaxation times shorter than 0.01 s (Kizilay et al., 2014). Flanagan et al (2015) investigated the size of the coacervates at an optimum molar ratio by using dynamic light scattering and found a value of Rh at ≈ 11.5 µm which corresponds to the formation of the largest species (Flanagan et al., 2015). Chapeau et al. (2016) demonstrated that the size of the coacervates ranged from 2 to 20 µm diameter, with a mean diameter around 8 µm (Chapeau et al., 2016).

2.2.4 Thesis objective and strategy:

LF/βLG couple constitutes an example of heteroprotein complex coacervation system. Previous studies on this system focused on the effect of pH, and the protein stoichiometry and concentration and a potential application of the LF/βLG coacervates as encapsulating agents. To extend the work already carried out and open up new application opportunities, this work aimed at determine sensitivity of LF/βLG coacervation process to change in ionic strength and its effect in addition to temperature effect on the structural changes in the network of formed coacervates.

To carry on this study, the optimum conditions of coacervation was set based on previous results from our group i.e. pH 5.5, βLG/LF stoichiometry = 10/1, total protein concentration of 0.55 mM (Tavares et al., 2015).

The sensitivity to ionic strength was studied at two different levels: first, molecular level using isothermal titration calorimetry and Monte Carlo simulation; then at macroscopic level, by following the coacervation process after either direct mixing of the proteins at low salt concentrations or during desalting after mixing the two proteins at very high salt concentrations.

In the second part of this thesis, we conducted an in-depth study on how small changes of ionic strength and temperature modulate the rheological properties of LF/βLG coacervates network.

Figure 2-16 summarizes the thesis steps and adopted strategy.

Ionic strength sensitivity of complex coacervation between β-lactoglobulin & lactoferrin

from protein-protein interactions to the characterization of the coacervates

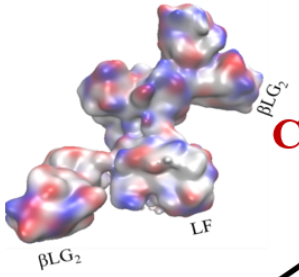

Chapter 1

Effect of mixing the proteins with **increasing** salt concentration From 0 – 100 mM

- Direct Mixing
- Isothermal titration calorimetry (ITC)
- Monte-Carlo simulation

Effect of mixing the proteins with **deacreasing** salt concentration From 400 – 0 mM

Desalting via dialysis

Chapter 2

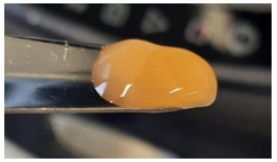

coacervation at optimum conditions

Effect of low ionic strength

Effect of temperature

Rheology

Figure 2-16: the thesis strategy: the chapters and the used methods

3 Results

3.1 Chapter 1: Insights into ionic strength influence on the interaction between Lactoferrin and β-lactoglobulin

3.1.1 Part 1: Ionic strength dependence of the complex coacervation between Lactoferrin and β-lactoglobulin

Preamble

Previous studies from different reasearch groups had put huge efforts in identifying the optimum conditions for βLG and LF coacervation. Optimum conditions have thus been determined for the highest coacervates yield . In addition to that, the vast majorties of these works studied the effect of pH, protein concentration and stoechiometry on coacervation. However, Since coacervation is driven mainly by electrostatic interactions, changes in the ions concentration of the medium can drastically affect its process. For this reason, the present work aimed to complete the previous ones by investigating the influence of the ionic strength on the LF/βLG complex coacervation.

Main objectives:

- Identify the critical salt concentration above which the coacervation is abolished.
- Study the mixing the proteins at high salt concentration using desalting techniques.
- Study the effect of salt concentration on the interactions between βLG and LF at a molecular level.

In order to investigate the effect of the presence of salt on the complex coacervation between βLG and LF, we monitored the turbidity, the coacervates yield and the shape of the formed coacervates during direct mixing and desalting protocols. Moreover, an in-depth investigation of the interactions that possibly took place between the proteins during the coacervation at different ionic strength were conducted using Isothermal Titration Calorimetry (ITC).

Main results:

- LF/βLG coacervation process is highly sensitivity to ionic strength.
- Above 20 mM of added NaCl no LLPS was detected.
- The presence of low salt tuned the electrostatic interactions between the two proteins.
- Starting with high ionic strength does not modify the observed sensitivity of the process to salt.

*Soussi Hachfi, R., Hamon, P., Rousseau, F., Famelart, M-H., & Bouhallab, S. (2023). Ionic strength dependence of the complex coacervation between lactoferrin & β-lactoglobulin. Submitted in Foods

Abstract

Heteroprotein complex Coacervation is an assembly formed by oppositely charged proteins in aqueous solution that leads to liquid-liquid phase separation. In a previous work, we reported on the ability of Lactoferrin and β-lactoglobulin to form complex coacervates at pH 5.5 under optimal protein stoichiometry. The goal of the current study is to determine the influence of ionic strength on the complex coacervation between these two proteins using direct mixing and desalting protocols. We showed that the initial interaction between Lactoferrin and β-lactoglobulin and subsequent coacervation process were highly sensitive to the ionic strength. No microscopic phase separation was observed beyond a salt concentration of 20 mM. The coacervates yield decreased drastically with increasing added NaCl from 0 to 60 mM. The charge-screening effect induced by increasing the ionic strength is attributed to a decrease of interaction between the two oppositely charged proteins throughout a decrease in Debye length. Interestingly, as shown by isothermal titration calorimetry, small concentration of NaCl around 2.5 mM promoted the binding energy between the two proteins. These results shed new light on the electrostatically driven mechanism governing the complex coacervation in heteroprotein systems.

Keywords: Complex coacervation; ionic strength; proteins; desalting

3.1.1.1 Introduction

Oppositely charged polymers interacting mainly through electrostatic interactions can undergo a spontaneous liquid−liquid phase separation (LLPS) into polymer-rich dense phase called coacervates and a less concentrated phase called the dilute phase. Complex coacervation, known as liquid−liquid phase separation phenomenon has been, and still is, a subject of intense experimental and theoretical interest since the pioneer research of Bungenberg De Jong and Kruyt one century ago(Bungenberg De Jong & Kruyt, 1929). Although several theoretical models have been provided to describe complex coacervation none of them were able to perfectly explain it (Overbeek & Voorn, 1957; Sato & Nakajima, 1974; Tainaka, 1967; Veis, 2011; Veis et al., 1967). Several studies, based on those models, described complex coacervation phenomenon as a four-step process; the first step is the spontaneous formation of both symmetrical and random heterocomplexes by electrostatic attraction (building blocks). The building blocks, also called primary units, come together to form soluble complexes. The third step involves the rearrangement of soluble complexes into spherical micrometric droplets, characteristic of complex coacervation (X. Wang et al., 2021). Finally, the droplets coalescence forming thus the dense phase of the coacervates (Jho et al., 2017). Interest in complex coacervation is remarkably increasing, as it is an ambitious undertaking that will open enormous opportunities for numerous applications in the food, cosmetics, pharmaceutical and biological fields (Costalat, Alcouffe, et al., 2014; Xiao et al., 2014). Moreover, complex coacervation can occur across a wide-variety of charged macromolecules such as proteins/polysaccharides, proteins/synthetic polyelectrolytes, polyelectrolytes/polyelectrolytes and proteins/proteins mixtures. However, heteroprotein complex coacervation (HPCC) i.e. involving two or more proteins is comparatively understudied (Adal et al., 2017; Croguennec et al., 2017; Desfougères et al., 2010; Zheng et al., 2021). Part of the published works on heteroprotein complex coacervation focused on the assembly between lactoferrin (LF) as basic protein and β-lactoglobulin (βLG), as acidic protein. In these studies, multiscale characterization of the LF/βLG formed coacervates were conducted using biophysical tools such as SAXS measurements (Kizilay et al., 2014) or solid state NMR (Peixoto et al., 2016). The potential applications of LF/βLG coacervates in food and their effectiveness for

encapsulation of bioactives was also reported (Chapeau et al., 2016). For HPCC, the most subtle is to set the physico-chemical parameters (pH, stoichiometry, concentration, etc.) for optimal coacervation. Yan et al. (Yan et al., 2013) reported that LF/βLG coacervation is favored under narrow range of pH 5.7 to 6.2, with lower ionic strength value and a total protein concentration between 10 and 40 g/L. For their part, Anema & de Kruif (Anema & de Kruif, 2014), noticed that LF/βLG coacervates were formed in pH region of 5.0-7.3 and ionic strength lower than 100 mM. In our previous work, we had narrowed the pH range more showing that optimal and maximum LF/βLG coacervation occurred at pH 5.5 (G. M. Tavares et al., 2015). Furthermore, we compared the coacervates yield when mixing LF with the two isoforms A and B of βLG. Interestingly, we found that a higher coacervates yield was recovered with the most acidic isoform, i.e. βLG isoform A (one more aspartic acid residue). These results underline the high sensitivity of LF/βLG coacervation to a small variation in the net protein charge (Croguennec et al., 2017; G. M. Tavares et al., 2015). Behind the pH, the ionic strength is another important parameter that controls the net protein change and consequently the electrostatically driven heteroprotein complex coacervation. Therefore, the aim of this present work is to gain more insight on the effect of the presence of salt on the interaction and complex coacervation between LF and βLG.

3.1.1.2 Materials and methods

A. Materials

LF with a purity of 90 g/100 g and iron saturation of 10–20 mol iron/mol protein according to technical specification was purchased from Fonterra Cooperative Group (Auckland, New Zealand) and used without further purification. Commercial bovine βLG containing both A and B variants was further purified before use. As βLG is prompt to self-aggregation during long storage, the non-native and aggregated species were regularly removed by dispersing in ultrapure water (30 g/L), adjusting to pH 5.2 with 1 M HCl and then storing at 30 °C for 10 min to precipitate aggregated and non-native forms. The dispersion was then centrifuged at 36 000 g for 10 min at 25 °C (Avanti, J-26S XP BioSafe Three-Phase Non-IVD Centrifuge, Beckman Coulter, Villepinte, France). The supernatant containing native

βLG was adjusted to pH 7.0 with 1 M NaOH, freeze-dried and stored at -20 °C until later. The protein purity in obtained powder was around 95% as assessed by HPLC analysis. Sodium chloride (NaCl) was purchased from VWR Chemicals (Rosny-sous-Bois, France). (2-(N-morpholino) ethanesulfonic acid hydrate (MES) was purchased from Sigma-Aldrich (St. Louis, MO, USA) and all other chemicals were of analytical grade.

B. Methods

Preparation of samples and direct mixing

MES buffer (10 mM) was used as solvent in all experiments and was prepared by solubilizing MES powder in ultra-pure water. Solid NaCl was added to reach targeted concentration and then adjusted to pH 5.5 using 1 mM NaOH solution.

LF and βLG Protein powders were solubilized in the desired concentration of NaCl (0-400 mM) and the pH was readjusted if needed to 5.5 value using 1 M NaOH or HCl. This pH value was found to be optimal for complex coacervation between the two whey proteins at the current stoichiometry and total protein concentration (Chapeau et al., 2016). The exact protein concentrations were determined in the two stock solutions by absorbance at 280 nm (SAFAS UV MC2, Safas, Monaco) using 0.96 L/g.cm and 1.47 L/g.cm as extinction coefficients for βLG and LF, respectively.

For direct mixing experiments, conducted in duplicate, solutions of βLG and LF prepared in MES buffer 10 mM at various NaCl concentrations were mixed at room temperature to reach a final concentration of 0.5 mM and 0.05 mM for βLG and LF, respectively, which means a LF/βLG molar ratio of 1/10.

Complex coacervates by desalting

The formation of complex coacervates between the two proteins prepared at various salt concentration (0, 100, 200 and 400 mM NaCl) was monitored during continuous desalting against 10 mM MES buffer, pH 5.5 using dialysis membranes. 10 mL of each mixtures were put into a 6-8 KDa molecular weight cut-off (MWCO) dialysis membrane (diameter = 14.6 mm) (Spectra/Por, Repligen Corporation,

California, USA). The dialysis membrane was then submerged into a dialysis bath containing 1 L of MES buffer under constant stirring at room temperature. Fourteen aliquots were taken from the dialysis bag at different times during the 24 h of dialysis for analyses. Dialysis experiments of the 10 mM MES buffer with studied NaCl concentrations and without proteins were also performed as dialysis control experiments.

During dialysis experiments, conductivity of the dialysis bath was measured using an electrical conductivity meter (HI98192, Hana instrument, Strasbourg, France). The probe of the conductivity meter (HI763133, Hana instrument, Strasbourg, France) was submerged into the bath throughout the dialysis time to make sure that the ion exchange between the dialysis bag and the bath is taking place. Different samples were collected from inside the bag and the salt concentration was measured using an electrical conductivity meter (HI98192, Hana instrument, Strasbourg, France). The dialysis experiments were conducted at least in duplicate.

Turbidity measurements

The turbidity caused by the spontaneous formation of coacervates as spherical droplets in LF/βLG direct mixtures and during the dialysis experiments was measured at 600 nm using a microplate spectrophotometer (Multiskan™ GO, Fisher Scientific, Strasbourg, France). In fact, the spectrophotometer provides absorbance measurements that could be converted to turbidity using the following equation 3:

$$Turbidity\ (cm^{-1}) = \frac{2.303.A}{L} \qquad 3\text{-}1$$

Where A is absorbance at 600 nm and L (cm) is the light path length corresponding to the height of the liquid column into the microplate well.

Coacervates yield

Protein partition was determined by protein quantification after phase separation. Dilute and coacervates phases were separated by centrifugation (Heraeus Biofuge Primo, Thermo Scientific, Waltham, MA, USA) at 28000 g for 30 min. Protein quantification was performed by liquid chromatography (UltiMate 3000 HPLC, Thermo Fisher Scientific, Waltham, USA) using a PLRP-S column (300Å, 2.1 x 150 mm, 8 µm) with a flow rate of 0.2 mL/min (Agilent Technologies, Santa Clara, USA). Milli-Q water containing 1.06 ‰ (v/v) of trifluoroacetic acid and an 80/20 acetonitrile/milli-Q water (v/v) mixture containing 1.0 ‰ (v/v) of trifluoroacetic acid were used for elution. The absorbance at 280 nm was measured during the elution using a Waters 2487 detector.

The coacervates yield was calculated using the following equation 4:

$$The\ coacervates\ yield = \frac{final\ protein's\ mass\ in\ the\ coacervates}{Total\ proteine's\ mass}\ X\ 100 \qquad 3\text{-}2$$

Phase contrast Microscopy

Optical microscopy was used to check that coacervates rather than amorphous aggregates were formed during direct mixing and dialysis experiments. Observations were conducted at room temperature using an Olympus phase contrast microscope (BX51TF, Rungis, France) set at the magnifications 100X.

Isothermal titration calorimetry (ITC)

The ITC experiment was performed at two temperatures, 25 °C and 35 °C, using a VP-ITC micro-calorimeter (MicroCal VP-ITC, Malvern Panalytical, Malvern, UK) by successive injections of LF solution (0.25 mM) into a βLG solution (0.1 mM) loaded in sample cell (1.425 mL). Titration experiments were performed at different NaCl concentrations between 0 and 20 mM. All solutions, prepared in 10 mM MES buffer pH 5.5, were degassed under vacuum before titration experiments. The reference cell was filled with NaCl solutions in the respective concentration for each measurement and the sample cell was filled with βLG solution. The LF solution in the syringe was also set at the same

NaCl concentration. βLG was titrated with 25 successive injections of 10 µL of LF solution. The initial delay was set at 60 s and the stirring rate inside the sample cell was set at 300 rpm to ensure the homogeneity of the cell solution during titration. The interval between injections was 200 s to reach the thermodynamic equilibrium. For each ITC experiment, a reference titration was performed by titrating LF solutions directly into 10 mM MES buffer containing the studied NaCl concentration. A negligible signal was associated to this reference injection, which was subtracted from the corresponding experimental signal. The ITC data were fitted using graphical user interface of PyTC, an open-source python software (Duvvuri et al., 2018). All the ITC experiments were performed at least in duplicate.

3.1.1.3 Results and discussion

A. Interactions between βLG and LF

Direct mixing experiments

The effect of ionic strength on the interaction/complex coacervation was studied by preparing individual proteins in the required salt concentration before mixing. Figure 3-1 shows the turbidity and the protein yield in the coacervates at different ionic strengths from 0 mM to 100 mM. Turbidity and coacervates yield were maximal without added salt and decreased with increased ionic strengths to reach a value close to zero at 20 mM. At this concentration, no LLPS was detected.

These results are in agreement with those reported by Yan et al. (2013) for the same coacervates system at a close pH value, say pH 5.9. In their study, the yield in βLG and LF have been monitored as a function of NaCl concentrations (0−100 mM) using size exclusion chromatography. Both proteins showed a decrease in their yield with the increase of the ionic strength. A concentration of 20 mM of NaCl was also found to be a critical salt concentration for coacervation. Moreover, in the same paper, the authors noticed that at this salt concentration, and after centrifugation, a white precipitate of βLG aggregates was observed instead of LF/βLG coacervates (Yan et al., 2013)

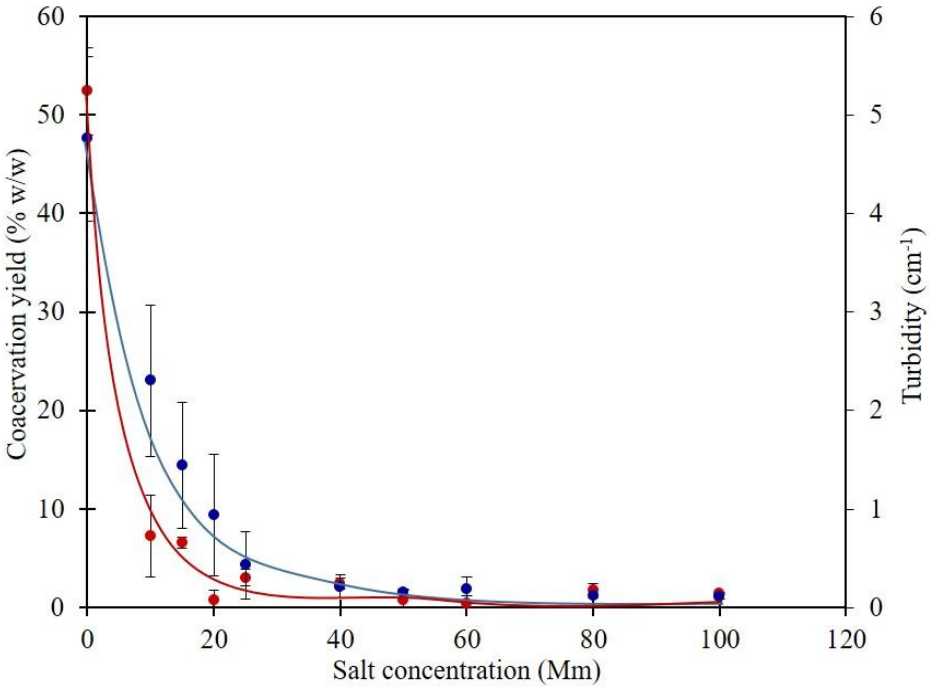

*Figure 3-1: Evolution of lactoferrin/β-lactoglobulin coacervates yield (**red**) and turbidity (**blue**) as a function of salt concentration after direct mixing in 10 mM MES buffer, pH 5.5. Total protein concentration of 0.55 mM*

. The effect of NaCl on the heteroprotein coacervates was also conducted on another protein system, β-casein/LF (Anema & (Kees) de Kruif, 2012). Similar ionic strength dependency of complex coacervation between these two proteins at pH value of 6.5. However, for those two proteins, complex coacervation was still observed even for ionic strength higher than 140 mM, a value 7 times higher than that found for LF/βLG. Hence, the concentration of NaCl tolerated by LF/βLG system is lower than that tolerated by β-casein/LF system. This difference might be explained by the random coil structure of β-casein as intrinsically disordered protein with high hydrophobicity compared to βLG. Consequently, the subtitle sensitivity to salt is completely protein structure dependent.

The coacervates yield decreased drastically with increasing ionic strength (Figure 3-1). The same tendency was reported for complex coacervation between whey protein and gum Arabic at pH 4 where the yield decreased from 0 to 100 mM NaCl (Weinbreck, Tromp, et al., 2004). However, visually and

from turbidity measurement, the coacervation was prevented beyond 60 mM of NaCl, a value higher than that found in the present work for LF/βLG system. In addition to that, the same authors reported that the kinetics of the phase separation slows down upon addition of salt because the coalescence of the coacervates droplets takes more time and water being slowly released from the coacervates phase.

Even though the decrease in the coacervates yield is a great proof of the effect of ionic strength on the formation of coacervates, turbidity measurement is also a powerful indicator of the coacervation. A slight increase of NaCl concentration induces a rapid decrease of turbidity (Figure 3-1). As checked by microscopic observations, addition of salt decreased both the size and the number of formed droplets. This behavior is not specific to HPCC since it was generally observed for several system such as polysaccharide/polysaccharide and polysaccharide/protein (Boral & Bohidar, 2010; Xiong et al., 2016). Such evolution of the turbidity as a function of the increase in the ionic strength highlights the predominant role of attractive electrostatic forces in the complex coacervation process. Hence, a stronger attractive interactions between biopolymers lead to a more turbid solution (Mjahed et al., 2010). The major difference lies in the salt sensitivity threshold, which is strongly dependent on the structures of the mixed macromolecules.

This huge dependency of LF/βLG complex coacervation on ionic strength obey to the mechanism explained a long time ago by Bungenberg de Jong: the presence of microions screens the charges of the polymers, which weakened attractive forces between them and disrupted the intermolecular electrostatic interactions (Bungenberg De Jong & Kruyt, 1929). As complex coacervation is an electrostatically driven process, the weakening of the electrostatic interaction hampers the complex formation and hinders the occurrence of LLPS. As a matter of fact, the theory of Overbeek and Voorn elucidates that before reaching a critical salt concentration, the polymer mixture was able to get separated into a polymer-rich and a polymers-poor phase (the LLPS) (Overbeek & Voorn, 1957). Overall, our results show the high sensitivity of LF/βLG complex coacervation to salt with a critical NaCl concentration of 20 mM above which the coacervation can no longer occur.

LF/βLG interaction energy

ITC experiments were conducted to provide a detailed thermodynamic description on how low ionic strength affects the interaction and association between βLG and LF. The heat flow versus time (raw data) profiles associated with the titrations of LF into βLG at different NaCl concentration and at 25°C are shown in the top panels of Figure 3-2. The actual heat associated with the interactions (Figure. 3-2 bottom panels) were obtained by integrating the peaks of the top panels and subsequently subtracting the heat produced from the titration of LF into the buffer. Based on the resulting titration profiles, the heat flow was negative ($\Delta H<0$), meaning that the sum of interactions and other phenomena taking place is an exothermic process.

The presence of NaCl affects signal intensity but did not change the negative signature, suggesting that the nature of non-Coulombic interactions (such as hydrophobic interactions and hydrogen bonding) was not altered by the salt-shielding effect. Exothermic processes during the interaction between two oppositely charged macromolecules have been reported for various other systems (Dong et al., 2015; Kayitmazer, 2017; Kutscher et al., 2015; Santos et al., 2018; G. M. Tavares et al., 2015; Zheng, Gao, Ge, Wu, et al., 2022). The exothermic nature of an enthalpically driven complexation process is generally attributed to the predominance of electrostatic interactions.

During the titration at very low added salt, a higher response in heat change was observed during the first injections, which gradually decreased over the titration and tended to saturation with increased protein molar ratio.

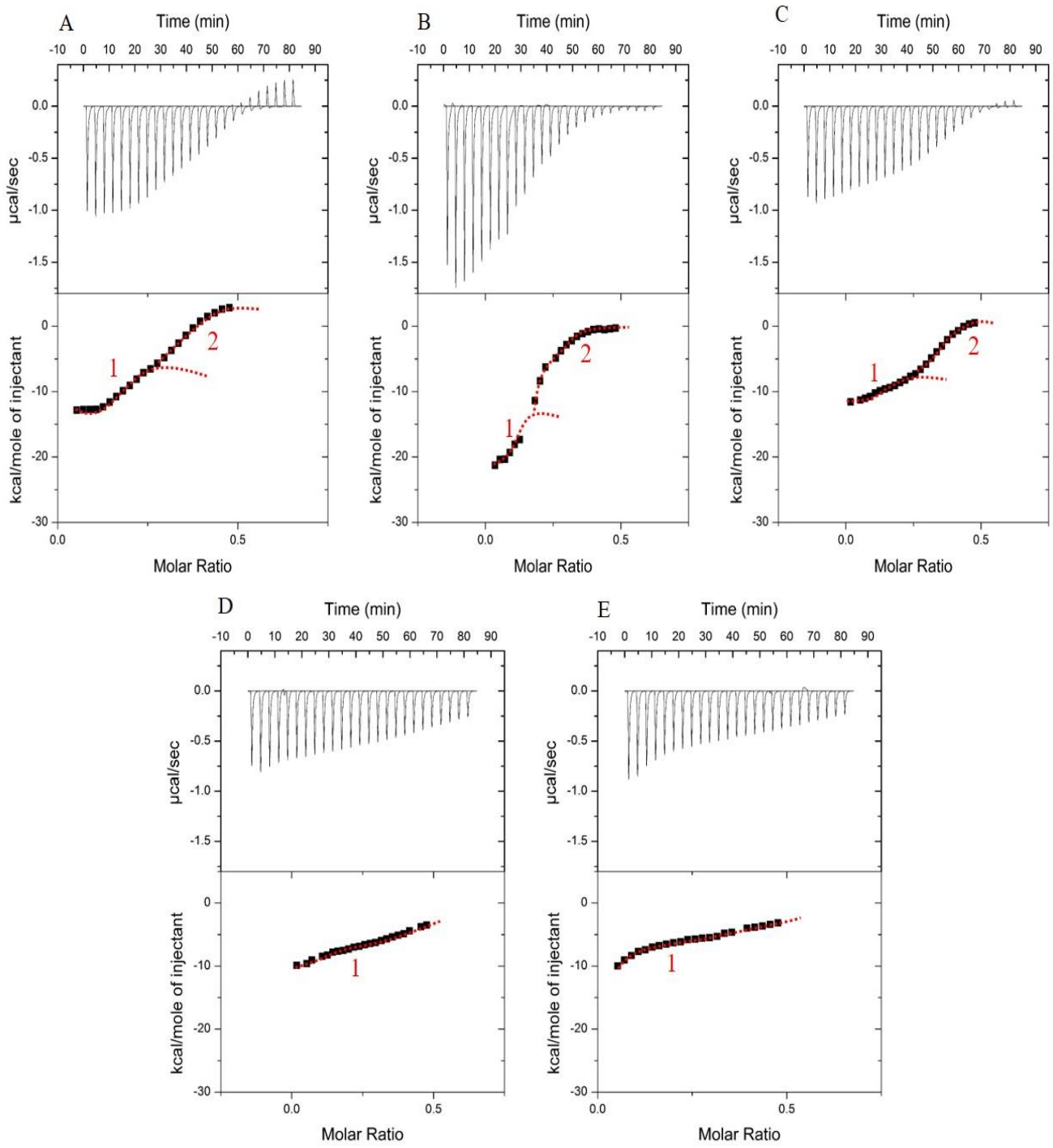

Figure 3-2: Heat flow thermogram as a function of the time (upper panel) obtained during the titration of βLG (0.1 mM) by LF (0.25 mM) at different salt concentrations in MES buffer 10 mM pH 5.5 and at 25 °C. Bottom panel: graphical representation of the integrate data of enthalpy versus the molar ratio of LF: βLG. A: without added salt; B: with 2.5 mM added NaCl; C: with 5 mM added NaCl; D: with 15 mM added NaCl; E: with 20 mM added NaCl. The red line is just to guide the eyes to distinguish when applicable the two inflection points.

The thermograms at very low salt concentration (Fig. 3-2 A-C) show two inflexion points that could describe two successive steps which means that two possible events came into play during the complexation of βLG with LF. The second inflexion point (above molar ratio of 0.2) disappeared with higher ionic strength values (Fig. 3-2 D and E). We assume that this second event is hampered by the reinforcement of the hydrophobic interactions since increasing the ionic strength can enhance those types of interactions. To confirm this hypothesis, the same ITC experiment was conducted without added salt, but at 35 °C as a temperature increment promotes hydrophobic interactions. As illustrated in Figure 3-3, when temperature increased from 25 to 35 °C without added salt, the second complex was lost. This might confirm the hypothesis that hydrophobic interactions might prevent the second mechanism that normally took place at a high molecular ratio. The formation of coacervates according to a two-step process as detected by ITC, has been described for other macromolecular systems (Kayitmazer, 2017; Priftis et al., 2012; Vitorazi et al., 2014). The first enthalpy-driven step is attributed to electrostatic interactions or ion pairing and lead to the formation of soluble complexes. The second step, rather entropy-driven, is attributed to the self-aggregation of these complexes into coacervates. This explanation fits well for LF/βLG system studies here, since the second inflexion point was suppressed with increasing ionic strength, concomitantly to the disappearance of LLPS as shown by turbidity measurements presented above. The second event can thus be assigned to the complex coacervation step between the two proteins. The explanation of what happens during the two steps is not easy since, for macromolecular interactions, each thermodynamic signal is a result of the contribution of several phenomena: interaction, protein conformational change, release of water, protons and other ions, complexation, reorganizations, aggregation, etc. The overall measured signal therefore comes from endothermic and exothermic reactions whose final absolute value is the result of the dominant energy.

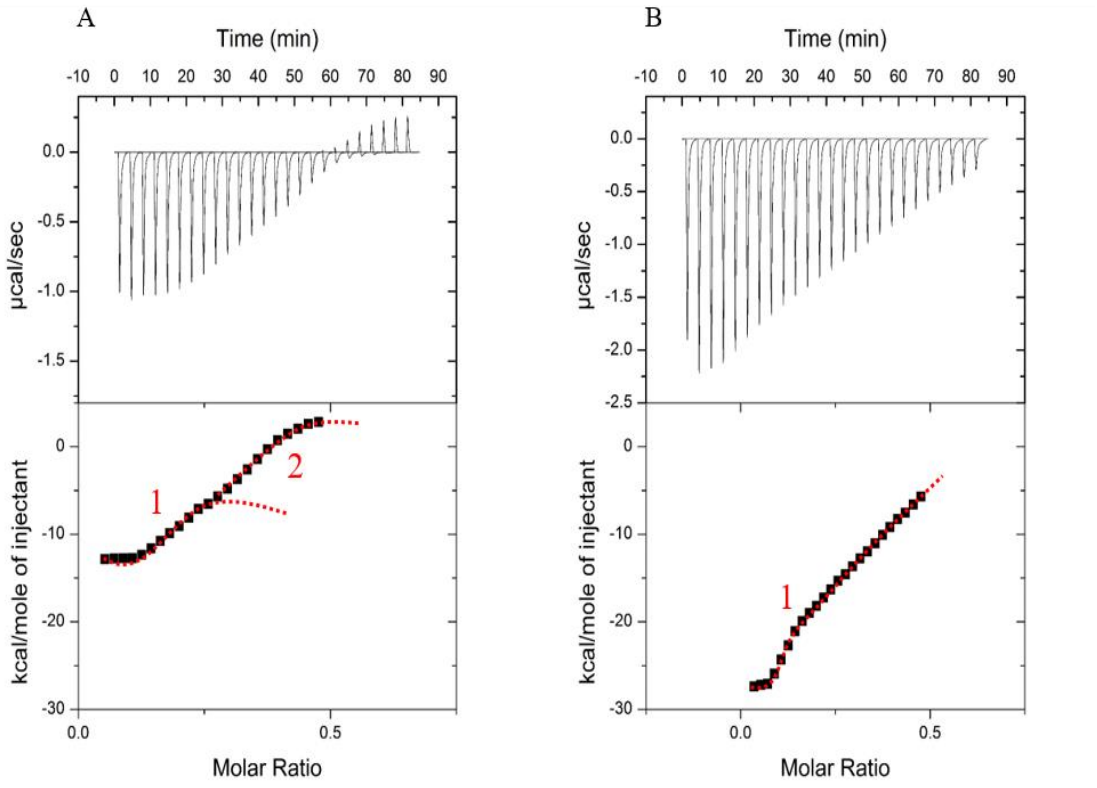

Figure 3-3: Heat flow thermogram as a function of the time (upper panel) obtained during the titration of βLG (0.1 mM) by LF (0.25 mM) in MES buffer 10 mM pH 5.5 at 25 °C (A) and 35 °C (B). Bottom panel: corresponding graphical representation of the integrated data of enthalpy versus the molar ratio of LF: βLG with no added salt. The red line is just to guide the eyes to distinguish when applicable the two inflection points.

To go further in the exploration of the thermodynamic changes occurring during titration, the binding isotherms were fitted using PyTC to determine the enthalpy and associated binding constant (Table 3-1). Without added salt, the interaction exhibited high enthalpy change and high binding constant K_a in the micro molar range. Interestingly, the addition of 2.5 mM NaCl further promotes the interaction with a +25% gain in enthalpy value and 2-fold increase of the affinity constant. Hence, a small amount of added salt favors the interactions between the two oppositely charged proteins. For higher added NaCl concentrations, the screening effect of salt on the interaction and association between the two proteins started to be observed as reflected in the ITC signals and in the significant decrease of K_a and ΔH values (Table 3-1).

Table 3-1: The binding constant (K_a) and the enthalpy (ΔH) as a function of the salt concentration measured [NaCl] by the GUI of PyTC

[NaCl] (mM)	K_a (M^{-1}) x 10^5	ΔH (Kcal/mol)
0	4.21 ± 0.06	-18.8 ± 0.04
2.5	9.72 ± 0.05	-24.7 ± 0.02
5	2.75 ± 0.05	-14,6 ± 0,04
15	0.847 ± 0.02	-12.09 ± 0.01
20	0.332 ± 0.015	-8.944 ± 0,03

Burgess (1990) reported that the general trend of gelatin/acacia coacervates yield increased with an increase in ionic strength up to a maximum and then decreased with a further increase in ionic strength (Burgess, 1990). This ‘‘salting-in like’’ trend was explained as a consequence of the effect of added salt on the extent of coiling and charge densities of the involved macromolecules. The results found here for LF and βLG are consistent with such reported data except that the concentration of NaCl tolerated by LF/βLG (HPCC system) is much less than that tolerated by gelatin/acacia coacervates. In general and compared to HPCC, higher concentration of salt is needed to screen the interaction/complexation in protein/polysaccharide systems and a relatively small amount can indeed promote the complexation as confirmed recently for pea protein/chitosan and ovalbumin/carboxymethylcellulose (Xiong et al., 2017; Q. Zhang et al., 2021).

The enthalpy change reflects the contribution of hydrogen bonds, electrostatic and van der Waals interactions and its decrease is hence expected with screening effect at increasing salt concentration (Santos et al., 2018). In fact, the presence of Na+ ions and Cl− ions reduced the strength of the electric field around charged groups in the proteins causing the saturation of their binding sites and lowering their interactions. The decrease of enthalpy and binding affinity with increasing NaCl (5 to 60 Mm) were also reported for β-conglycinin/lysozyme system (Zheng, Gao, Ge, Wu, et al., 2022).

The ITC experiments revealed that βLG and LF complexation was enthalpically favorable, and that small amount of salt ions promoted the interactions between the two proteins. Those results provided one more proof on the major role played by the ionic strength on the complex coacervation of βLG and LF. As a next step, we aimed to understand the kinetics of formation of coacervates via a desalting technique.

B. LF/βLG Complex coacervation via desalting

Unlike the direct mixing presented in the section **A**, desalting is an alternative protocol to better determine the ionic strength sensitivity of a complex coacervation process. Desalting was proposed as gentle method to build and better control assemblies of nanoparticles and complex biological assemblies (Fresnais et al., 2009). The desalting protocol involves first the mixing of the two macromolecules at a sufficiently high ionic strength in which the interactions are inhibited (charge screening). This mixed ‘‘inactive’’ solution is then dialyzed to decrease continuously the ionic strength around the mixed macromolecules (Berret, 2011; Costalat, David, et al., 2014).

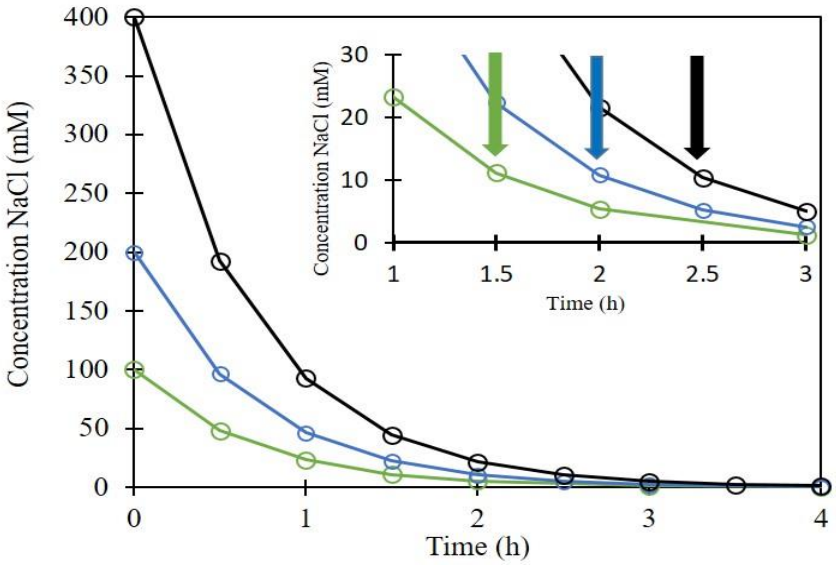

*Figure 3-4: Evolution of ionic strength inside the dialysis tube as monitored by conductivity during hours of dialysis of LF/βLG mixed at various initial ionic strength: 100 mM (**green**), 200 mM (**blue**) and 400 mM (**black**). Insert: zoom on the four first hours. Dialysis experiments were conducted against 10 mM MES buffer at pH 5.5.*

In the current study, we have monitored the behavior during continuous dialysis against MES buffer of mixtures of LF and βLG prepared at three high salt concentrations prior to mixing them. The decrease of salt concentration inside the dialysis tubes monitored by conductivity measurements followed an expected exponential behavior (Figure 3-4). The higher the initial concentration, the longer the dialysis time to reach the final equilibrium concentration. Whatever the initial salt concentration in the range 100 to 400 mM, almost total elimination of salt is achieved after 3.5 hours of dialysis in our experimental conditions. Costalat et al. (2014) reported the similar kinetics of chloride elimination where 100% of salt was removed after 5h and 6h for NaCl starting concentrations of 2 M and 6 M, respectively (Costalat, David, et al., 2014). Figure 3-5 shows the visual aspect and the corresponding microscopic images of the mixture in the dialysis tube at 100 mM NaCl during 24h of dialysis. At the beginning of the dialysis, the solution in the tube was almost transparent and no interaction was detected between the two proteins at this ionic strength.

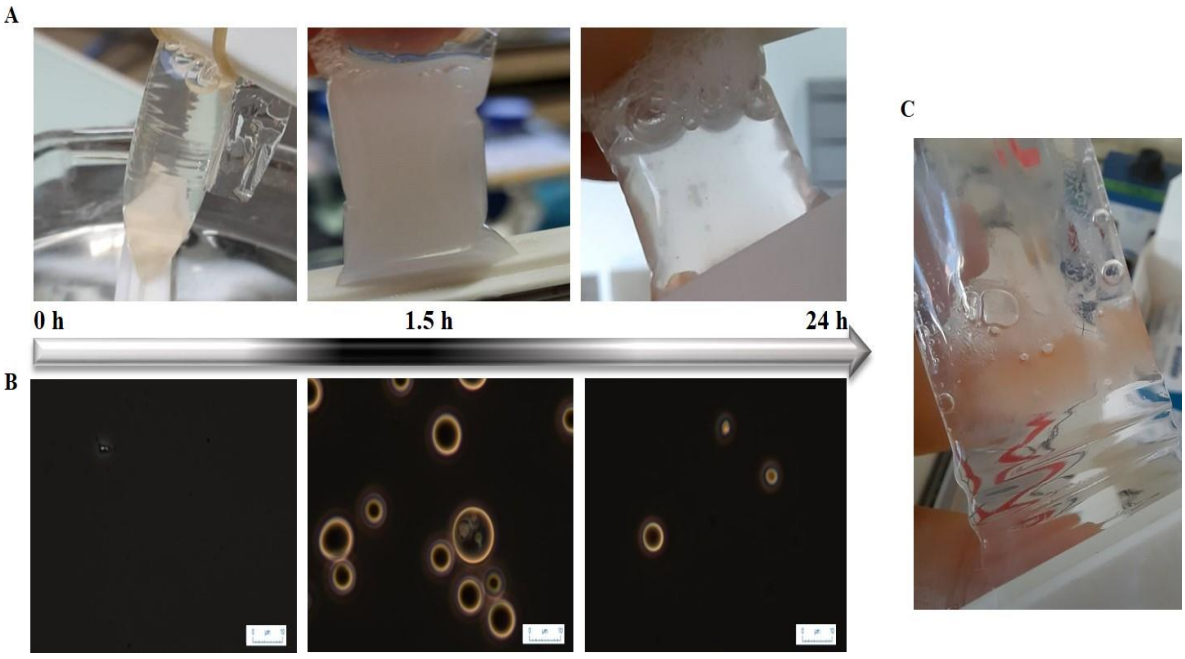

Figure 3-5: Appearance of LF/βLG coacervates during desalting protocol as a function of dialysis time for the initial salt concentration of 100 mM. (A) visual aspect inside the dialysis tube; (B) corresponding microscopic images showing the formation of coacervates droplets; (C) An image of the coacervates at the bottom of the dialysis tube at the end of the dialysis experiment. Dialysis was performed against 10 mM MES buffer at pH 5.5. Scale bar: 10 µm.

Once the dialysis begun, the solution in the dialysis tube started getting turbid until reaching a maximum. At the end of the 24h of dialysis, the solution was once again transparent as the LLPS took place (Figure 3-5 C). This move toward a transparent solution is explained by the progressive formation of highly turbid micro-droplets (microphase separation) that progressively coalesce leading to the observed LLPS. Turbidity measurements over time during dialysis confirmed the visual and microscopic observations as shown in Figure 3-6. First, it is worth mentioning that without added salt, the protein solution exhibited spontaneously a maximum value of turbidity as shown for direct mixing experiments (Figure 3-1). The turbidity decreased continuously in parallel with the occurrence of LLPS inside the dialysis tube. On the other hand, for LF/βLG mixture exposed to high ionic strengths, the turbidity during the dialysis first increased progressively until reaching a maximum and then decreased to almost zero. The areas under the curves are substantially identical for the three-dialysis experiments.

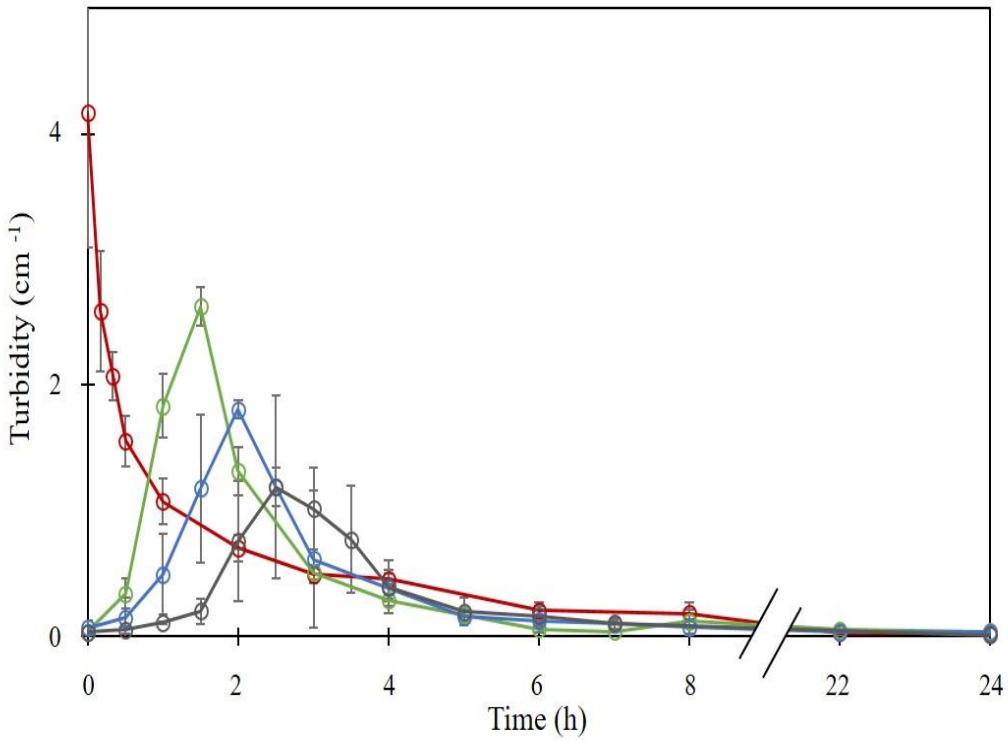

*Figure 3-6: Evolution of turbidity inside the dialysis tube during 24h desalting experiment of LF/βLG mixed at total protein concentration of 0.55 mM in 10 mM MES buffer, pH 5.5 at various initial salt concentrations. No added salt (**red**); with added NaCl at concentrations of 100 mM (**green**), 200 mM (**blue**) and 400 mM (**black**).*

The dialysis time needed for maximum turbidity depended on the initial salt concentration, which is to be correlated to the desalting kinetics shown in Figure 3-4. As illustrated in Figure 3-4 insert, the highest turbidity value was reached when the salt concentration inside the tube was around 10 mM for the three desalting experiments. This means that the transition from unassociated state to complexation/coacervation between LF and βLG occurred at an optimal and constant ionic strength (10 mM), confirming the high salt sensitivity of the studied heteroprotein system. By superimposing the results of Figures 3-4 and 3-6, a significant level of turbidity (complex coacervation) was reached around 10 mM NaCl inside the dialysis tubes.

The overall size of the coacervates droplets formed during dialysis experiments varied from 1 to 10 µm as assessed by microscopic observations. However, we noted that their number was significantly lower for the sample with an initial NaCl concentration of 400 mM (data not shown). However, Fresnais et al. (2009) reported that dialysis leads to the formation of nanoparticle-polymer clusters with a size 3 to 5 fold larger than that obtained with direct mixing protocol at the same ionic strength (Fresnais et al., 2009). The same research group concluded that the decrease of the desalting rate lead to an increase in the hydrodynamic diameter of copolymers complexes (Berret, 2011). This explication can fit with the results of LF/βLG system, as the decrease of the desalting rate is equivalent to conducting dialysis with a higher initial concentration. A higher initial salt concentration delays the on-set of the complexation/ coacervation process during dialysis experiments (i.e. turbidity change, Figure 3-6).

The evolution of the coacervates yield was also monitored during desalting experiments (Figure 3-7). During the initial dialysis time, like turbidity, the increase of the coacervates yield was slowed down by a higher salt concentration. It is obvious that without added salt the coacervates yield sharply increased to a plateau value after 3h of dialysis. However, in the presence of high salt concentrations, the coacervates yield increased slowly during time owing to the strengthening of the electrostatic interactions and the release of the binding sites that caused the coacervates to form progressively.

Initial high salt concentrations do not appear to greatly affect the final coacervates yield recovered after desalting, which varied from 55% to 65% (Figure 3-7).

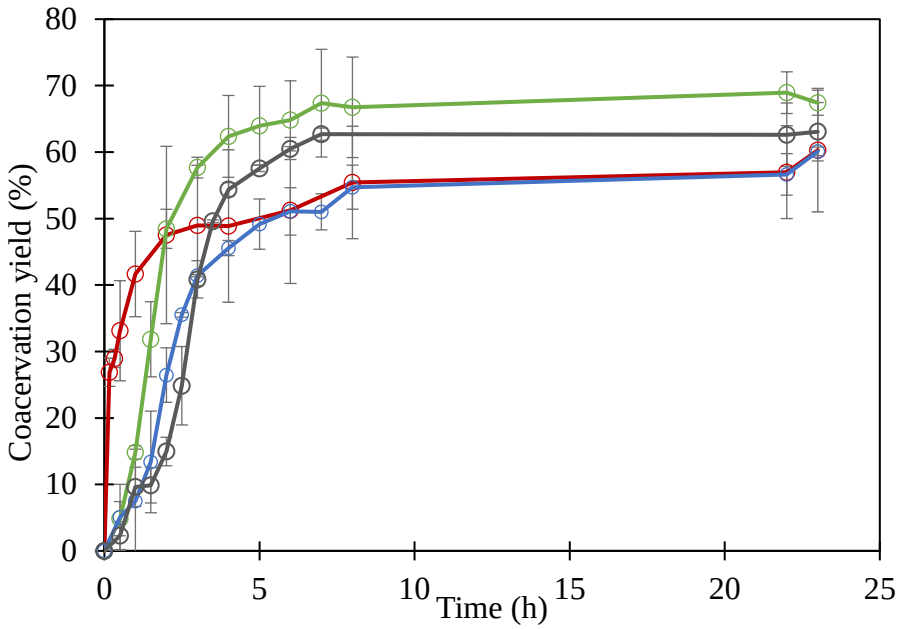

*Figure 3-7: Evolution of the coacervates yield inside the dialysis tube during desalting experiment of LF/βLG mixed at total protein concentration of 0.55 mM in 10 mM MES buffer, pH 5.5 at various initial salt concentrations. No added salt (**red**); with added NaCl at concentrations of 100 mM (**green**), 200 mM (**blue**) and 400 mM (**black**).*

3.1.1.4 Conclusion

In a previous work, we reported on the ability of Lactoferrin and β-lactoglobulin to form heteroprotein complex coacervates under optimal conditions of pH and molar stoichiometry of 5.5 and 10 respectively. Here, the influence of ionic strength on such complex coacervation process was demonstrated using direct mixing and desalting protocols. We showed that whatever the protocol used, the interaction and subsequent assembly of LF and βLG are highly sensitive to ionic strength of the medium. The molecular interaction between the two proteins can be tuned at very narrow window of added salt concentration (i.e. 0-20 mM), while no microscopic phase separation was detected at higher ionic strength. These

results are useful for targeting potential applications of LF/βLG complex coacervates. Studies are ongoing to determine how the salt sensitivity observed here changes at higher total protein concentrations and at other pH values.

3.1.1.5 Supplementary results

So far, the ionic strength effect on the coacervation was conducted using different concentrations of NaCl. We have also studied the effect of KBr, another salt, on the LF/βLG complex coacervation. This salt, in contrast to NaCl, has been shown to be efficient on the dissociation on polyelectrolyte coacervates networks (Fares et al., 2018). Dialysis experiments at 100 mM of salt concentration was repeated using KBr. The turbidity of the solution as well as the coacervates yield during 24 h of dialysis in 100 mM of KBr vs 100 mM NaCl is shown in Figure 3-8.

Figure 3-8 illustrates that the changes in turbidity and the coacervates yield of the coacervates during dialysis were similar regardless of the used salt. However, the maximum of turbidity was lower and was reached 30 min earlier for dialysis at 100 mM of KBr as compared to NaCl. The conclusion is thus that at the same ionic strength value, changing the ion identity didn't affect the coacervation. This can be explained in terms of the Hofmeister series where Cl- and Br- were found to have the same properties. Another assumption could be that both ions have the same strength of interaction with the proteins (Sing & Perry, 2020; Y. Zhang & Cremer, 2006). Consequently, we did not evidence any difference between NaCl and KBr during the process of progressive formation of HPCC.

Perry et al. (2014) studied the effect of different salt ions on the formation of polyelectrolytes coacervates. They found that, for ionic strength lower than 1 M, no huge difference was observed. However, for ionic strength higher than 1 M, divalent cations were found to disfavor coacervates formation more deeply than divalent anions. These authors, reported that the difference on the size and charge density of the ions, as well as their hardness and solvation can explain their effect toward coacervation (Perry et al., 2014).

Therefore, to complete our study, the investigation of the effect of ions identity should include polyvalent ions and should be conducted during both the formation and the dissociation of the coacervates network.

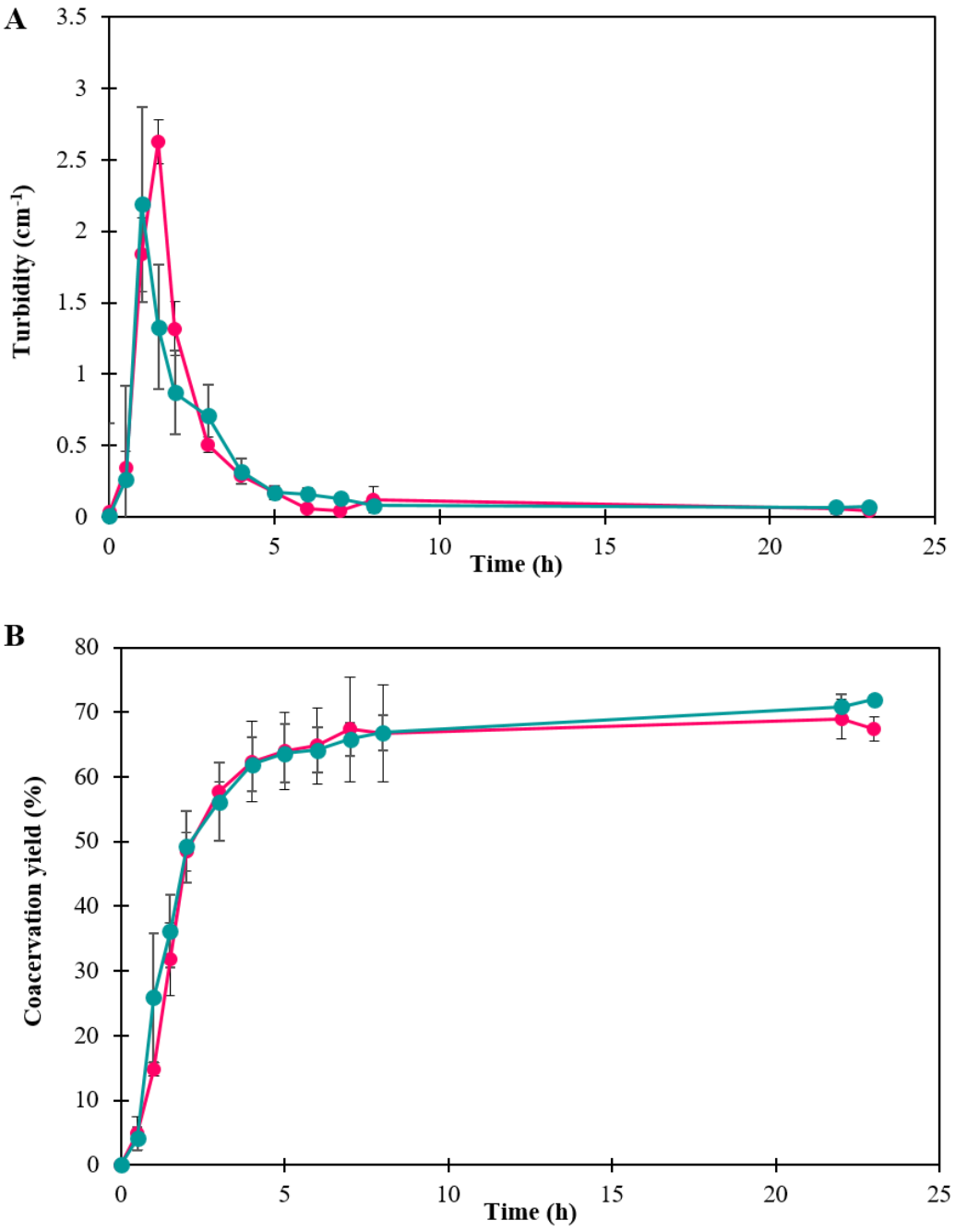

*Figure 3-8: Evolution of A- the turbidity and B- the coacervates yield inside the dialysis tube during desalting experiment of LF/βLG mixed at total protein concentration of 0.55 mM in 10 mM MES buffer, pH 5.5 at 100 mM of KBr (**teal**) and NaCl (**pink**).*

3.1.2 Part 2: Ionic strength effect on lactoferrin - β-lactoglobulin interactions: Monte-Carlo simulation

Preamble

Main objectives:

- Measuring the net charge of individual proteins as a function of pH and ionic strength.
- Identify the contribution of multipolar terms involved in the electrostatic energy of interaction between the two proteins and their response to increasing ionic strength.
- Study the effect of ionic strength on the free energy of interaction between the two proteins.
- Study the configuration of the primary unites of the coacervates.

The influence of ionic strength on LF/βLG complex coacervation was conducted using mainly experimental techniques. Molecular simulation made proof of a huge efficiency in investigating ion effect on protein-protein interactions. Here, we use Faunus, a Monte Carlo simulation code, in order to investigate the ionic strength influence on the lactoferrin - β-lactoglobluin dimer interactions as the building blocks of the studied coacervates was found to be the binding of LF with two βLG dimers.

Monte Carlo simulation was performed to first, measure the net charges of each protein as a function of a large range of pH and ionic strength. Secondly, the multipole contribution in the total electrostatic energy and the effect of salt on each multipole term were evaluated. Moreover, the effect of increasing the ionic strength on the free energy of interactions was also sampled.

Finally, the investigation of the contact between residues of LF and βLG dimer led to identifying the structure of the primary unit of the coacervates.

Main results:

- The increase in the ions concentration in the medium led to an increase in the absolute value of the protein net charge.
- Ion-ion interactions had the strongest contribution in the total electrostatic energy.
- The alignment of βLG and LF was diminished after increasing ionic strength.
- The increase in the ionic strength progressively reduced the attraction between the proteins until the disappearance of almost all attraction at 100 mM.
- MC simulation confirmed that two βLG dimers can bind into the LF surface on two different sites

Abstract

Several experimental techniques were used in order to study the interaction between β-lactoglobulin and lactoferrin. These two highly charged globular proteins, was proved able to form spherical coacervates under specific conditions. The LF/βLG coacervates are very senstive to changes in ionic strength. In this present study, the effect of implicit salt on the interaction between LF/βLG was investigated using Monte Carlo simulation. In agreement with the experimental results, Mc simulation showed that the increase of ionic strength led to a dramatic decrease in the attraction between the proteins hence a decrease in the free energy of interaction. Sampling βLG and LF binding proved that LF is able to bind with two βLG dimers in two different sites.

Keywords: Complex coacervation; ionic strength; Monte-Carlo simulation; protein-protein interaction.

3.1.2.1 Introduction

Proteins are essential biopolymers for humans' health thanks to their rich diversity of functional, physico-chemical and biodegradable properties. These biopolymers are of a major interest in the food industry. It was proved that proteins can modify food's color, flavor, physicochemical and textural properties (Damodaran & Paraf, 1997). As proteins exhibit a rich diversity of functional properties, various works focus on their ability to form a large diversity of nano- and microstructures throughout diverse interactions between them. Protein-protein interactions in aqueous solution was and still attracting much attention and many studies aimed to understand the processes taking place during these interactions. The protein surface is chemically heterogeneous and is composed of different regions of charged, polar, and apolar groups which made them capable of interacting with ions as well as other proteins via electrostatic interactions. These interactions between oppositely charged proteins can undergo a liquid liquid phase separation (LLPS) into protein rich phase called coacervates and a protein poor phase called dilute phase. This phenomenon is also called heteroprotein complex coacervation. β-lactoglobulin and lactoferrin, two highly charged globular proteins, was proved able to form spherical coacervates under specific condition of pH and proteins concentration and ionic strength (Anema & de Kruif, 2014; G. M. Tavares et al., 2015; Yan et al., 2013). Several works used various experimental techniques such ITC (Tavares et al., 2015), MNR (D'Silva et al., 2005; Peixoto et al., 2016) and SAXS (Kizilay et al., 2014) were used to investigate β-lactoglobulin and lactoferrin interactions. In addition to these methods, numerical simulation was conducted using docking simulations in order get insights about the LF/βLG coacervates molecular structures (Peixoto et al., 2016). As ionic strength plays a major role in the electrostatically driven heteroprotein complex coacervation, this study focused of the effect of the ionic strength on the interaction between β-lactoglobulin and lactoferrin using simulation techniques. Monte Carlo simulation was performed to investigate the effect of implicit salt on the interaction between these two proteins. Using a Faunus software (Stenqvist et al., 2013), we measured the net charges of each proteins as a function of both pH and ionic strength. Moreover, the electrostatic interactions between βLG and LF in the present of salt as well as the multipole contribution in the total electrostatic energy have been evaluated. The effect of increasing ionic strength on the free energy of

interaction was also sampled. Finally, the structure of the primary unit of the coacervates including one LF and two βlG dimers were investigated by studying the residues that gets into contact during the complexation.

3.1.2.2 Methodology

Model

Metropolis-Hastings Monte Carlo (MC) simulations was conducted to explore the interaction between βLG dimer (PDB id: 1BEB) and LF (PDB id: 1BLF) using the Faunus framework (Stenqvist et al., 2013). The two proteins structures are kept rigid and coarse grained so that each amino acid is represented by a spherical bead of size σ_i, which could be charged, or neutral depending on residue type and solution pH represented. These amino acids interact with a combined Lennard-Jones and Debye-Hückel potential to account for short-range repulsion and attraction, as well as electrostatic interactions in an aqueous electrolyte solution. The ionization state of each amino acid is fluctuating according to its pKa value and solution pH. The MC system energy function used is:

$$U = \sum_{i}^{N-1} \sum_{j=i+1}^{N} \left\{ 4\epsilon_{ij} \left[\left(\frac{\sigma_{ij}}{r_{ij}} \right)^{12} - \left(\frac{\sigma_{ij}}{r_{ij}} \right)^{6} \right] + k_B T \frac{\lambda_B Z_i Z_j}{r_{ij}} e^{-k r_{ij}} \right\} \qquad 3\text{-}3$$

where λ_B = 7 Å is the Bjerrum length, κ is the inverse screening length, Z are residue charge numbers, r_{ij} is the distance between the ith and jth particle, ϵ = 0.05 $k_B T$ the Lennard-Jones interaction strength and N is the number of interaction sites. The temperature was set to 300 K for all simulations.

Proteins charges fluctuations

The net charge of each protein βLG dimer and LF was calculated during simulation. In fact, Faunus calculated the average charge and standard deviation per atom, and the most probable species (atom name) averaged over all present molecules.

Interaction free energy calculation

The mass centers of the two rotating proteins are fixed on a connecting line along which they are allowed to translate. In addition to rotational and translation MC moves, move attempts are also performed to deprotonate acidic and basic residues. During simulation, we sample the radial distribution function, *g (R)*, where *R* is the mass-center separation between the two proteins. The radial distribution function, *g(R)* is related to the angularly averaged potential of mean force *w (R)*.

$$w\,(R) = -kB\,T\,ln\,g\,(R) + w_0 \qquad 3\text{-}4$$

w_0 is a reference state and is chosen such that *w (R)* tend toward 0 for large *R*.

Simulation bias

Due to the strong electrostatic attraction between the oppositely charged βLG and LF, only short separations are sampled and almost no sampling is done at large distance. For this reason, the reference state w_0 became difficult to determine within reasonable simulation times. Therefore, to promote sampling at large separations, we added a *bias potential B (R)* to the MC energy function as showed in equation 7.

$$U = \sum_{i}^{N-1} \sum_{j=i+1}^{N} \left\{ 4\epsilon_{ij} \left[\left(\frac{\sigma_{ij}}{r_{ij}} \right)^{12} - \left(\frac{\sigma_{ij}}{r_{ij}} \right)^{6} \right] + K_B T \, \frac{\lambda_B Z_i Z_j}{r_{ij}} \, e^{-k r_{ij}} \right\} + B(R) \qquad 3\text{-}5$$

The used bias potential follows the equation 8.

$$B(R) = -K_B\,T\,Z_1 Z_2 \left(\frac{sinh(Ka)}{Ka}\right)^2 \left[\frac{1+Ka\,coth(Ka)}{R} - \frac{K}{2}\right] e^{-kR} \qquad 3\text{-}6$$

The use of the bias potential *B (R)* makes the observed potential of mean force *biased* and unphysical *w' (R).* However, since *B (R)* depends only on the separation, *R* we can simply unbias by subtraction to recover the true free energy *w (R)* as mentioned in the equation 9

$$w(R) = w'(R) - B\ (R) \qquad 3\text{-}7$$

B (R) is the monopole-monopole interaction in an electrolyte solution from Sogame-Ise theory (Wu et al., 1998), and effectively removes a large part of the electrostatic attraction (note the negative sign). Z_1 and Z_2 denote the average protein charges and a=36 Å is an effective diameter, chosen such that *w' (R)* is reasonably flat over a large range of ionic strengths. The measurement of the potential mean force is conducted in 4 steps. First the radial distribution function *g (R)* is measured than converted to a free energy *w' (R)*. Later *the w' (R*) is shifted to zero at a large separation distance R in order to be find the reference state w_0. Once the w_0 is measured, that is when we unbias to obtain the actual free energy *w (R)* for different salt concentration (10 – 100 mM).

Virtual translation moves

Another way to measure the potential of mean force for increasing salt concentration (10 – 100 mM) can be conducted using *virtual translation moves (VTM)*. A virtual displacement is performed for one single molecule and then the force is measured by perturbation. During *VTM*, the system is momentarily perturbed so that one of the proteins is slightly displaced along the mass-center connection vector. The linear perturbation theory was used in order to obtain the *force*, *f (R)* which can be numerically integrated to yield the interaction free energy, *w'(R)*. For these simulations the bias potential mentioned above was also used to get the enhance sampling of the true interaction free energy, *w (R).*

Electrostatic energy and multipole decomposition

The electrostatic energy between the two proteins in terms of an electrostatic multipole expansion was measured as a function of salt concentration at a *fixed* mass-center separation, *R* corresponding to the

minimum free energy distance. During simulation, the two proteins rotate and we can sample the direct inter-protein Coulomb interaction.

$$U_{exact}(R) = K_B T < \sum_i^{N_{LF}} \sum_j^{N_{\beta LG}} \frac{\lambda_B Z_i Z_J}{r_{ij}} > \quad 3\text{-}8$$

At a fixed *R* and for each configuration, the instantaneous protein monopole, dipole and quadrupolar moments were calculated. From those moments, and by the use of a multipole expansion, the electrostatic energy and the sum of all terms (ion-ion, ion-dipole, dipole-dipole, and ion-quadrupole) was measured. At the lowest salt concentration *i.e.* 10 mM, the multipolar contributions to the total electrostatic energy as percentage was also presented.

Contact map in the free energy minimum

During the complexation of the βLG dimer and LF at low ionic strength equal = 10 mM, the residues of both proteins that get in contact with each other are reported into a contact map. This is done by analyzing 1000 frames from a trajectory collected at ionic strength =10 mM and at pH 5.5. The contact is defined when the residue-residue center distance is less than 20 Å.

The visual representation is performed using the Visual Molecular Dynamics (VMD) software.

3.1.2.3 Results and discussion

Proteins charge

As a first step of the simulation, we will be studying single proteins and focusing on their protonation states as a function of pH and salt concentration.

Figure 3-9 A and B show the net charge as a function of both pH and ionic strength of βLG and LF respectively. We can see that regardless of the salt concentration, the increase of the pH from 4 to 12 led to a decrease of the net charge of both βLG and LF. Same results were reported by Anema & de Kruif, (2014) who calculated the net charge of βLG and LF using the Scripps protein calculator on a

protein sequence download from the Swiss Protein Data Bank. These results were expected in this pH range as βLG and LF have pI, the pH in which the protein electrically neutral, around 5 and 9 respectively. In fact, βLG and LF contains a large number of charged amino acid residues (around 47 for βLG and 167 for LF) that can be protonated or deprotonated.

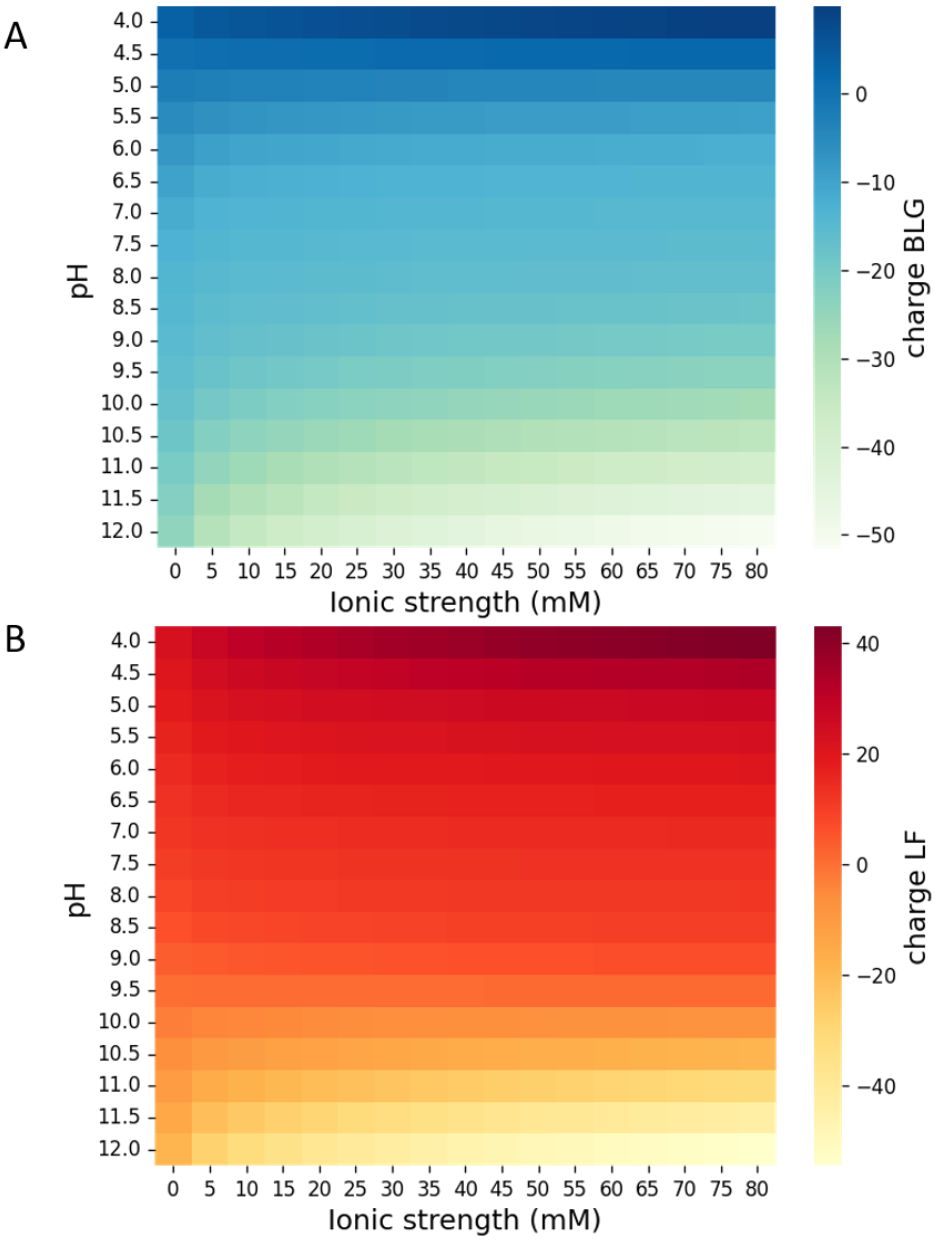

Figure 3-9 : The net charge as a function of pH and the salt concentration A- βLG and B- LF

This is why the net charge of these two proteins strongly depends on the pH. At pH values below the pI, the protein is protonated hence the positive net charge. However, the protein donate protons and acquire a negative charge when increasing the pH to value above the pI. (Jachimska et al., 2018).

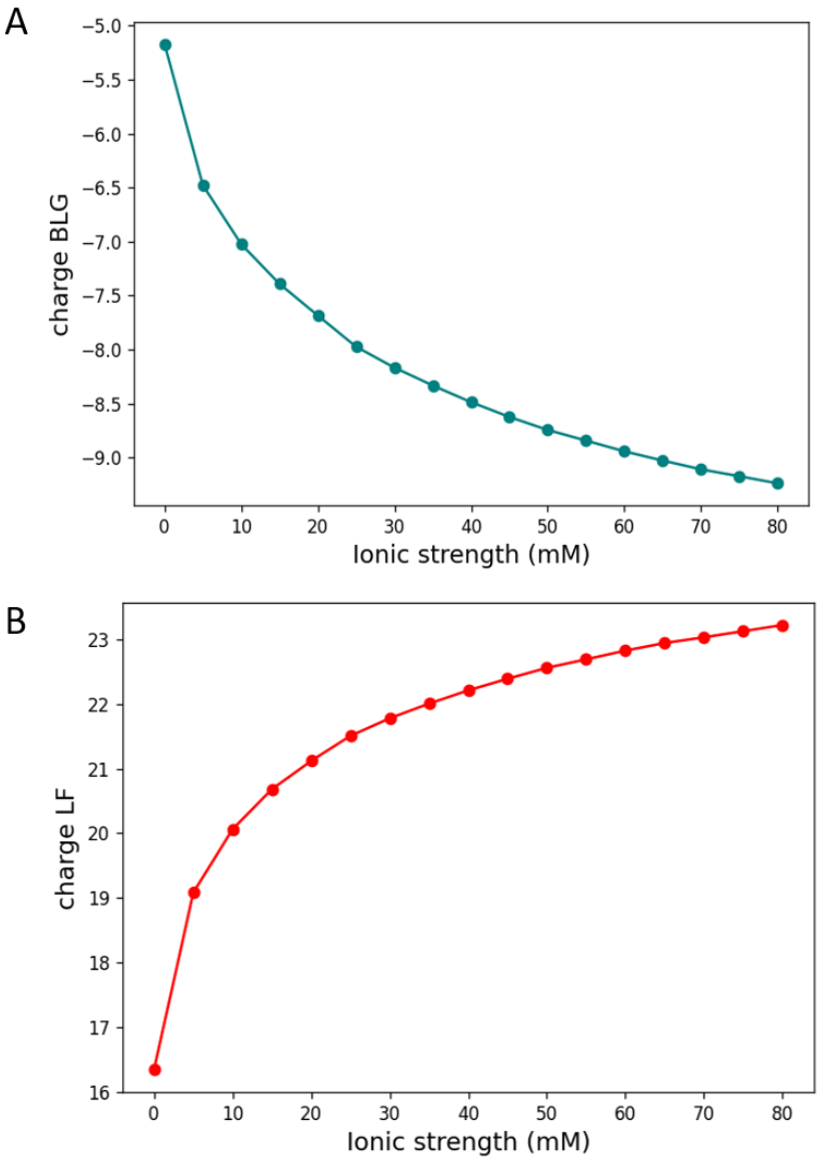

Figure 3-10: The net charge as a function of salt concentration at pH = 5.5 for A- βLG and B- LF

Figure 3-10 shows the net charge of the two proteins as a function of ionic strength (0 – 80 mM) at pH 5.5, the experimentally observed optimum pH for coacervation between βLG and LF. The increase of

the ions concentration in the medium led to an increase in the absolute value of the protein net charge. These results can be explained by the fact that salt ions screen the intramolecular electrostatic interactions so that at high ionic strengths the protein can accommodate a higher net-charge. Another way to express this, is that the apparent pK_a values become more and more ideal as salt is added. Same charge tendency were reported for two other proteins; Thermomyces lanuginosa Lipase (TLL) and γ-crystallin (Hladílková et al., 2016; Kurut & Lund, 2013). It can be seen in Figure 3-10 that with further increase of the salt concentration the net charge tends to a plateau. This observation is related to a progressively lower association of the ions on the two whey proteins due to the saturation of the proteins binding sites at sufficiently high salt concentrations (Gokarn et al., 2011; Kurut & Lund, 2013). Moreover, the magnitude of the increase of the absolute net charge of LF was twice as high as that of the βLG.

Lactoferrin - β-lactoglobulin potential of mean force

After investigating the charges of each protein individually, the interaction between the two proteins together is now sampled. The potential of mean force in an ionic strength range going from 10 to 100 mM is measured.

We first sampled the radial distribution function, *g (R)* between the two proteins at different NaCl concentrations (data not shown). It was proved that the optimal distance where the attraction between βLG and LF is maximum is around 56 Å.

From the radial distribution function, we deduced the LF- βLG potential of mean force, *w (R)* as a function of distance for different salt concentrations (see Figure 3-11).

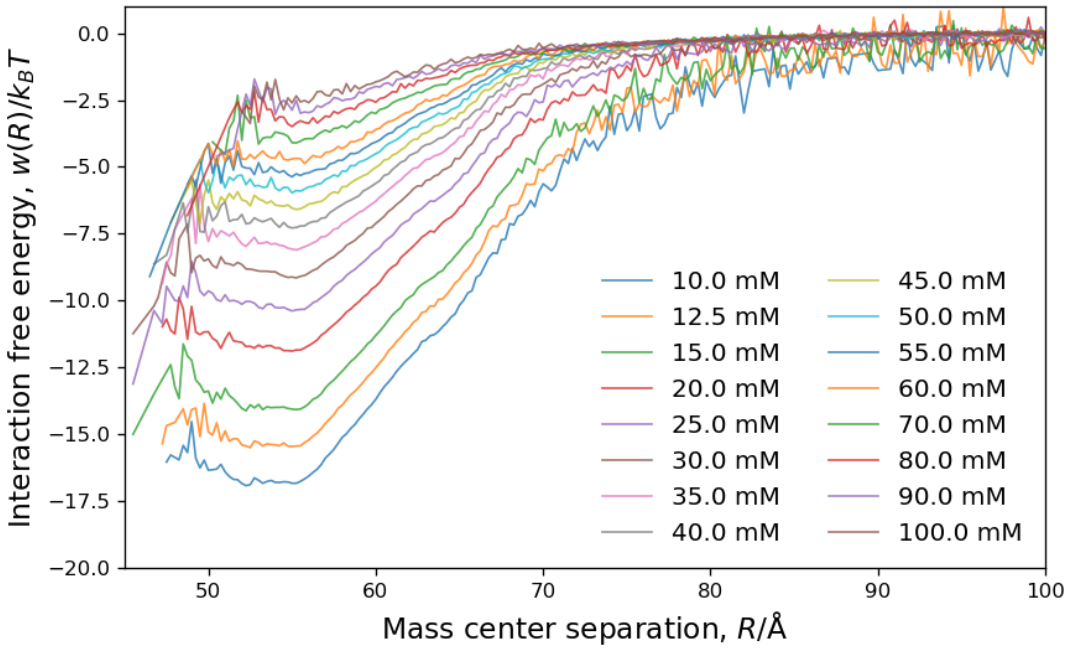

Figure 3-11: Simulated free energy of interaction w(R) between a β-lactoglobulin dimer and lactoferrin as a function of their mass center separation R at different ionic strength from 10 mM to 100 mM at pH 5.5.

In Figure 3-11, we show the simulated potential of mean force between β-lactoglobulin dimer and lactoferrin as a function of the mass center separation *R*. It is seen that regardless of the ionic strength value, the minimum of the free energy of interactions always took place at a distance close to R = 56 Å. Figure 3-11 also demonstrated that at low concentration of salt a long-range repulsion, indicated by a negative *w (r)*, was measured. This behavior is due to electrostatic attraction between the two proteins. The increase of the ionic strength progressively reduced the attraction between the proteins. A further addition of salt ions until reaching 100 mM led to the disappearance of almost all attraction between proteins. In fact, at low ionic strength, the two proteins strongly aligned at a specific distance hence a strong attraction. This attraction is progressively suppressed while adding salt due to charge screening, which underlines the importance of electrostatics interaction in the interaction between β-lactoglobulin and lactoferrin. Similar results were reported for lysozyme/α-lactalbumin interaction in salt solution

where the increase of the salt concentration from 5 mM to 100 mM led to reduced electrostatic interactions (Lund, 2016).

An alternative calculation for the free energy of interaction *w (R)* was conducted by virtual translation moves (VTM) using linear perturbation theory. The results of this methods are shown in Figure 3-12.

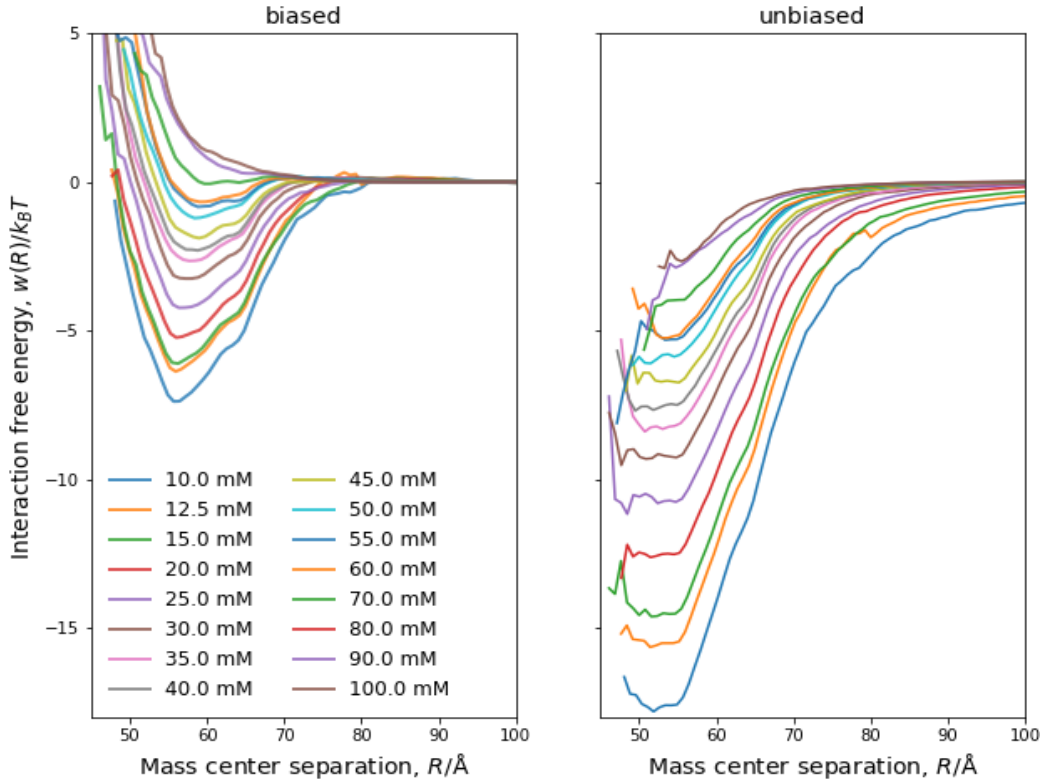

Figure 3-12: Simulated free energy of interaction w(R) between a β-lactoglobulin dimer and lactoferrin as a function of their mass center separation R at different ionic strength from 10 mM to 100 mM at pH 5.5 using linear perturbation theory with a bias potential

It is seen in Figure 3-12 that the use of the perturbation theory gave practically the same results, as the classical methods shown in Figure 3-11. However, the curves plotted using *(VTM)* are slightly smoother, indicating that the method is computationally more efficient as the two types of analysis are made on the same set of equilibrium configurations (i.e. from the same simulation).

Lactoferrin - β-lactoglobulin electrostatic energy

Just like the last section, a simulation of both proteins is conducted here as well. Since multipoles are a first approximation to mathematically describe charge patches on the protein surface, an analysis of the contribution of Coulomb interactions, including the ion-ion, dipole-ion, dipole-dipole and dipole-quadrupole interactions, on the electrostatic energy of interaction between LF and βLG and its behaviors toward increasing ionic strength is conducted.

Figure 3-13 A shows the multipolar contributions in the lactoferrin - β-lactoglobulin total electrostatic energy of interaction using a pie chart. The simulation was conducted at distance R = 56 Å as the strongest attraction was proved to take place around that distance.

Figure 3-13 A clearly indicates that the ion-ion interactions had the strongest single contribution *i.e.* almost 50% of the total electrostatic energy. The ion-dipole interaction contribution was also important as it represented almost one-fifth of the total energy. On the other hand, ion-quadrupole and dipole-dipole interactions had the lowest contribution. However, if combined, all the “anisotropic” contributions are roughly equal to the “isotropic” monopole-monopole contributions.

It is know that the dipole-dipole interactions become important only when dipoles are far enough from other electrostatic sources or in a medium with a high dielectric constant (Polimeni, 2021). The remaining interactions not included in our finite multipole expansion was assigned in the pie chart presentation to "higher order moments".

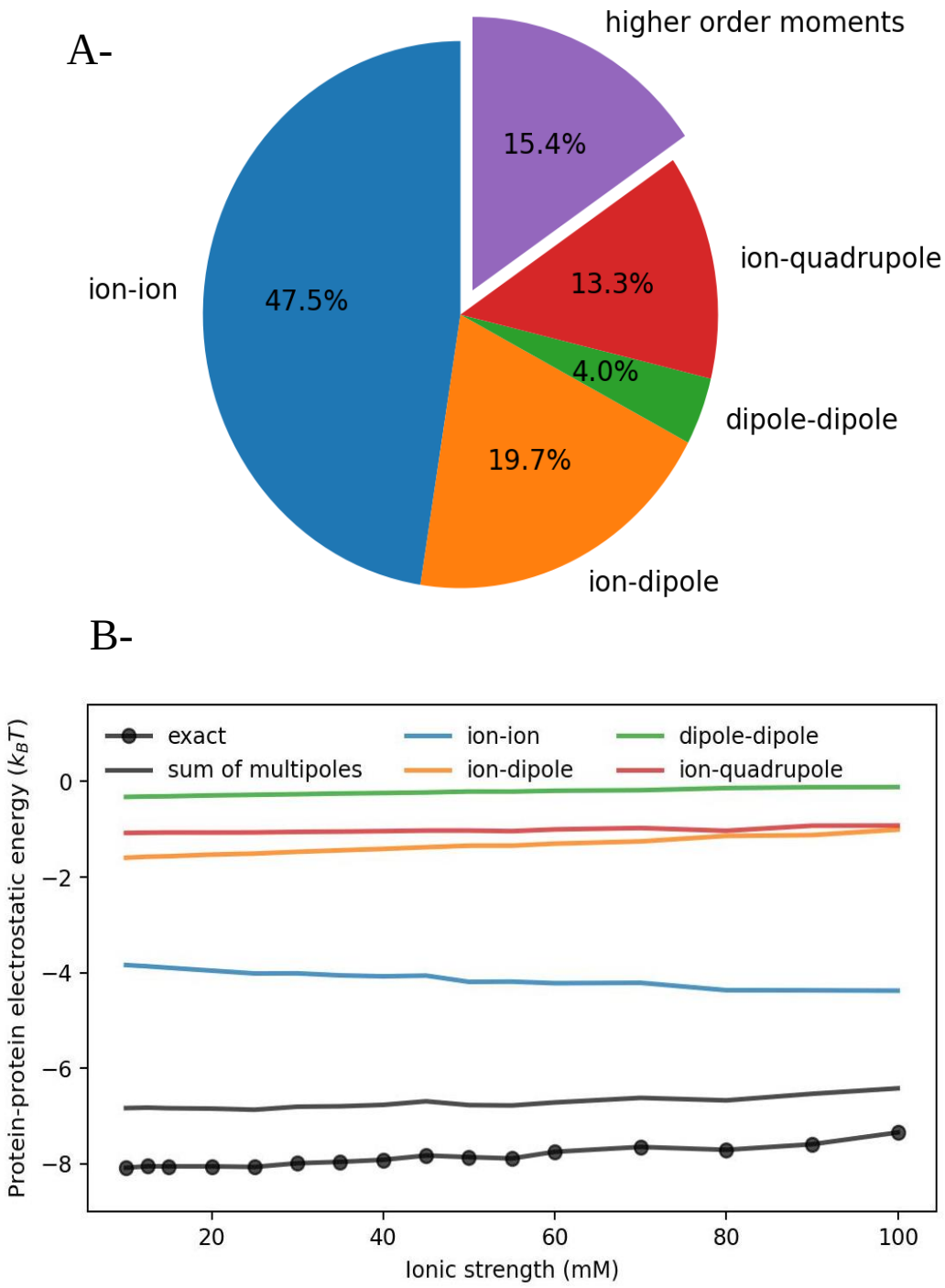

Figure 3-13: Pie chart of the multipole contributions in the lactoferrin and β-lactoglobulin electrostatic energy of interaction. B- The electrostatic energy between lactoferrin and β-lactoglobulin in terms of an electrostatic multipole expansion as a function of ionic strength. Simulation is conducted at R = 56 Å, at the lowest ionic strength 10 mM and pH 5.5.

Figure 3-13 B shows the electrostatic energy between the two proteins in terms of an electrostatic multipole expansion as a function of the ionic strength. The latter Figure confirmed the results reported in the pie chart representation. In fact, at the lowest ionic strength, the ion-ion interactions inside the coacervates were the strongest as it was twice as high as the other multipoles value.

The ion-dipole and ion-quadrupole terms give roughly equal contributions and both are attractive. Figure 3-13 B also shows the respond of each term after increasing the ionic strength from 10 mM to 100 mM. The ion-ion term gets more negative with increasing ionic strength, which merely reflects that the net-charge of LF/βLG complex increases due to the charge screening caused by increasing salt ions. The anisotropic terms (ion-dipole, dipole-dipole, ion-quadrupole) slightly decreases with ionic strength, showing that the alignment is diminished which is expected. It is worth mentioning that these energies exclude salt-protein interactions, but the configurational space on which the averaging is done do fully incorporate salt at the mean-field level, *i.e.* Debye-Hückel.

The binding of β-lactoglobulin dimer and lactoferrin

A study of the contact between the residues that get involved in the complexation of the βLG dimer and one LF at low ionic strength (10 mM) was conducted. During this simulation, we reported a contact map summarizing all the βLG and one LF residues that gets into contact during the complexation. The results of this simulation are reported in Figure 3-14.

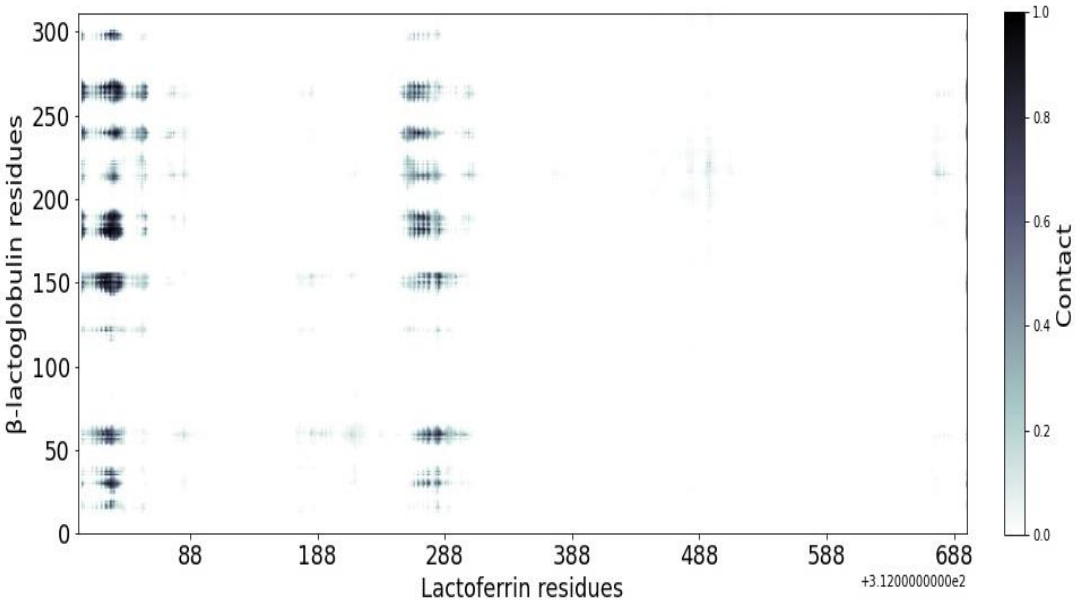

Figure 3-14: A contact map of the β-lactoglobulin and lactoferrin residues at 10 mM ionic strength

Figure 3-14 shows that the βLG dimer interact mainly with the same region in the LF. We are assuming that this LF region have the highest density of positively charged residues. Therefore, the electrostatic interaction between βLG and LF are the strongest around this region.

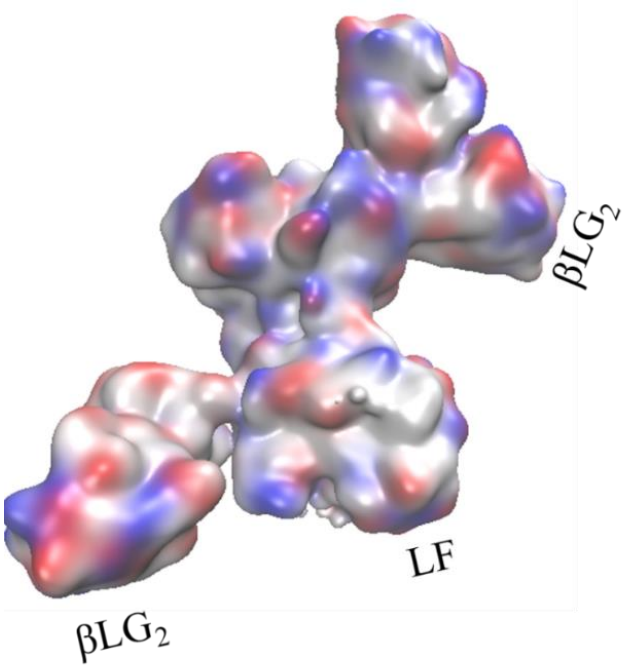

Figure 3-15: A representative simulation snapshot of LF binding with two βLG dimers at ionic strength = 10 mM. Colors represents charged residues.

Figure 3-15 show a visual representation of the binding of two β-lactoglobulin dimers and one lactoferrin. The formed complex (LF ($\beta LG_2)_2$) shows that the LF has two binding sites for the two βLG dimers. Peixoto et al. (2016) reported similar results for the same protein couple using docking simulations. These authors showed that two βLG_2 are able to bind into the LF surface on two different sites called the S and M sites (Peixoto et al., 2016).

3.1.2.4 Conclusion

Monte-Carlo simulation was proved a useful method for the analysis of the protein – protein interactions. In this present study, Monte Carlo simulation was performed to investigate the effect of the presence of ions in the medium on the interaction between two globular proteins: βLG and LF. The measurements of the net charge of each protein individually revealed that the increase of the ionic strength led to an increase in the absolute value of the protein net charge. The radial distribution function, *g (R)* and the free energy, *w (R)* proved that LF/βLG maximum interaction occurs at a distance around R= 56 Å. The maximum free energy was observed at the lowest ionic strength, the increase of the salt concentration progressively reduced the attraction between the proteins until the disappearance of almost all attractions at 100 mM. In addition to that, sampling the binding of the two proteins showed that two βLG dimers can bind into the LF surface on two different sites.

3.2 Chapter 2: Rheological characterization of β-lactoglobulin/lactoferrin complex coacervates

3.2.1 Part 1: Rheological characterization of β-lactoglobulin/lactoferrin complex coacervates in the optimum conditions

Preamble

The objective of this present study was to investigate in depth for the first time the rheological properties of the β-lactoglobulin/lactoferrin complex coacervates obtained under their optimum conditions of coacervation i.e. pH 5.5, a low ionic strength of 4 mM (10 mM MES buffer), a total protein concentration of 0.55 mM and molar ratio βLG:LF of 10:1

Main objectives:

- Comparing the viscosity of the individual proteins to that of the coacervates to emphasize the importance of internal organisation and interaction in the rheological properties of the coacervate network.
- Study of the viscoelastic behaviour of the coacervates under a large frequency range.
- Study of the coacervates respond to an instantaneous stress

Dynamic apparent viscosity was determined by flow experiments under a wide shear rate range from 0.01 s^{-1} to 300 s^{-1}. Viscoelastic properties of the coacervates were also studied using two techniques:

- frequency sweep at 628 – 0.628 rad/s
- Creep and recovery for 10 min each using increasing stress values of 0.5 – 5 Pa.

Main results:

- βLG/LF coacervates exhibited viscoelastic properties, with a dominate liquid-like behavior.
- βLG/LF coacervates showed an extremely high viscosity, 2500 times higher than that of individual proteins at the same concentration.
- A flow-dependent and time-dependent de-structuring of the coacervates was observed, that was also reversible

*Soussi Hachfi, R., Famelart, M.-H., Rousseau, F., Hamon, P., & Bouhallab, S. (2022). Rheological characterization of β-lactoglobulin/lactoferrin complex coacervates. LWT- Food Science and Technology, 163, 113577. https://doi.org/10.1016/j.lwt.2022.113577

Abstract

Heteroprotein complex coacervation between lactoferrin (LF) and β-lactoglobulin (βLG), two oppositely charged proteins from whey, occurred under specific conditions of pH, ionic strength and protein molar ratio. The present work aims at characterizing the rheological properties of the concentrated phase called coacervates obtained after phase separation. Unlike some polysaccharide/protein coacervates, LF/βLG heteroprotein coacervates exhibit a liquid-like behavior; the loss modulus G" being 100 times higher than the storage modulus G' at low frequencies. This behavior was confirmed under creep-recovery tests. The heteroprotein coacervates exhibited a Newtonian viscous flow under low shear rate and a shear thinning behavior above 10 s^{-1}. The coacervates are exceptionally viscous, reaching a viscosity value of 55 ± 10 Pa.s which is ~2500 times higher than that measured on individual protein solutions of equivalent total concentration. Also, a structural change occurred in the coacervates, probably due to the weaknesses of electrostatic interactions inside the protein network at high shear rates. The observed time-dependent structural rearrangement was proved to be reversible. These findings open new ways for the use of coacervates as texturizing agents in food matrices.

Key words: Food heteroprotein; Viscoelasticity; Rheology; liquid-liquid phase separation

3.2.1.1 Introduction

Complex coacervation is an electrostatically and entropically-driven associative liquid-liquid phase separation (LLPS) process which most often takes place between two oppositely charged macromolecules (Kizilay et al., 2011). Since the pioneer research on complex coacervation of gelatin and gum Arabic by Bungenberg De Jong and Kruyt one century ago (Bungenberg De Jong & Kruyt, 1929), the biopolymer-based coacervates continue to be a fundamental research focus. Nowadays, the research programs on complex coacervation and more generally on LLPS are burgeoning not only in order to generate new materials and new applications for food or pharmaceutical industries but also to understand the intra-cellular biological assemblies and the origin of some neurodegenerative diseases. (For more details, see reviews by (Croguennec et al., 2017; Kapelner et al., 2021; Yewdall et al., 2021). The main promising applications for food and pharmaceutical industries are macromolecular purification, encapsulation for protection and delivery of bioactives and nutrients and also elaboration of biomaterials with new textures and functionalities (Blocher & Perry, 2017; Croguennec et al., 2017).

The generic process of complex coacervation leading to LLPS can be summarized into four main steps: initially, a spontaneous attractive interaction between macromolecules of opposite charges leads to formation of primary units whose stoichiometry is system dependent (Croguennec et al., 2017). Then, the formation of soluble complexes from these primary units (building blocks) according to a not completely elucidated mechanism. The third step is the growth step with the formation of micrometric droplets characteristic of complex coacervation (X. Wang et al., 2021) and finally, the coalescence of these droplets with gentle LLPS into a dense phase (coacervates) and dilute phase (Jho et al., 2017).

Various research works allowed progress in the understanding of the mechanisms of the complex coacervation. However, the vast majority are centered on proteins/polysaccharides, proteins/synthetic polyelectrolytes and polyelectrolytes/polyelectrolytes mixtures. Studies focusing on complex coacervation involving proteins of opposite charge, called heteroprotein complex coacervation (HPCC) are more recent and therefore less well documented (Croguennec et al., 2017; Zheng, Tang, et al., 2020).

As recently reviewed, HPCC constitutes a special case of LLPS because its process is highly sensitive to the ionic strength, occurs at narrow range of pH and follows the principle of charge and size compensation (Boire et al., 2018). Indeed, the formed dense phase is composed of at least two different proteins with opposite charges. During this last decade, several couples of oppositely charged proteins, from both animal and plant origins, were used to understand the main mechanism that drives HPCC (Croguennec et al., 2017). These different works have mainly focused on the optimal conditions for HPCC, the properties of primary units and the formed micrometric droplets, but little on the structural characterization of the final dense phase.

The HPCC based on two milk proteins, Lactoferrin (LF) and β-lactoglobulin (βLG), is the most studied system (Anema & (Kees) de Kruif, 2012; Chapeau et al., 2016; Kizilay et al., 2014; G. M. Tavares et al., 2015). These studies provided several fundamental elements on i- the physico-chemical conditions for optimal complex coacervation including pH, ionic strength, stoichiometry and protein surface charge, ii- the molecular nature of the primary units; iii- the structure of formed βLG-LF droplets and their ability to encapsulate a bioactive molecule. Moreover, two studies have attempted to characterize the structure and properties of the final coacervates by combining SAXS and rheology (Kizilay et al., 2014) or Fluorescence recovery after photo-bleaching and solid state NMR (Peixoto et al., 2016). They concluded that the coacervates phase is a dynamic network with a complex molecular composition. The aim of the present work is to extend these studies by a combination of rheological methods for in-depth characterization of the coacervates formed between βLG and LF. Rheological analysis provides insight into the internal structure of biomaterials very useful for potential processing (Abraham et al., 2017). LF/βLG coacervates were prepared under optimal coacervation conditions, i.e. at pH 5.5 and 0.01 mol/L ionic strength and separated from diluted phase. Dynamic apparent viscosity was determined by flow experiments under a wide shear rate range. The viscoelastic proprieties of the coacervates were proved using two techniques first the frequency sweep then the creep-recovery tests.

3.2.1.2 Materials and methods

A. Materials

LF with a purity of 90 g/100 g and iron saturation of 10 to 20 mol iron/mol protein according to technical specification was purchased from Fonterra Cooperative Group (Auckland, New Zealand). LF powder was used without further purification. Industrial bovine βLG containing both variants A and B was further purified before use. As βLG is prompt to self-aggregation during long storage, the non-native and aggregated species were regularly removed by acidic precipitation. The βLG powder was dispersed in ultrapure water (30 g/L), adjusted to pH 5.2 with 1 mol/L HCl and then kept at 30° C for 10 min to precipitate aggregated and non-native forms. The dispersion was centrifuged at 36 000 g at 25° C for 10 min (Avanti, J-26S XP BioSafe Three-Phase Non-IVD Centrifuge, Beckman Coulter, Villepinte, France). The supernatant containing native β-lactoglobulin (purity > 95 g/100 g powder as assessed by HPLC) was adjusted to pH 7.0 with 1 mol/L NaOH, freeze-dried and stored at -20° C until use. Whey protein isolate (WPI) was purchased from Lactalis Ingredients (Bourgbarré, France) and contained 84 g total proteins per 100 g of the powder. 2-(N-morpholino) ethanesulfonic acid hydrate (MES) was purchased from Sigma-Aldrich (St. Louis, MO, USA) and all other chemicals were of analytical grade.

B. Preparation of heteroprotein coacervates

MES buffer 0.01 mol/L was prepared by solubilizing MES powder in ultra-pure water and adjusted to pH 5.5 by 1 mol/L NaOH solution. Protein powders were solubilized in 0.01 mol/L MES buffer adjusted at pH 5.5 using 1 mol/L HCl solution. This pH value was found to be optimal for complex coacervation between the two whey proteins at chosen stoichiometry and total protein concentration (Chapeau et al., 2016). The protein concentrations were determined in these two stock solutions by absorbance at 280 nm (SAFAS UV MC2, Safas, Monaco) using 0.96 L/g.cm and 1.47 L/g.cm as extinction coefficients for βLG and LF, respectively.

In order to prepare the coacervates, The optimized protocol published previously was applied (Chapeau et al., 2017). Briefly, an equivalent volume of the two protein solutions were mixed at room temperature

to reach a final concentration of 0.5 mM and 0.05 mM for βLG and LF, respectively, which means a LF/βLG molar ratio of 1:10. Mechanical stirring was performed by stirring the solution in a vessel containing a propeller pale of 2.5 cm diameter, with three blades. The propeller was set in rotational motion by the mean of an electric motor set at 360 rpm. The spontaneous formation of coacervates as spherical droplets was monitored by turbidity measurements at 600 nm (SAFAS UV MC2, Safas, Monaco) and microscopic observations on a phase contrast microscope (BX51TF, Olympus, Rungis, France). This mixture was stored for 12 h and then centrifuged at 37 000 g for 30 min at 20° C in order to separate the two liquid phases and extract the coacervates phase. From an experiment to another, a coacervates yield of 55 to 65 g of proteins in the coacervates/ 100 g initial total proteins was recovered. For each experiment, a total volume of 100 mL was implemented to get about 0.7 - 0.9 g of the coacervates enough to perform 3 to 4 rheological measurements. After centrifugation, the protein content in the coacervates phase was quantified by HPLC as previously reported (Chapeau et al., 2017). About 25 to 30 g of proteins were quantified for 100 g of recovered hydrated coacervates.

C. Rheological measurements

Rheological measurements of the coacervates were carried out using a stress-controlled rheometer (DHR2, TA Instruments, Guyancourt, France) with a cone - plate geometry (angle of 2°, diameter = 20 mm, truncature = 51.5 µm) and a parallel plate geometry (diameter = 20 mm) with gap values of 250 µm and 500 µm.

Whatever geometry is used, around 200 mg of coacervates samples were loaded on the Peltier plate at 20° C and allowed to rest for 2 min before measurement.

All rheology measurements were performed at least twice and plotted as means and standard deviations and fitting of data was performed with python (version: 3.9.5) and excel software.

Flow measurements

Flow measurements were performed in an upward shear rate sweep (0.01 - 300 s^{-1}) followed by a downward one. Measurements were performed by averaging for 20 s after an equilibrium time of 100 s at low shear rates (0.01 s^{-1} to 0.1 s^{-1}) and for 5 s after 10 s equilibrium at higher shear rates (0.1 s^{-1} to 300 s^{-1}). All the flow measurements were performed using a cone - plate geometry and a parallel plate geometry.

Flow measurement plus constant shear rate

Flow experiment was performed as above in a cone-plate geometry, but once a shear rate of 1 s^{-1} was reached during the upward and downward sweep, this shear rate was maintained for 6 min and the viscosity was measured versus time.

Frequency sweeps

Frequency sweeps were carried out from 100 to 0.1 Hz with an oscillatory strain amplitude of 0.001, which was in the linear viscoelastic regime, in a cone-plate geometry.

Creep and recovery tests

Creep and recovery were conducted with a cone-plate geometry using stress values (σ) of 0.5 -5 Pa for 10 min each.

3.2.1.3 Results and discussion

Figure 3-16 illustrates the steps of liquid-liquid phase separation that led to the formation of LF/βLG complex coacervates. The process starts with spontaneous increase of solution turbidity to reach 2.8 ± 0.15 cm-1, a characteristic value of complex coacervation between these two whey proteins in solution (Chapeau et al., 2016; Yan et al., 2013). The spontaneous formation of spherical droplets, with a mean diameter between 5 to 10 µm, a signature of the complex coacervation process was attested by phase

contrast microscopy (Figure 3-16 B). The spontaneous formation of these droplets corresponds to the microphase separation step of the complex coacervation process. The coalescence of the droplets leads to the macrophase separation at the end as indicated by the white arrow (Figure 3-16 A).

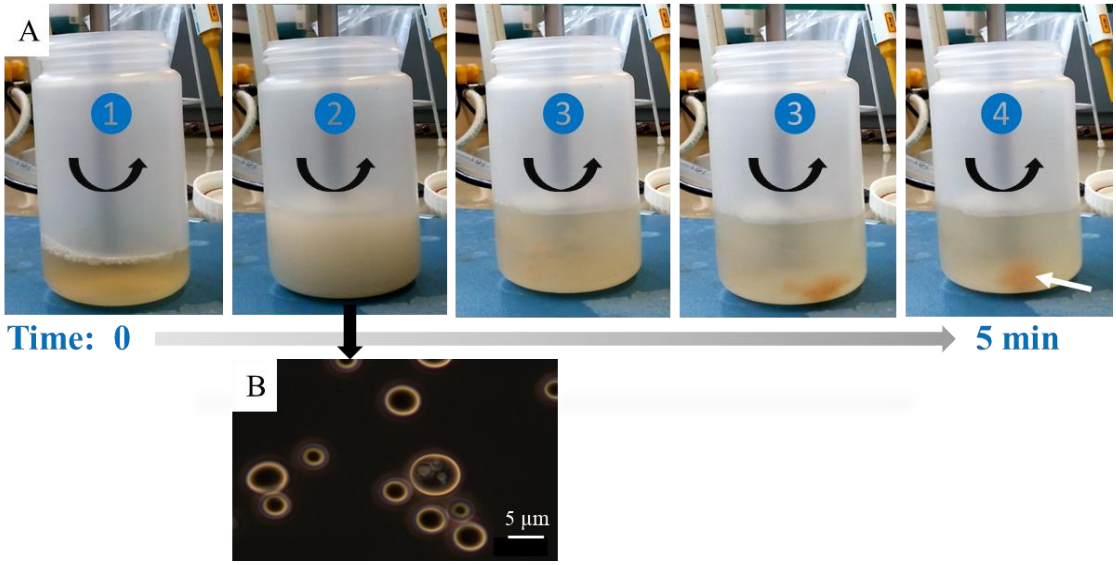

Figure 3-16: A- Visual monitoring over time of the liquid-liquid phase separation i.e. complex coacervation between lactoferrin and β-lactoglobulin under continuous stirring in 0.01 mol/L MES buffer pH 5.5. Total batch mixing volume = 100 mL. 1*: Solution of lactoferrin at 0.05 mM;* 2 *At t0, addition of 0.5 mM β-lactoglobulin solution with spontaneous appearance of turbidity. This step corresponds to the microphase separation of complex coacervation with the formation of micrometric droplets (B), characteristic of the coacervation process;* 3*: Initiation and progression of liquid-liquid phase separation;* 4*: Macrophase separation with the formation of coacervates indicated by the white arrow.*

The coacervates yield obtained at used total protein concentration of 13 g/L varied from 55 to 60 g of proteins in the coacervates/ 100 g initial total proteins, as already described in details (Chapeau et al., 2016).

A. Flow

As a first experiment, the apparent viscosities at low shear rates were measured (Figure 3-17). The plot showed a behavior close to Newtonian fluids, with a slight decrease in viscosity at increasing rates, with increasing and decreasing steps almost superimposed. Consistency and behavior indexes from the power law were K = 51.9 ± 0.9 Pa.s and n = 0.94 ± 0.03, respectively, confirming a behavior index close to 1. Given that βLG is the main component of whey protein isolates (WPI) and also the major protein in the βLG/LF coacervates phase (Peixoto et al., 2016), The viscosity of coacervates was compared with that of a WPI solution at the same pH and total protein concentration of 250 g/L.

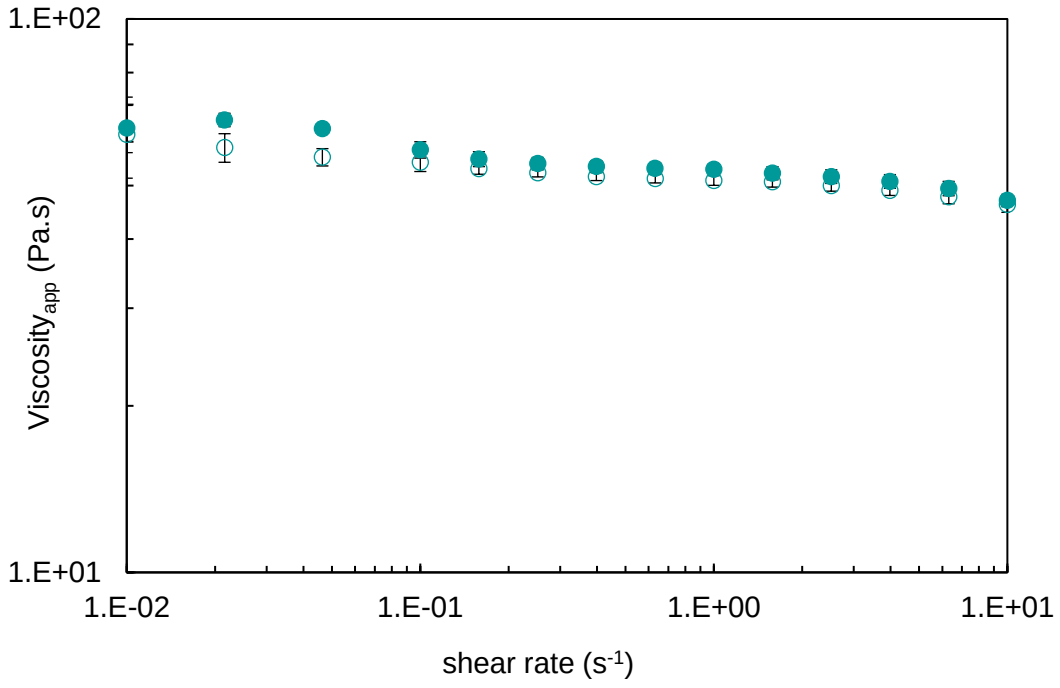

Figure 3-17: Apparent viscosity of coacervates at strain rates from 0.01 to 10 s^{-1} as measured at 20° C. Values from three preparation of coacervates with cone-plate geometry. Close symbols: upward shear rate; open symbols: downward shear rate. Mean and standard deviations from three measurements are plotted.

At this concentration, WPI shows homogeneous solution with no phase separation nor coacervation. Using the same protocol, WPI solution exhibited a Newtonian behavior with a viscosity value of 23 ±

0.5 mPa.s at 10 s^{-1} (data not shown), a value 2000 - 3000 times lower than the viscosity of βLG/LF coacervates at 10 s^{-1}. This high difference underlines that the internal organization/interaction play a major role in the rheological properties of the coacervates network, which deserves to be studied in-depth the apparent viscosities of βLG/LF coacervates in a much wider shear rates range is shown in Figure 3-18. For higher shear rates, the dynamic viscosity decreased sharply and it showed a high hysteresis between the upward and downward steps. Despite the dramatic decrease of the viscosity during the upward shear rate, the initial viscosity of the coacervates was fully recovered by the end of the flow cycle. This behavior was similar with the cone-plate and the plate-plate geometry, although the viscosity was slightly lower with the plate-plate than with the cone-plate geometry and the hysteresis loop was slightly larger with the cone than with the plate.

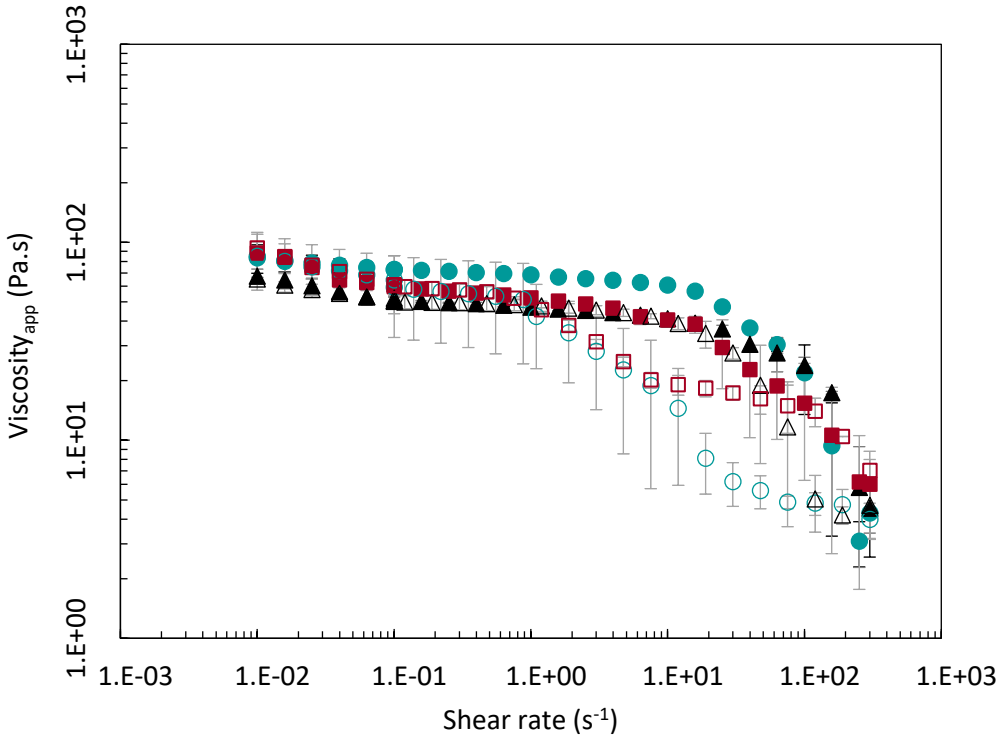

Figure 3-18: Apparent viscosity of βLG/LF coacervates as a function of shear rate from 0.01 s^{-1} to 300 s^{-1} at 20° C. Cone-plate (●) (three measurements), plate-plate gap = 250 µm (▲) (two measurements), plate-plate gap = 500 µm (■) (two measurements). Close symbols: upward shear rate; open symbols: downward shear rate. Mean and standard deviations of all measurements are plotted.

Similar behavior has been already reported for other coacervates systems: whey protein/gum Arabic coacervates at pH 4 above a critical shear rate of 30 s^{-1} (Weinbreck, Wientjes, et al., 2004), ovalbumin-gum Arabic coacervates at pH 2.7 - 3.7 above 5 - 10 s^{-1} (Niu et al., 2018) and polyelectrolyte/surfactant coacervates (Liberatore et al., 2009).

To better understand what happened between 1 and 300 s^{-1}, an extra experiment was performed during the flow measurement. The experiment of Figure 3-18 was duplicated but at 1 s^{-1} the viscosity was measured as a function of time during the upward and the downward flow. Figure 3-19 shows the obtained results at constant shear rate experiment at 1 s^{-1}. During the upward flow curve, the viscosity remained constant, meaning that the coacervates was in an equilibrium state. However, in the downward flow curve, the viscosity increased over time. This thixotropic behavior was also observed in the case of coacervates made from protein/polysaccharide (Niu et al., 2018; Weinbreck, Wientjes, et al., 2004) and from polyelectrolyte/surfactant (Liberatore et al., 2009; R. C. W. Liu et al., 2002). Weinbreck et al. (2004) explained the drop in viscosity above a critical shear rate as the one observed in Figure 3-18 by a breakdown of the structure due to the breakup of physical bonds in the coacervates network at high shear. Once a critical shear rate is reached, the electrostatic interactions inside the protein network is weakened, which causes a change in the coacervates structure (Weinbreck, Wientjes, et al., 2004). This behavior was the same regardless of the selected geometry or the gap value in the plate-plate geometry. The breakdown of the structure at high shear rate was not due to an artefact from the geometry such as a non-laminar shear nor a wall slip of the sample but rather to the changes in the coacervates structure.

Hence, the disrupted coacervates was able to recover its initial structure during the downward flow in agreement with the hysteresis loop observed between increasing and decreasing flow rate (Figure 3-18). The structural changes were fully reversible but needed time to reform and restore similar original state of the network. This hypothesis is confirmed in Figure 3-19 where the recovery of the coacervates structure brought about by the rearrangement of the physical bonds between βLG and LF was proved to be time dependent. These results were similar to those reported for the OVA-GA complex coacervates (Niu et al., 2018).

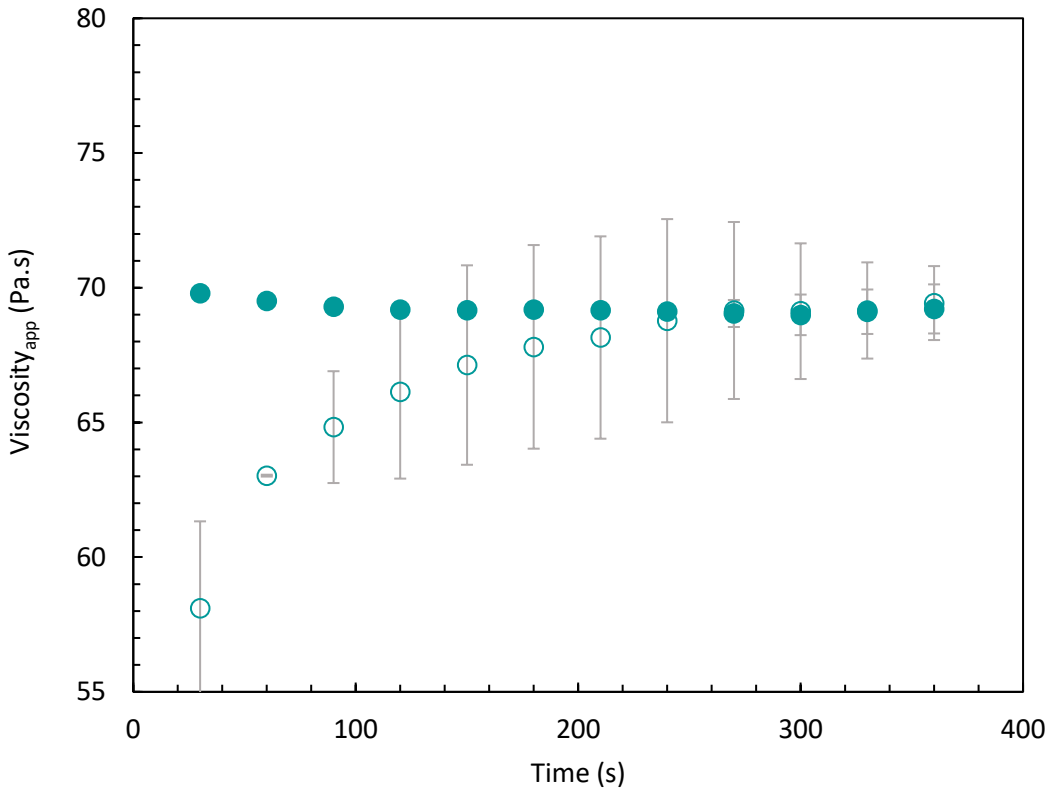

Figure 3-19: Apparent viscosity of LF/βLG coacervates as a function of time during a constant shear rate at 1 s^{-1}: upward flow curve (close circle) and downward flow curve (open circle). Mean and standard deviations from duplicate

Alongside the hypothesis of a shear-induced breakdown of the coacervates structure, other assumptions could be invoked such as a microscale structural reorganization of the interspersed phases of the complex coacervates (Kaur et al., 2011). This structural rearrangement is due to a temporary breaking up of the attractive interactions between two polymers aggregated in dense particles in the dispersion (Niu et al., 2018). Another assumption was given by Liberatore et al. (2009) who explained the drop of the viscosity by a shear-induced phase separation; using a simultaneous characterization by rheology and small angle light scattering they observed that, once the shear rate increases, a phase separation took place leading to a shear thinning behavior of the coacervates (Liberatore et al., 2009). Another supposition could be related to the sample leaving the geometry gap under high shear rate that leads to a lower viscosity value. The possibility of shear banding at high shear rate should also be taken into account.

According to the latter authors, the Cross rheological model (Cross, 1965) described in equation 11 can fit the viscosity data:

$$\eta = \eta_\infty + \frac{\eta_0 - \eta_\infty}{1+(t.\Sigma)^m} \qquad 3\text{-}9$$

where η_0 and η_∞ are the zero-shear and the high-shear viscosity, respectively, t is the relaxation time i.e. the inverse of the onset of shear thinning, $\Sigma$the shear rate and m the shear thinning index, also known as the rate constant. A value of m equal to 0 means a Newtonian behavior, whereas the higher the m value, the more intense the shear thinning behavior. The fitting of the data gives a value of m equal to 0.53. According to Liberatore et al. (2009), a stress plateau is obtained at values of m equal to 1 or more. This plateau could be an indication of a possible shear banding in the geometry. Shear banding can originate from many behaviors, such as disentanglement of polymers, shear-induced phase separation due to spatial fluctuation of polymer concentrations, and particle scission and reformation dynamics. For the LF/βLG coacervates, a plateau of stress was hardly fitted with m adjusted to values around 0.5.

The aim of the flow experiments was to study the viscous properties of LF/βLG coacervates over a wide shear rate range. LF/βLG heteroprotein coacervates had two different behaviors depending on the shear rate applied; a Newtonian behavior at low shear rates and a shear thinning behavior above 10 s^{-1}. In addition to that, a hysteresis loop between the upward and downward flow was observed likely due to a slow and progressive recovery and reconstitution of electrostatic interactions inside the protein network. The weakness of electrostatic interactions could also lead to weak elasticity inside the coacervates structure therefore a study of the viscoelastic properties of the coacervates was carried out by frequency sweep measurements and creep-recovery tests.

B. Frequency sweeps

Figure 3-20 shows the viscoelastic behavior of LF/βLG coacervates at 20° C. Over the whole range of angular frequencies studied, G'' dominated the behavior, mostly at low frequencies where the value of G'' was 10 times higher than G' which meant that the coacervates had a liquid-like behavior. This behavior is close to the one depicted on the coacervates between βLG and LF performed under other experimental conditions (Kizilay et al., 2014) as well as with others types of polyelectrolyte complexes (PECs) (Marciel et al., 2018). Using a discrete fitting of relaxation times with the Maxwell model and plotting G' and G'' for enlarged frequencies (TA Instruments utilities, data not shown) allowed a raw estimation of the crossing frequency. The fitting generally required more than one single element, as usually for complex systems (R. C. W. Liu et al., 2002).

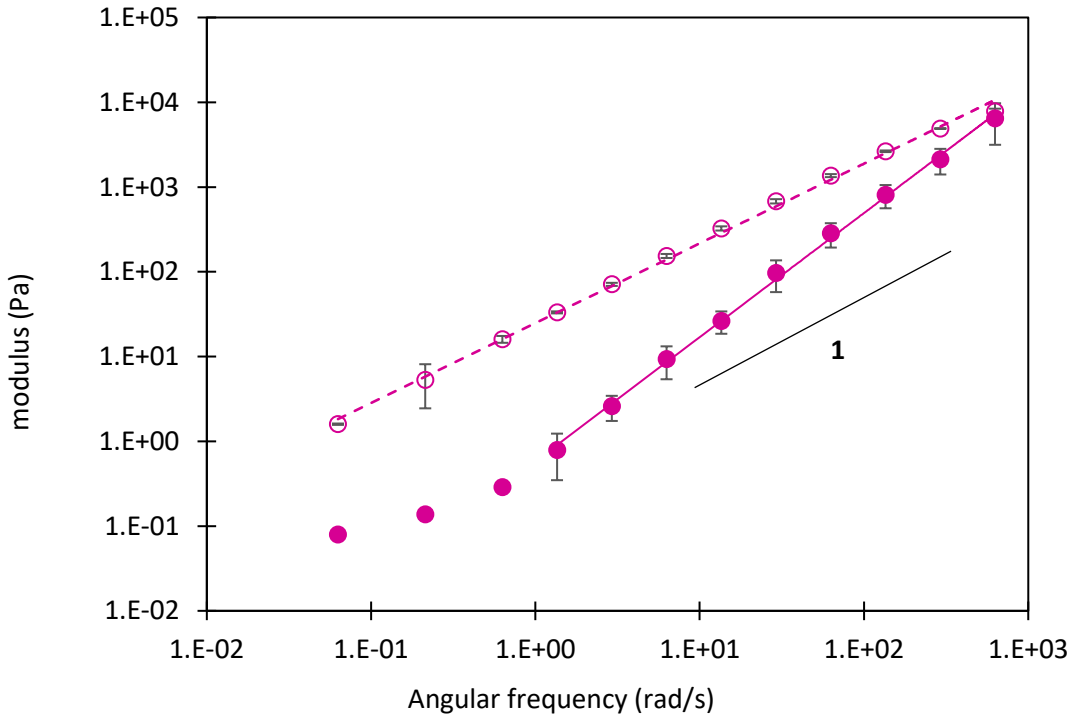

Figure 3-20: Storage modulus (full symbols ●) and loss modulus (open symbols o) of LF/βLG coacervates as function of angular frequency at 20° C (two measurements). Solid line: G' frequency power law scaling above 1 rad/s. Dashed line: G'' frequency power law scaling. Mean and standard deviations are plotted.

Crossing frequencies were estimated at 760 rad/s. The interconnected structures responsible for the viscoelastic properties inside LF/βLG coacervates have a relaxation lifetime around 8 ms. This value is of the same order of magnitude as determined for the same heteroprotein coacervates at pH 6 which was found to be 1 ms (Kizilay et al., 2014). A very low lifetime for interconnecting electrostatic interactions between polymers gives transient network properties, as it was shown, and a behavior clearly dominated by viscous properties.

While G'' was linearly dependent to the angular frequency during its whole range, G' trend toward a plateau and did not follow a linear fit in the low frequency regime. Both G' and G'' thus followed a power law of frequency, for the G'' with an exponent close to 1 (0.95 +/- 0.01) and at frequencies larger than 1 rad/s for the G' with an exponent of 1.47 +/- 0.01. Others have reported deviation from the typical Maxwellian behavior of G' as a function of frequency. This deviation has been attributed either to a contribution of a distribution of relaxation times in the tested frequency domain, for instance between ion pairs considered as the sticky points of the transient network (Ali & Prabhu, 2018; H. B. Bohidar, 2015). Or to a limited sensibility of the rheometer at low frequencies (Boire et al., 2018; Marciel et al., 2018; Tang et al., 2015) or to the presence of a very weak elastic network (H. Bohidar et al., 2005; Dardelle & Erni, 2014). Sticky Rouse relaxation phenomenon has also been advanced to explain the behavior in coacervates made from weak polyelectrolytes due in fact to the mobility of free non-interacting polyelectrolytes (Marciel et al., 2018; Tang et al., 2015). For a large number of coacervates involving oppositely charged molecules, low-salt environment results in stronger electrostatic interactions between ion pairs with higher solid-like properties, whereas high salt concentrations weakens ion-pair strength, leading to labile sticky connections and increased liquid-like properties (H. B. Bohidar, 2015; Chai et al., 2014; Y. Liu, Momani, et al., 2017; Y. Liu, Winter, et al., 2017; Xiong et al., 2017). However an inversed effect of salt has also been reported (Priftis et al., 2013) and pH can also alter the viscoelastic behavior of coacervates (Kizilay et al., 2014; Marciel et al., 2018; Raei et al., 2018; Weinbreck, Wientjes, et al., 2004). All these effects act by modulating the strength of electrostatic interactions between the two polymers in the coacervates phase. Peixoto et al. (2016) reported on the

composition, dynamic and internal structure of LF/βLG coacervates using solid-state NMR experiments combined with in silico docking. In particular, the co-existence of three types of molecular entities with specific dynamics and Rh properties has been shown in the current coacervates network. The smaller one is assigned to βLG2 and βLG monomers (Rh = 2 nm), which is used in excess in the initial mixture. The other entities with Rh of 7 nm and ≈ 30 - 60 nm are assigned to heterocomplexes involving LF and βLG_2, the association of which built the overall "skeleton of the coacervates" (Peixoto et al., 2016). The high mobility of some of these species and the weak connectivity between them could explain the observed viscoelastic properties of the overall network of LF/βLG heteroprotein coacervates.

C. Creep-recovery tests

Figure 3-21 a reports the plot of strain versus time at various stress values. Once the stress was applied, the coacervates underwent deformation without an instantaneous elastic response. However, in the recovery test, two different behaviors were noticed: the coacervates had a slight recovery at 0.5 and 1 Pa, whereas the recovery was hardly detectable at higher applied stress. The coacervates thus showed a viscoelastic response at low stress values, but only a liquid-like behavior under higher stress. This result agrees with a dominant liquid-like behavior of the coacervates with the possible presence of a very weak elastic network as previously hypothesis in other coacervates systems (H. Bohidar et al., 2005) with mechanical spectra showing a turn in G' at low frequency. The observed viscoelastic behavior at low stress is consistent with the results reported for the gum Arabic/whey protein isolate coacervates and gum Arabic/chitosan coacervates (Tavares & Noreña, 2020; 2019) for applied stress<1 Pa and for fish gelatin and sodium alginate complexes (Derkach et al., 2021). Applying high stress values for 10 min might cause a breakdown in the protein network, which caused a reorganization in the coacervates structure and therefore a loss of the weak elasticity. J (t) defines the creep compliance J (t) = ε(t)/σ, the coacervates had a liquid-like dominant behavior, which meant that the creep compliance would be a linear function of time (t) as mentioned in equation 12:

$$J(t) = a.t \qquad 3\text{-}10$$

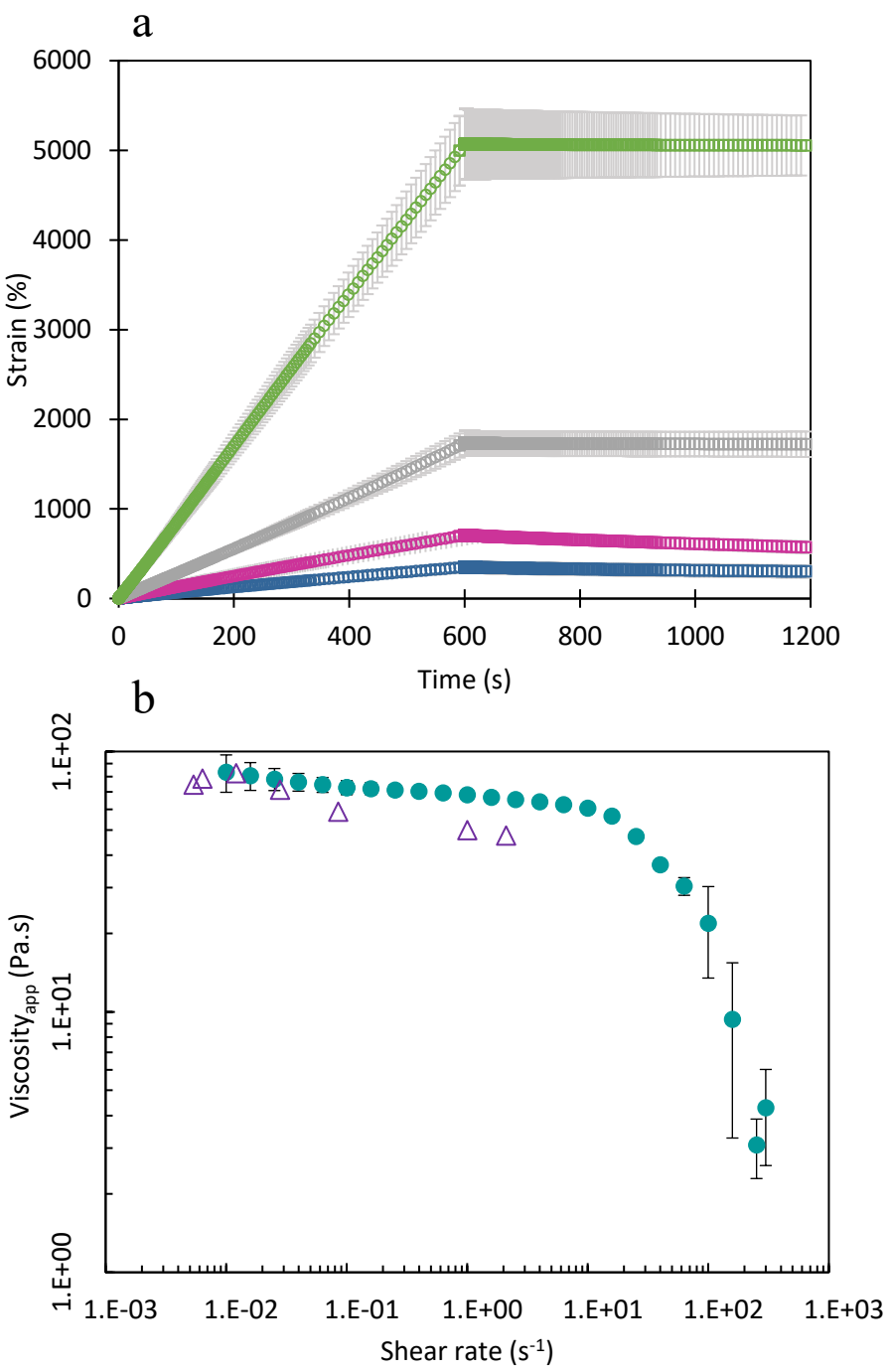

Figure 3-21: a- Strain versus time in creep (0 - 600 s) and recovery test (600 – 1200 s) of LF/βLG coacervates at 20° C. Applied stress: 0.5 Pa (----), 1 Pa (----), 2 Pa (----) and 5 Pa (----). b- Apparent viscosity of βLG/LF coacervates as function of shear rate in flow (●) and creep tests (Δ).

The creep compliance versus time plots were linear (not shown) and their slopes allowed the evaluation of the dynamic viscosity at their respective strain rates. Figure 3-21 b shows the comparison of the viscosity of the coacervates measured in the flow and creep tests. Viscosity results are in reasonably good agreement and confirmed the liquid-like dominant behavior of the current coacervates. The behavior under creep-recovery tests of coacervates made from oppositely charged proteins is clearly elucidated here for the first time.

3.2.1.4 Conclusion

The aforementioned results clearly demonstrated the exceptional rheological properties of complex coacervates made from two oppositely charged proteins βLG and LF. A dominant liquid-like behavior is demonstrated, together with the presence of a weak elastic network probably due to electrostatic interactions between βLG and LF, and responsible for shear thinning and thixotropy in the flow behavior and to non-Maxwellian and non-zero recovery behavior in oscillation and creep-recovery tests. The formed coacervates, composed of 250 g of proteins /kg, constitute a hydrated network with exceptional viscosity close to 60 Pa.s, while the viscosity of individual proteins at equivalent concentration is of the order of a few mPa.s. The observed rheological properties are the result of weak and reversible interactions. Hence, the combination of the rheological methods used here allowed for the understanding the behavior of heteroprotein coacervates and to the best of our knowledge, this is the first time that such in-depth characterization is reported. Information on the composition and the physical properties of heteroprotein coacervates is very useful for identifying and exploring their potentials for specific applications including encapsulation and protection of bioactive molecules but also in controlling the texture of protein enriched food formulations. Studies on how the rheological properties of heteroprotein coacervates can be tuned by changes in ionic strength and temperature are in progress.

Acknowledgements

We gratefully acknowledge the financial support provided by the regional council of Brittany and INRAE.

Conflicts of interest

The authors declare no conflicts of interest.

Credit Author Statement

Rima Soussi Hachfi: Execution of experiments, Investigation, Methodology, Data analysis, Writing.

Marie-Hélène Famelart: Supervision, Proposition of experiments, Validation, data analysis, writing-Review.

Florence Rousseau: Execution of experiments, Methodology, Data analysis.

Pascaline Hamon: Execution of experiments, Methodology, Investigation.

Saïd Bouhallab: Conceptualization, Project supervision, Writing – Review & Editing.

3.2.2 Part 2: Ionic strength and temperature effects on the rheological properties of lactoferrin/ β-lactoglobulin coacervates

Preamble

In our previous study, a complete rheological characterization of the β-lactoglobulin/lactoferrin complex coacervates prepared under their optimum conditions of coacervation in terms of pH and protein concentration was conducted. Here, we aimed to investigate the effect of both added salt (0 – 8 mM) and temperature (5 – 30 °C) on the rheological properties of the coacervates. The effect of temperature (5 – 30 °C) was studied on coacervates already prepared at 20°C, while for ionic strength; the coacervates were prepared at various salt concentrations.

Main objectives:

- Comparing the viscosity of the individual proteins and that of the coacervates under increasing temperatures.
- Study the effect of ionic strength and of the temperature on the viscosity and the viscoelasticity of the coacervates.
- Study the temperature effect on the relaxation mechanism of the coacervates using TTS.

The rheological measurements were performed by:

- Flow measurements under increasing and then decreasing shear rates,
- Frequency sweeps
- TTS (only for the temperature effect).

Main results:

- The reinforcement of the hydrogen bonding between proteins and the reduction in polymer mobility at low temperature led to an increase in both the viscosity and viscoelasticity of the coacervates.
- The relaxation mechanism of the coacervates was independent of the temperature.
- An increase in ionic strength probably reinforced the hydrophobic interactions between the proteins hence a more viscous coacervates and a higher elastic modulus.

*Soussi Hachfi, R., Famelart, M.-H., Rousseau, F., Hamon, P., & Bouhallab, S. (2023). Rheological properties of lactoferrin/β-lactoglobulin coacervates: ionic strength and temperature effects. Submitted

Abstract

The various applications of heteroprotein complex coacervation have made it of great interest in many fields including food industry. Several works studied the efficiency of protein-based coacervates for encapsulation of bioactive molecules. However, the respond of these coacervates to slight changes in the physico-chemical environment deserves to be better understood. In the present study, heteroprotein complex coacervation between positively charged Lactoferrin (LF) and negatively charged β-lactoglobulin (βLG) was investigated. An in-depth study of the effects of a slight increase in ionic strength (lower than 8 mM NaCl) and of temperature changes (5-40°C) on the rheological properties of LF/βLG coacervates was conducted, as these parameters were proved to be critical for practical applications. The LF/βLG coacervates showed a high sensitivity to temperature, as they become more liquid-like and less viscous at high temperature. Whatever the temperature, the apparent viscosity of these coacervates was exceptionally higher compared to that of a pure protein. Time temperature superposition TTS principle showed that the interaction involved in the coacervation process as well as the relaxation mechanism of the coacervates were independent of temperature. The slight increase in ionic strength led to the increase of viscosity and viscoelastic modulus. These results allow a better understanding of the interactions involved in concentrated protein coacervates in order to modulate their use in the food industry.

Keywords: Complex coacervation, β-lactoglobulin, Lactoferrin, Rheology, Ionic strength, Temperature

3.2.2.1 Introduction

Complex coacervation (CC), also known as liquid-liquid phase separation (LLPS), is an electrostatically and entropically driven phenomena that takes place between two oppositely charged macromolecules and leads to the formation of two phases; a polymer-rich dense phase called the coacervates and a less concentrated phase called the dilute phase. Several theoretical models described the process of complex coacervation as such; first, a spontaneous formation of heterocomplexes or building blocks by electrostatic attraction. These building blocks come together to form micrometric droplets. This step is called micro-phase separation. Then, the coalescence of those droplets leads to the formation of the coacervates (Overbeek & Voorn, 1957, 1957; Tainaka, 1967; Veis, 2011; 1967). The pioneer research on complex coacervation was conducted on gelatin and gum arabic by Bungenberg De Jong and Kruyt one century ago (Bungenberg De Jong & Kruyt, 1929). Since then, interest on biopolymer based coacervates kept growing and turned into a subject of intense experimental and theoretical interest (Chai et al., 2014; Dong & Cui, 2019; Niu et al., 2018; Schmitt et al., 1998; Weinbreck, Tromp, et al., 2004; Xiong et al., 2017). To achieve complex coacervation, a number of parameters should be taken into consideration; pH, usually taken between the isoelectric points of the two macromolecules, ionic strength, concentrations and stoichiometry between mixed macromolecules (Schmitt et al., 1998). The relevance of complex coacervation is evident in numerous applications in various disciplines such as food, pharmaceutical, cosmetics and biomedicine industry. CC and subsequent LLPS were extensively reported for a wide variety of charged macromolecules such as proteins/polysaccharides, proteins/synthetic-polyelectrolytes, polyelectrolytes/polyelectrolytes and proteins/proteins mixtures. Despite being a promising technique for the design of natural functional foods (Chapeau et al., 2016), heteroprotein CC, i.e., involving two or more proteins, is comparatively understudied (Adal et al., 2017; Croguennec et al., 2017; Desfougères et al., 2010; Zheng et al., 2021). Part of the published works on heteroprotein complex coacervation focused on the assembly between lactoferrin (LF) as basic protein and β-lactoglobulin (βLG) as acidic protein. Some of these studies aimed to characterize LF/βLG coacervates by using biophysical tools such as SAXS measurements (Kizilay et al., 2014) or solid-state NMR (Peixoto et al., 2016). LF/βLG system was shown to be highly sensitive to physico-chemical

parameters such as pH, stoichiometry and concentration of macromolecules. Several works focus on investigating the optimal condition for LF/βLG coacervation. Yan et al. (2013) and Anema and de Kruif (2014) found that a narrow range of pH and an ionic strength lower than 100 mM were favorable for the coacervation process (Anema & de Kruif, 2014; Yan et al., 2013). During our previous work (Chapeau et al., 2016; G. M. Tavares et al., 2015), we have shown that a high coacervates yield is obtained at pH 5.5 and 20°C with less than 20 mM ionic strength. We further showed that the complex coacervates formed under these conditions exhibit exceptional rheological properties (Soussi Hachfi et al., 2022). The aim of the present investigation was to determine the sensitivity of these rheological properties to relatively small changes in temperature and ionic strength, two critical parameters for potential applications. Therefore, viscosity and viscoelasticity of LF/βLG coacervates were monitored at different ionic strengths and temperatures. Moreover, we applied the principle of time temperature superposition (TTS) to further illustrate the effect of temperature on the dynamic oscillatory modulus. In fact, the TTS is a well-known procedure applied to determine the temperature dependence of the rheological behavior, in particular the relaxation mechanisms, the thermal stability of the materials as well as their physical changes inside the coacervates networks (van Gurp & Palmen, 1998)

3.2.2.2 Materials and methods

Materials

LF with a purity of 90% and iron saturation of 10-20% according to technical specification was purchased from Fonterra Cooperative Group (New Zealand). LF powder was used without further purification. Industrial bovine βLG containing both A and B variants was further purified before use. As βLG is prompt to self-aggregation during long storage, the non-native and aggregated species were regularly removed by acidic precipitation. Therefore, βLG powder was dispersed in ultrapure water (30 g/L), adjusted to pH 5.2 with 1 M HCl and then kept at 30°C for 10 min to precipitate aggregated and non-native protein. The dispersion was centrifuged at 36 000 *g* (15000 rpm, in JLA-16.250 rotor, Avanti, J-26S XP BioSafe Three-Phase Non-IVD Centrifuge, France) at 25°C for 10 min. The supernatant

containing native βLG (purity > 95% as assessed by HPLC) was adjusted to pH 7.0 with 1 M NaOH, freeze-dried and stored at -20°C until use. Whey protein isolate (WPI) was purchased from Lactalis Ingredients company (Bourgbarré, France) with a total protein content of 84% (w/w; N × 6.38). 2-(N-morpholino) ethanesulfonic acid hydrate (MES) from Sigma-Aldrich (St. Louis, MO, USA). All other chemicals were of analytical grade.

Methods

Preparation of heteroprotein coacervates

MES buffer 10 mM was prepared by solubilizing MES powder in ultra-pure water and adjusted to pH 5.5 with 1 M NaOH solution. Required solid NaCl was dissolved in this MES buffer to cover a concentration range from 0 to 8 mM and the pH readjusted if needed to pH 5.5.

Whey protein isolate (WPI) solution was prepared by solubilizing WPI powder at 250 g protein /kg. This solution was used as a control reference of homogeneous dispersion of protein at high concentration as this concentration is the one found in LF/βLG coacervates produced without NaCl addition (Peixoto et al., 2016).

βLG and LF powders were solubilized at the target concentration of NaCl (0-8 mM) and the pH of the solutions was adjusted to pH 5.5 using 1 M NaOH and HCl solutions for LF and βLG, respectively. Chapeau et al. (2016) found this pH value to be optimal for complex coacervation between the two whey proteins at a chosen stoichiometry of βLG/LF = 10 and at a total protein concentration of 0.55 mM. The protein concentrations were determined by absorbance at 280 nm (SAFAS UV MC2, Safas, Monaco) using 0.96 L g^{-1} cm^{-1}, 1.47 L g^{-1} cm^{-1} and 1.046 L g^{-1} cm^{-1} as extinction coefficients for βLG, LF and WPI, respectively.

In order to prepare the coacervates, we applied an optimized protocol (Chapeau et al., 2017). Briefly, an equivalent volume of the two protein solutions were mixed at room temperature to reach a βLG/LF

molar ratio of 10:1 equivalent to final concentrations of 0.5 mM and 0.05 mM for βLG and LF, respectively. Mechanical stirring was performed by stirring the solution in a vessel containing a propeller pale of 2.5 cm diameter, with three blades. The propeller was set in rotational motion by the mean of an electric motor set at 143 *g*. The spontaneous formation of coacervates as spherical droplets was monitored by turbidity measurements at 600 nm (SAFAS UV MC2, Safas, Monaco) and microscopic observations on a phase contrast microscope (BX51TF, Olympus, Rungis, France). This mxture was stored at 4°C for 12 h and then centrifuged at 36 000 *g* for 30 min at the studied temperatures (5 to 40°C) in order to separate the two liquid phases and extract the coacervates phase. At the end of the centrifugation, the coacervates yield, i.e., the amount of proteins in the coacervates/initial amount of proteins was measured. For each experiment, a total volume of 100 mL was implemented to get ca. 0.5 and 0.9 g of the coacervates at 8 mM NaCl and without salt, respectively.

Rheological measurements

Rheological measurements of the coacervates with and without added salt and of the WPI sample were carried out using a stress-controlled rheometer (DHR2, TA Instruments, France, Guyancourt) with a cone-plate geometry (angle of 2°, diameter = 20 mm, truncature = 51.5 µm) or a parallel plate geometry (diameter = 20 mm, gap = 500 µm).

Regardless of the used geometry, around 200 mg of sample were loaded on the Peltier plate at the studied temperature (5 - 40°C) and allowed to rest for 15 min for thermal equilibration. All rheological measurements were performed at least twice, plotted as means and standard deviations and fitted with TRIOS software (TA Instruments, Guyancourt, France).

Flow measurements

Flow measurements were performed using the cone-plate geometry in an upward shear rate sweep (0.01-300 s^{-1}) followed by a downward one. Measurements were performed by averaging for 20 s after an

equilibrium time of 100 s at low shear rates (0.01-0.1 s^{-1}) and for 5 s after 10 s equilibrium at higher shear rates (0.1-300 s^{-1}).

Frequency sweeps

Frequency sweeps were carried out from 628 to 0.628 rad/s with an oscillatory strain amplitude of 0.1%, i.e., in the linear viscoelastic regime with the cone-plate geometry.

Time-Temperature Superposition (TTS)

A series of frequency sweep measurements were carried out using the plate-plate geometry at different temperatures from 5 to 40°C. Samples were loaded onto the plate and were equilibrated for 15 min at each working temperature before measurements.

3.2.2.3 Results and discussion

The effect of ionic strength on the coacervation process was studied by varying NaCl concentration at 20°C. The effect of temperature was investigated on coacervates formed at 20°C without added NaCl.

Effect of temperature

Figure 3-22 shows the apparent viscosity of LF/βLG coacervates at different temperatures and, for comparison, that of the WPI solution at 250 g/kg, without added NaCl. The WPI solution showed a Newtonian-like behavior for all the studied temperatures. On a much wider shear rate range, the coacervates showed a viscosity 3 to 4 log higher than that of individual protein (WPI) at a given temperature. Moreover, the viscosity of coacervates presented two different stages; a Newtonian behavior at low shear and a shear thinning behavior once the shear rate increased. This reversible structural change was proved time-dependent and probably due to the weaknesses of electrostatic interactions inside the protein network at high shear rates (Soussi Hachfi et al., 2022). For all studied temperature, the coacervates kept the same 2-stages behavior. The increase in temperature led to a decrease in the apparent viscosity of the coacervates, but also and in a less pronounced way for WPI

protein solutions. At 1 s^{-1}, when the temperature increased from 5 to 40°C, the LF/βLG coacervates viscosity dropped dramatically from 332 ± 39 Pa.s to 8 ± 0.68 Pa.s. However, around a shear rate closer to 1 s^{-1}, the apparent viscosity dropped from 73 ± 10 mPa.s to 20 ± 4 mPa.s for the WPI solution. This huge fall in the coacervates viscosity compared to that of WPI suggests that increasing the temperature brought about a structural change inside the coacervates. Moreover, an outstanding decrease in the hysteresis loop between upward and downward steps of measurement as well as in the amplitude of the shear thinning behavior were observed at higher temperatures.

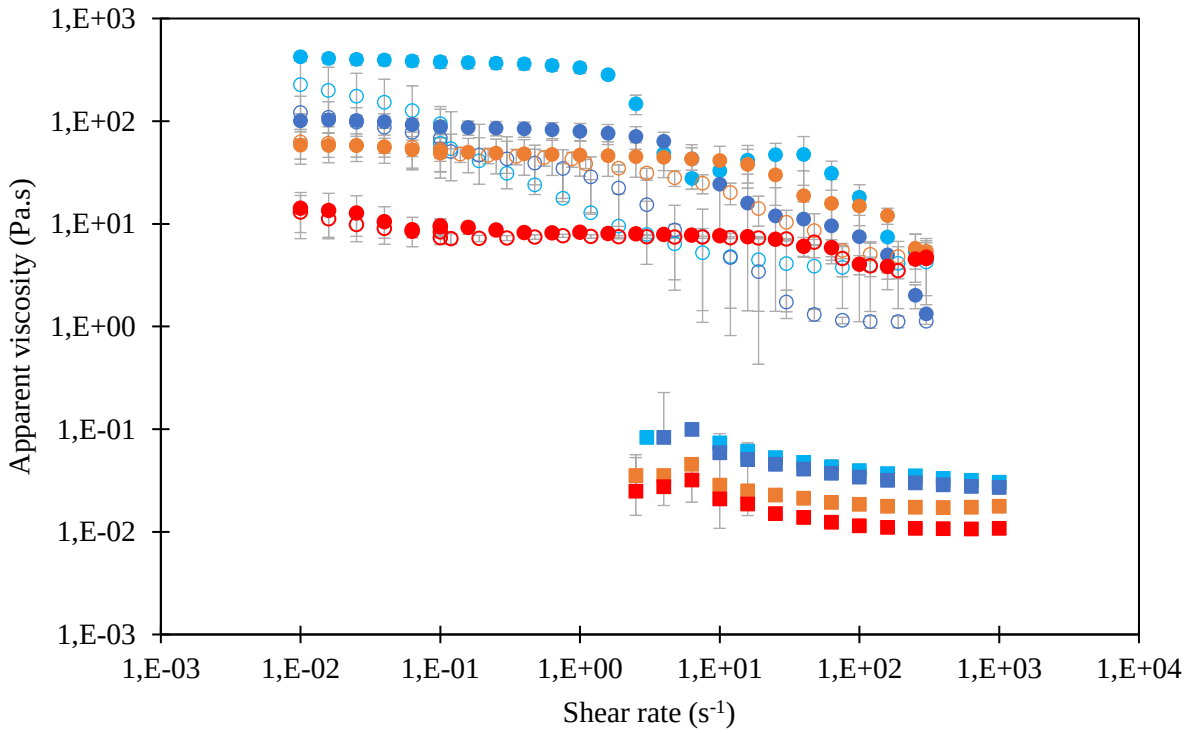

*Figure 3-22: Viscosity at different temperatures of LF/βLG coacervates formed at 20°C in 10 mM MES buffer, pH 5.5 (●) and of WPI solution (concentration control) (■) as function of shear rate: 5 °C (**light blue**), 10 °C (**dark blue**), 20 °C (**orange**), 40 °C (**red**). Upward shear rate (fill symbols) and downward shear rate (open symbols). Coacervates were formed by mixing the two proteins at initial total protein concentration of 0.55 mM.*

Similar trends were reported for other complex coacervation systems including proteins-polysaccharides (Anvari et al., 2015; Kayitmazer et al., 2007) and proteins/polyelectrolytes systems (Dubin et al., 2008; Liberatore et al., 2009). Anvari et al. (2015) studied the rheology of fish gelatin (FG) / gum arabic (GA) coacervates at pH 3.5 and control without coacervates at pH 8. These authors reported a decrease in the viscosity for the coacervates as well as for the control samples with increasing temperature. In fact, they explained that at low temperature, the mobility of the biopolymers and solvent was reduced, but the hydrogen bonding between biopolymers was enhanced which led to a higher viscosity. Furthermore, just like the LF/βLG coacervates, Anvari et al observed that at 1 s^{-1}, the viscosity of the coacervates remarkably dropped while the viscosity of the control remained the same (Anvari et al., 2015). Other protein-polysaccharides coacervates study was conducted by Kayitmazer et al. (2007). These authors measured the viscosity of chitosan and Bovine Serum Albumin (BSA) coacervates at two temperatures, 12 and 25°C. As for the LF/βLG coacervates and the FG/GA coacervates, the viscosity of chitosan-BSA coacervates was much higher and also more shear thinning at low temperature. These Authors explained this difference by the fact that chitosan-BSA coacervates undergo a further phase separation inside the coacervates for temperature lower than 18°C, which means that the shear thinning behavior is directly related to the phase separation inside the coacervates. Similarly to LF/βLG coacervates, the temperature effect on chitosan/BSA coacervates is much greater than the influence of temperature on chitosan alone (Kayitmazer et al., 2007). Polyelectrolyte based coacervates showed a similar behavior with the highest viscosity being observed at low temperatures (Dubin et al., 2008; Liberatore et al., 2009). In fact, Dubin et al. (2008) noticed the coexistence of two domains within the coacervates: a dense continuous domain and a dilute domain. The rise in temperature increased the contrast between these two domains, and eventually led to a phase separation. The same authors explained this by the fact that an increase of the temperature induced a contraction of the two domains and a decrease in their connectivity. Therefore, the overall rheological properties were dominated by the dilute domain, explaining the lower observed viscosity at high temperature. According to these authors, the phase separation inside the coacervates into a denser domain and a dilute one explains the decrease in the viscosity and the reduction in the shear thinning behavior at higher temperatures. In our case, the shear thinning behavior increased at low

temperature leading us to think that decreasing the temperature can induce a phase separation inside the LF/βLG coacervates. The reason behind this structure transition is not quite clear and could be explained by different assumptions such as a decrease in the connectivity of the physical network in the coacervates at high shear rates and the formation of metastable states before a sharp drop of viscosity (Le Meins & Tassin, 2001).

Table 3-12 shows the comparison of the activation energy between LF/ βLG coacervates, the whey protein solution at the same concentration as the coacervates and the water.

Table 3-2: The activation energy (Ea) of the LF/ βLG coacervates, the WPI solution (at 250 g kg-1) and water calculated from the viscosity values at different temperatures

	LF/ βLG coacervates	WPI	Water
Ea (KJmol-1)	62.13	25.98	17.47

The activation energy was calculated using the data from figure 1 and the equation 1:

$$\eta = A.e^{-Ea/RT} \qquad \textit{Equation 3-11}$$

where η is the mean dynamic viscosity at low shear rates i.e., during the Newtonian behavior, T is the temperature in Kelvin, A is a temperature-independent pre-exponential factor, Ea is the activation energy and R is the universal gas constant. Ea was also calculated from G', G'' and the torque at 10 rad s^{-1} during the oscillation and from the shift factor aT.

The activation energy of the coacervates is more than 3 times higher than that of the water and 2 times higher than that of the WPI solution in the same temperature range. This observation implies that the influence of the temperature on the coacervates network is not only due to the temperature impact on hydrogen bonding and the individual proteins. Studying the temperature effect in depth could give

interesting insights on protein-protein and water interactions between proteins and between proteins and solvent inside the coacervates as well as on the mechanism of the coacervation.

The temperature influence on viscoelastic properties of LF/βLG coacervates was also investigated. Figure 2 shows the changes in storage modulus G' and loss modulus G'' as function of angular frequency at various temperatures from 5 to 30°C. The data points with a high raw phase, i.e. higher than 160° were excluded and not presented in figure 2.

Throughout the whole studied frequency range and for all tested temperatures, both the storage and the loss modulus followed a power law of frequency, with an exponent close to 1 for G" and close to 2 for G'. Moreover, G'' was always higher than G' indicating that regardless of the temperature, LF/βLG coacervates exhibited a viscoelastic liquid-like dominant behavior. Increasing the temperature from 5°C to 30°C led to the decrease of both moduli. In addition to that, the loss tangent ($tg(\delta) = G''/G'$) increased with increasing temperature (data not shown) proving that the liquid-like character became more dominant at higher temperatures. the increase in $tg(\delta)$ with an increase in temperature seems to be general as it was also observed for proteins/polysaccharide and proteins/polyelectrolytes systems (Anvari et al., 2015; P. L. Dubin et al., 2008; Kayitmazer et al., 2007). The dominance of such typical liquid-like character was attributed to the reinforcement of the molecular mobility and the weakness of the polymer−water hydrogen bonding network with increasing temperature (Anvari et al., 2015; P. L. Dubin et al., 2008; Kayitmazer et al., 2007; Qiao et al., 2014; Suarez-Martinez et al., 2019).

It should be noted that the modulus at the crossover between G' and G'' of the LF/βLG complex coacervates was not significantly modified by the temperature of centrifugation and measurement as it always took place around 628 rad/s. This means that the relaxation time of the actual coacervates was not affected by the temperature, unlike the chitosan/BSA complex coacervates for which the relaxation time decreased from 150 ms at 12°C to 22 ms at 25°C (Kayitmazer et al., 2007). The lifetime of interchain connectivity for chitosan-BSA coacervates can highly decrease with a relatively small

increase in temperature (Kayitmazer et al., 2007). The different oscillatory shear behavior regarding the temperature for each studied coacervates networks reflected distinct structures for each coacervates.

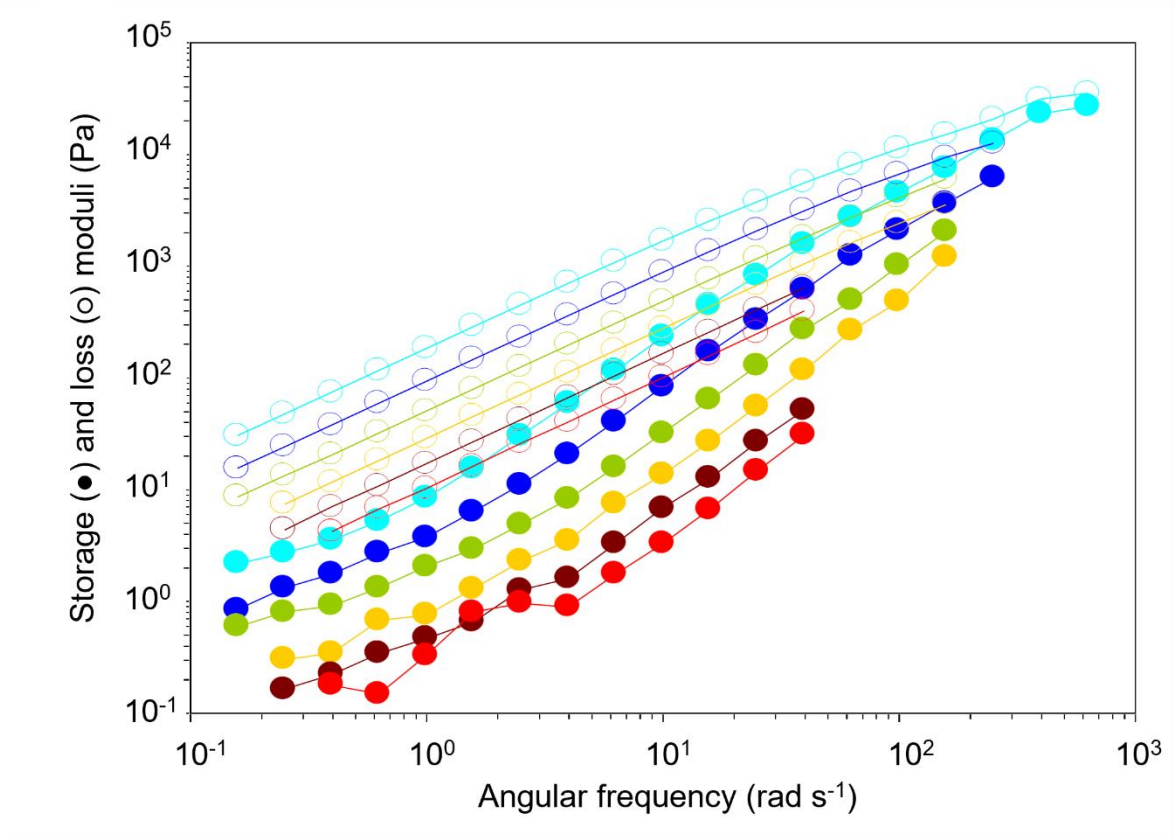

*Figure 3-23: Effect of temperature on storage, G' (●) and loss, G'' (○) moduli of LF/βLG coacervates as function of angular frequency at different temperatures of separation and measurement: 5 °C (**light blue**), 10 °C (**dark blue**), 15 °C (**green**), 20 °C (**orange**), 25 °(**brown**), 30 °C (**red**). The coacervates were produced at 20°C in 10 mM MES buffer, pH 5.5.*

Figure 3-24 shows the master curves after horizontal shifting with data at 15°C chosen as reference temperature of the moduli reported in Figure 3-23 for temperatures ranging from 5 to 30°C. Clearly, all the frequency-dependent viscoelastic data were superimposed which means that the viscoelastic spectra followed the time-temperature superposition (TTS) principle and can thus form a master curve by horizontal shifting. While the shifting curves was perfect for G'', the one for G' was less satisfactory as less good superposition was seen at low frequency. Van Gurp and Palmen (1998) think that local

frictional interactions influence the temperature-dependent dynamics leading TTS to fail. On the other hand, a plateau value of G′ at low frequency that failed to obey to the TTS theory was reported for another mixture of proteins/polymers coacervates using TTS (H. Bohidar et al., 2005). These authors think that a solid-like tenuous network embedded into a viscoelastic suspending fluid could explain data at low frequency, and that with increasing frequencies; the suspending fluid dominated the mechanical properties. This reflects the huge dependence of structure and dynamics of coacervates probed by frequency. Another possible explanation could be related to the lower sensitivity of rheological measurements of G' at low frequencies.

Figure 3-24 proved that TTS principle can be appropriate for LF/βLG coacervates and the master curve showed that the dynamic modulus at low temperature is shifted at high frequency and vice versa. The fact that all G' and G'' curves can superimpose reflects that the coacervates relaxation process and energy of activation had the same temperature dependence. Moreover, since the coacervates obey to TTS, we can assume that, in the studied temperature range, the coacervates did not undergo any changes in their chemical structure nor in their morphology (Menczel & Prime, 2009).

The application of the TTS principle is widely under-studied for biopolymer-based coacervates, e.g., proteins and polysaccharides and even less for heteroprotein coacervates, which made the comparison with our results quite difficult.

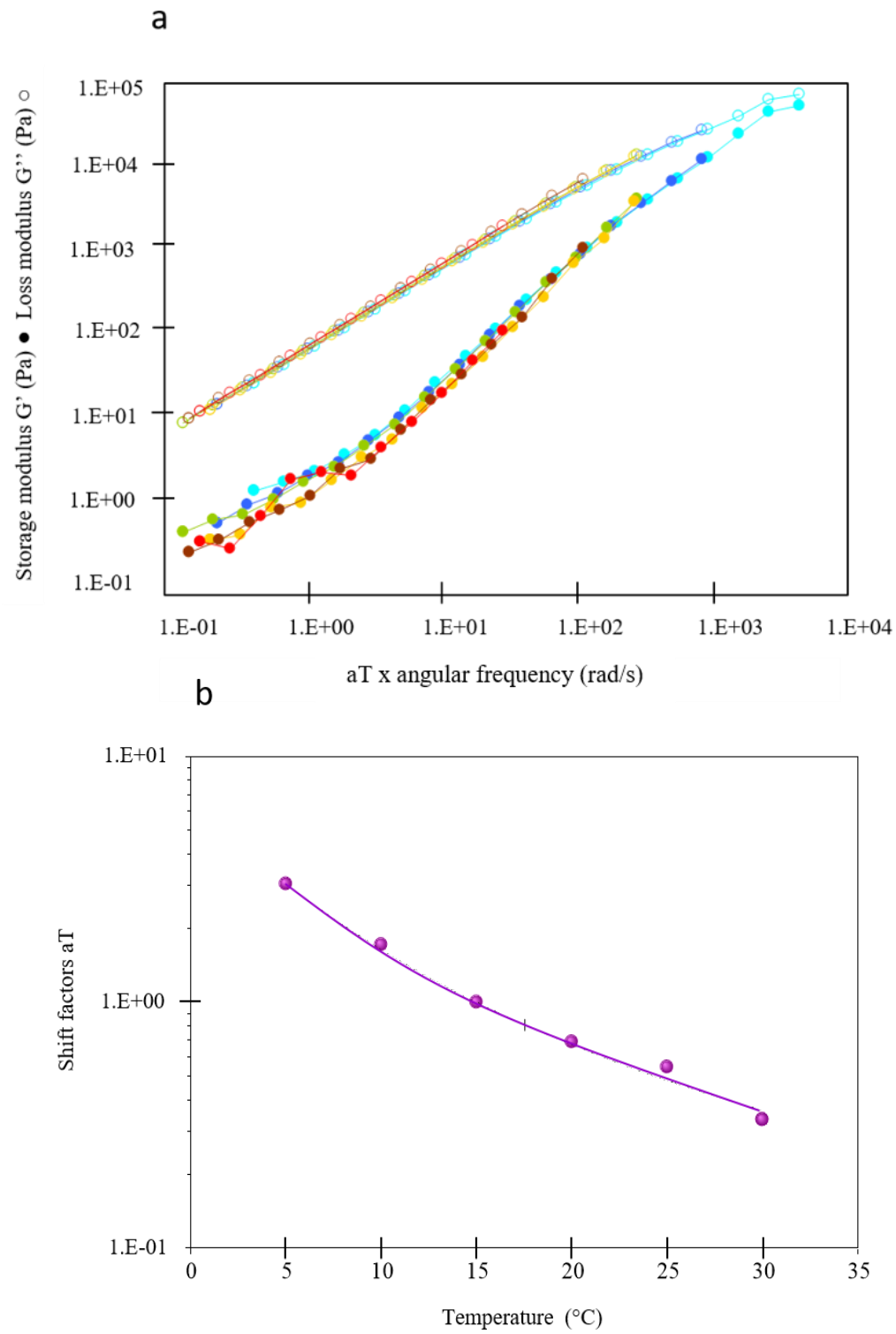

*Figure 3-24: a- Time temperature superposition master curve: Storage, G' (●) and loss, G'' (○) moduli as function of angular frequency shifted from different temperatures of LF/βLG coacervates with a reference temperature of 15°C. Temperatures: 5°C (**light blue**), 10°C (**dark blue**), 15°C (**green**), 20°C (**orange**), 25°C (**brown**), 30°C (**red**). b- the shift factor, aT, as function of temperature. Solid line stands for WLF fit. The coacervates were formed at 20°C in 10 mM MES buffer, pH 5.5*

However, several authors applied TTS on polyelectrolytes complex coacervation and reported the same trends as found for LF/βLG coacervates; a good overlapping curve that shifted well into a master curve. However, for polyelectrolytes, TTS could be conducted on a much wider frequency scale. In addition, polyelectrolytes coacervates showed a faster relaxation and exhibited a remarkable jump in modulus and in the temperature-dependent viscoelastic regime from liquid-like to almost glassy state with increasing both the temperature and the frequency (Ali & Prabhu, 2018; Suarez-Martinez et al., 2019; J. Wang et al., 2019; Yang et al., 2019).

The shift in frequency, known as the temperature shift factor aT (see Figure 3-24 b) was quantified. It is the ratio of the relaxation time at temperature T and at the reference temperature. Generally the curve of aT as function of the temperature can be fitted using either the Arrhenius equation or the Williams–Landel–Ferry (WLF) (Williams et al., 1955);

$$ln(aT) = \frac{-C_1\ (T-T_{ref})}{C_2 + (T-T_{ref})} \qquad 3\text{-}12$$

where, C_1 and C_2 are material-depend parameters equal to 1.9 and 49.4 K respectively and T_{ref} is the reference temperature (15°C). However, the WLF equation gives a better fit over a wide range of temperatures because it has two adjustable parameters against only one for the Arrhenius equation (Menczel & Prime, 2009). In the case where T_{ref} is equal to the glass transition temperature (T_g) of the polymer, C_1 and C_2 were found to be equal to 17.44 and 51.6 K respectively. (Williams et al., 1955)

Effect of ionic strength

In this section, the temperature of centrifugation and measurement was set at 20°C and the effect of small amount of salt in the solution before coacervation was investigated. The influence of added NaCl concentrations from 0 to 8 mM on the viscosity and the viscoelasticity of the LF/βLG complex coacervates is shown in Figure 3-25. The calculated Debye lengths decreased from 4.75 to 2.75 nm between 0 and 8 mM added NaCl. This narrow range of ionic strength was chosen because of the strong sensitivity of the LF/βLG coacervates to ionic strength (Yang et al., 2019). At concentrations higher

than 8 mM, the coacervates yield was very low, c.a. less than 10% w/w. In fact, 20 mM of NaCl is the critical salt concentration above which a yield close to 0% is measured.

The apparent viscosity of the coacervates at various NaCl concentrations (Figure 3-25-a) showed the same behavior as the one shown in Figure 3-22; a Newtonian behavior followed by a shear thinning one once the shear rate reached ca. 10 s^{-1}. Besides, for all the studied salt concentrations, the same thixotropic behavior between upward and downward flow was evidenced.

The viscosity of the coacervates slightly increased with the weak increase in ionic strength. In addition to that, the shear thinning behavior started at a lower shear rate for higher salt concentrations, i.e., at 15, 6.3 and 2.5 s^{-1} for 0, 5 and 8 mM, respectively, estimated as the shear rate where the decrease in viscosity was larger than 20%. This led us to think that even though the viscosity increased with increasing salt the stability of the coacervates under shear decreased. Several authors studied different coacervates systems and reported a decrease in viscosity with an increase in ionic strength even if the salt concentration ranges varied across the studied systems. In fact, it is known that complex coacervation is mediated by electrostatic attractions: at high salt concentration, interactions between the microions and the biopolymers provoked a decrease in the net charge of the biopolymers, and hence a decrease in electrostatic attraction. That can explain the decrease in viscosity for some coacervates systems (J. Liu et al., 2020; Niu et al., 2018; Priftis et al., 2013; Singh et al., 2007).

For the current LF/βLG coacervates, the very small increase of salt concentration induced an increase in apparent viscosity of the coacervates. A similar salt effect, was also found for chitosan/whey protein coacervates, but at higher salt levels (Bastos et al., 2010), with apparent viscosity at an ionic strength of 250 mM larger than the one at 100 mM. The occurrence of hydrophobic associations, as electrostatic repulsions throughout progressive protein charge screening vanished, may enhance the viscosity of the protein network (Dubin et al., 1994).

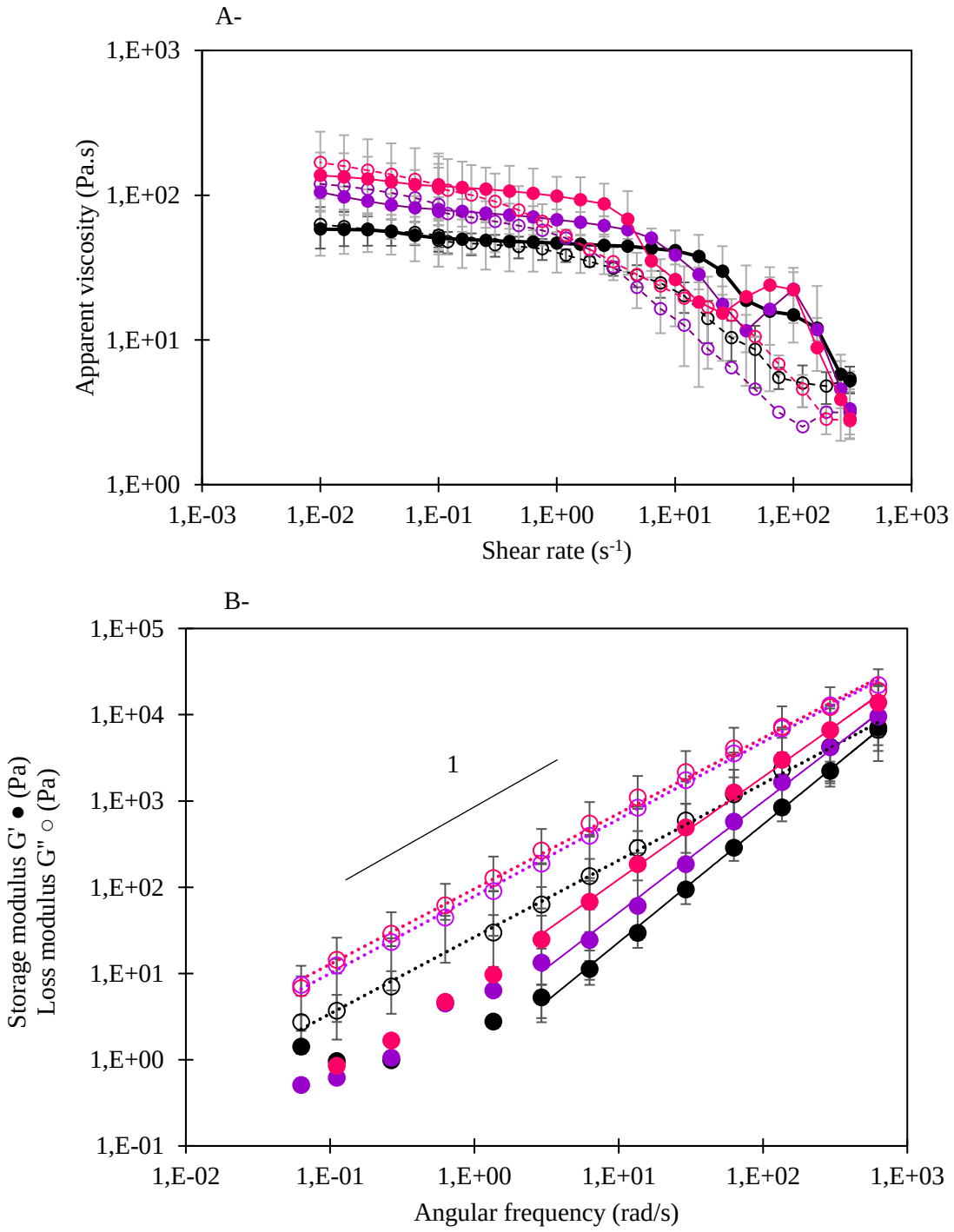

*Figure 3-25: a- Viscosity of LF/βLG coacervates as function of shear rate for different NaCl concentrations: upward shear rate (fill symbols); downward shear rate (open symbols). b- Storage modulus (fill symbols) and loss modulus (open symbols) as function of angular frequency for different NaCl concentrations: Solid line: G'. Frequency power law scaling. Dashed line: G'' frequency power law scaling. 0 mM (**black**), 5 mM (**purple**), 8 mM (**pink**). The coacervates were performed at 20°C in 10 mM MES buffer, pH 5.5 containing the indicated NaCl concentrations.*

Figure 3-25 B shows the viscoelastic properties of coacervates. Regardless of the studied ionic strength, the coacervates always exhibited a liquid-like behaviour with G″ larger than G′ throughout the whole frequency range. Figure 3-25 B also shows an increase in both moduli with increased salt concentration in parallel with a decrease in the loss tangent (data not shown). In addition to that, without added salt the crossover modulus was measured at 628 rad/s. However, for higher salt concentration, no crossover modulus was observed in the studied frequency range leading us to think that the relaxation time increased with increasing salt. The absence of a crossover modulus made the application of time salt superposition difficult to conduct.

Wang et al. (2007) and Xiong et al. (2017) studied the salt influence for βLG/pectin coacervates and ovalbumin/chitosan coacervates, respectively. The storage modulus G' for those coacervates systems increased with increasing the salt concentration until reaching a maximum and then decreased. Wang et al. explained that at acidic pH, an equilibrium between βLG monomers and dimers exists. The addition of salt will shift this equilibrium to the dimeric side and promote the self-aggregation of βLG molecules due to the salt screening of protein charges which causes a relatively larger protein coacervates. Likewise, Xiong et al. observed larger insoluble coacervates when increasing the ionic strength. These authors concluded that larger coacervates led to a tighter coacervates network hence a higher storage modulus (Wang et al., 2007; Xiong, 2017). Xiong et al. and Wang et al. hypotheses cannot explain LF/βLG coacervates as the increase of salt concentration did not induce larger coacervates.

An alternative explanation for the increase in dynamic moduli as function of ionic strength is that the salt mobile ions screened electrostatic repulsion instead of disturbing the electrostatic attraction between the biopolymers so the total interaction would be enhanced. Moreover, the salt ions can establish salt-bridges between the biopolymers enhancing the mechanical rigidity of the material. The reinforcement of the hydrophobic interactions after increasing the salt concentration can also explain the increase in the coacervates mechanical rigidity. (Boral & Bohidar, 2010; P. Dubin et al., 1994; X. Wang et al., 2007).

3.2.2.4 Conclusion

A complete and comprehensive study on the influence of temperature and ionic strength on the rheological behavior of complex coacervation phenomenon between βLG and LF was presented. We reported a remarkable increase in the viscosity and the viscoelasticity with decreasing temperature because of the reinforcement of hydrogen bonding between proteins and the reduction in polymer mobility. TTS measurements showed a relaxation mechanism of the coacervates independent of the temperature. We also showed that the coacervates became viscous and have a higher elastic modulus with an increase in ionic strength, possibly due to the reinforcement of hydrophobic interactions. These results provided new insights for the use of LF/βLG complex coacervates in mainly food applications, such as microencapsulation and texture adjustment where salt is almost omnipresent.

4 General discussion

Three research groups within the scientific community have been focusing on the LF/βLG complex coacervation. In these works the highly limited conditions under which the LF/βLG complex coacervation can occur was widely investigated (Kizilay et al., 2014; Peixoto et al., 2016; G. M. Tavares et al., 2015; Yan et al., 2013). In this thesis, we have extended the research work on this protein couple by studying first, the effect of ionic strength on the interactions between the two proteins at molecular level and subsequent complex coacervation throughout experimental and simulation approaches then the structure of formed coacervates network using rheological tools.

4.1 Insights into ionic strength influence on the interaction between LF and βLG

Monitoring the turbidity and the yield of the LF/βLG coacervation at different ionic strengths from 0 to 100 mM underlined the high sensitivity of the coacervation to ionic strength. In fact, the coacervates yield as well as the turbidity decreased drastically with increasing salt concentrations (0 - 100 mM) and 20 mM was enough to completely abolish the liquid-liquid phase separation. Microscopic observations confirmed that the addition of salt decreased both the size and the number of formed droplets. This behavior seems to be not specific to LF/βLG complex coacervation since the same tendency was reported for other protein-protein and protein-polysaccharides complex coacervation systems. However, the latter complexes are more resistant to ionic strength as their critical salt concentration, i.e. the concentration above which the LLPS was suppressed, varied from 60 to 140 mM compared to 20 mM for LF/βLG (Anema & de Kruif, 2012; Weinbreck et al., 2004). All the studied coacervates systems showed a strong salt dependency that highlights the predominant role of attractive electrostatic forces in the complex coacervation process. Bungenberg de Jong and Kruyt (1929) explained that the presence of microions screens the charges of the polymers, which weakened attractive forces between them and disrupted intermolecular electrostatic interactions . Therefore, the complex coacervation cannot occur. Similarly, our thermodynamic study provided by ITC experiments showed that the LF/βLG coacervation

is an enthalpically driven phenomenon, which confirms the predominance of electrostatic interactions. The increase of NaCl ions from 0 to 20 mM decreased the ITC signal intensity but did not change its sign, which proved that electrostatic interactions between proteins decreased, but the non-Coulombic interactions such as hydrophobic interactions and hydrogen bonding were not altered by the salt-shielding effect. On the other hand, it is well established that the coacervation is a two-step process (Tainaka, 1967; Veis, 2011), these two steps being detected by ITC for LF/βLG system . In fact, at low ionic strength, ITC thermograms clearly show two curve inflexions that can be interpreted as follow:

- The first one represents the enthalpy-driven step and is attributed to electrostatic interactions or ion pairing and leads to the formation of soluble complexes.
- The second inflexion reflects the second step of the coacervation, which is entropy-driven and is attributed to self-aggregation or coacervation (Kayitmazer, 2017; Priftis et al., 2012; Vitorazi et al., 2014).

Increasing the ionic strength leads to the suppression of the second inflexion point concomitantly to the disappearance of LLPS as shown by turbidity measurements. Interestingly, the fitting of our ITC data demonstrated that the addition of 2.5 mM NaCl promoted significantly the interaction with a +25% gain in enthalpy value and 2-fold increase of the affinity constant compared to the value measured without added salt. Hence, a small amount of added salt tuned up the interactions between the two oppositely charged proteins. With a further increase in the salt concentration, the screening effect of salt on the interaction and association between the two proteins started to be observed as reflected in the ITC signals and in the significant decrease of Ka and ΔH values. This ‘‘salting-in like’’ trend was first reported for other protein/polysaccharides coacervates and was explained as a consequence of the effect of added salt on the extent of coiling and charge densities of the involved macromolecules (Burgess, 1990).

Simulation using the Monte-Carlo method agreed with the ITC results by demonstrating that electrostatic attractions between the two proteins, indicated by a negative free energy *w (R)*, was

measured. The increase in ionic strength progressively reduced this attraction until the disappearance of almost all attraction at 100 mM, due to charge screening.

An alternative method to build and control assemblies of nanoparticles and biological complexes is desalting. This protocol involves first the mixing of the two proteins at sufficiently high salt concentrations (100-400 mM) where intermolecular interactions were inhibited. Then the so called 'inactive solution' is dialyzed to progressively decrease the ionic strength and initiate the interaction and the coacervation process. Monitoring the visual aspect during dialysis, the turbidity, the coacervates yield and microscopic observations inside the tube we showed that, at high ionic strength, no interaction between the two proteins was observed. However, once the dialysis begun, the solution in the dialysis tube started getting turbid until reaching a maximum of turbidity. Finally, the LLPS occurred at the end of the 24h of dialysis after a progressive formation and coalescence of highly turbid micro-droplets by microphase separation, without added salt, the protein solution spontaneously and rapidly exhibited a maximum coacervation but during the dialysis of LF/βLG mixture at high salt concentration (100 – 400 mM), the increase in both turbidity and coacervates yield was slower and progressive. However, for all tested added salt concentration (100 – 400 mM) the highest turbidity value was reached when the salt concentration inside the tube was around 10 mM. Therefore, the LF and βLG transition from unassociated proteins to complex coacervates always occurred at an optimal and constant ionic strength of 10 mM added NaCl. On the other hand, initial salt concentration value did not appear to greatly affect the final coacervates yield, which varied from 55% to 65% regardless of the initial salt concentration. Furthermore, microscopic observations showed that the overall size of the coacervates droplets formed during dialysis experiments varied from 1 to 10 µm. However, we noted that their number was significantly lower for the sample with an initial NaCl concentration of 400 mM than for the other tested concentration (100 – 200 mM). Other complex coacervates systems as the one reported by Fresnais et al. (2009) showed clusters with a size 3 to 5 fold larger during dialysis than that obtained with the direct mixing protocol at a constant and fixed ionic strength. For these complexes, the decrease of the desalting rate led to an increase in the hydrodynamic diameter of copolymers complexes.

4.2 Rheological characterization of β-lactoglobulin/lactoferrin complex coacervates

LF/βLG coacervates were 2500 times more viscous than WPI solution at the same pH and total protein concentration of 250 g/L. This exceptional difference underlined that the internal organization and involved interactions between the two proteins, and between proteins and water, play a major role in the rheological properties of the coacervates network. For this reason, an in-depth study of the rheological properties of the coacervates was conducted.

The apparent viscosity of LF/βLG coacervates in a wide increasing and decreasing shear rate range demonstrated the existence of two behaviors; a Newtonian one at low shear rates, followed by a sharp decrease of the viscosity for shear rate > 10 s^{-1}. In addition to that, an obvious high hysteresis between the upward and downward steps was recorded. By the end of the flow cycle, the initial viscosity of the coacervates was fully recovered despite the dramatic decrease of the viscosity during the upward shear rate step. Viscosity as a function of time at a constant shear rate showed that the structural changes that could be at the origin of the shear-thinning and thixotropic behaviors were fully reversible, provided that enough time was given to restore the original state of the network. Similar behaviors have been already reported for other proteins/polysaccharides and polyelectrolyte/surfactant coacervates systems (Liberatore et al., 2009; R. C. W. Liu et al., 2002; Niu et al., 2018; Weinbreck, Wientjes, et al., 2004). The drop of viscosity at elevated shear rate is explained by these authors by a breakdown of the structure due to the breakup of physical bonds and weakening of the attractive interactions in the coacervates network at high shear (Niu et al., 2018; Weinbreck, Wientjes, et al., 2004). Other assumptions were evoked in the literature such as a microscale structural reorganization of the interspersed phases of the complex coacervates or a shear-induced phase separation Liberatore et al., 2009). Changes in the rheometer and centrifugation temperature (5 – 40 °C) showed that the coacervates kept the same 2-stages behavior at any temperature. The increase in temperature led to a decrease in the apparent viscosity of the coacervates, that was much larger than the one obtained for equivalently concentrated

WPI solution. This suggests that increasing the temperature brought about a structural change inside the coacervates formed at 20 °C. At low temperatures, the mobility of the biopolymers and solvent was reduced, but the hydrogen bonding between biopolymers was enhanced which led to a higher viscosity (Anvari et al., 2015). Moreover, an outstanding decrease in the hysteresis loop between upward and downward steps of measurement as well as in the amplitude of the shear thinning behavior were observed at higher temperatures for the LF/βLG coacervates. This shear thinning behavior is probably related to a phase separation inside the coacervates at low temperature as observed in the literature (P. L. Dubin et al., 2008; Kayitmazer et al., 2007; Liberatore et al., 2009). The reason behind this structural transition is not quite clear and could be explained by different assumptions such as a decrease in the connectivity of the physical network in the coacervates at high shear rates and the formation of metastable states before a sharp drop of viscosity (Le Meins & Tassin, 2001).

It was seen in the above section that small changes in the ionic strength remarkably influenced the interaction between the two proteins. The study of the effect of small amount of salt in the solution (0 – 8 mM) on the viscous properties of the LF/βLG complex coacervates was thus investigated. This narrow range of ionic strength was chosen because of the strong sensitivity of the studied coacervates to ionic strength increases (Yang et al., 2019). In this range, the calculated Debye lengths decreased from 4.75 to 2.75 nm for 0 and 8 mM added salt respectively. The apparent viscosity of the coacervates showed the same 2-stages behavior as well as the same thixotropic behavior between upward and downward flow regardless of the ionic strength. However, the viscosity of the coacervates slightly increased with the low increase in ionic strength and the shear thinning behavior started at a lower shear rate for higher salt concentrations. This meant that even though the addition of salt increased the viscosity, either by increasing interactions between the proteins and water, between proteins themselves or by changing the volume fraction of proteins, the stability of these interactions could decrease under shear. Increasing interactions in the coacervates could be by increasing their number or strength or both, but changing their stability in the meantime could mean that new interactions with a lower stability formed at a slightly larger ionic strength. In fact, protein charge screening due to increasing ionic strength could abolish

electrostatic repulsions hence reinforce hydrophobic associations which may enhance the viscosity of the protein network (P. Dubin et al., 1994). These trends are not generic to all macromolecular systems as several authors reported a decrease in viscosity with larger ionic strengths (higher than 10 mM) , due to the weakening in electrostatic attraction (J. Liu et al., 2020; Niu et al., 2018; Priftis et al., 2012; Singh et al., 2007).

Studying the viscoelasticity of the coacervates showed that the coacervates had a viscoelastic liquid-like behavior mostly at low frequencies where G'' was 10 times larger than G'. G'' followed a power law of the frequency on the whole frequency range while G' trended toward a plateau at low frequencies. G' deviation at low frequency had been attributed either to a contribution of a distribution of relaxation times in the tested frequency domain, e.g. between ion pairs considered as the sticky points of the transient network (Bohidar, 2015; Ali & Prabhu, 2018), or to a low sensibility of the rheometer (Boire et al., 2018; Marciel et al., 2018; Tang et al., 2015) or to the presence of a very weak elastic network (Dardelle & Erni, 2014 ;Bohidar et al., 2005). In addition to that, no crossover modulus was seen in the studied frequency range. However, fitting the data showed that the crossing frequencies were estimated at 760 rad/s indicating that the interconnected structures responsible for the viscoelastic properties inside LF/βLG coacervates exhibit a relaxation lifetime around 8 ms, a very low value. Such a low lifetime for interconnecting electrostatic interactions between polymers could give transient network properties, and a behavior clearly dominated by liquid properties. According to Peixoto et al. (2016), the composition, dynamics and internal structure of LF/βLG coacervates showed the co-existence of three types of molecular entities with specific dynamics and Rh properties. The high mobility of some of these species and the weak connectivity between them could explain the observed viscoelastic properties of the overall network of LF/βLG heteroprotein coacervates. On the other hand, creep recovery test showed a viscoelastic response at low stress values, but only a liquid-like behavior under higher stress values. This result agrees with a dominant liquid-like behavior of the coacervates with the possible presence of a very weak elastic network that could only be demonstrated at extremely low solicitations. This

behavior of the coacervates does not seem to be specific to LF/βLG coacervates as it was already reported for other coacervates systems Tavares & Noreña, 2019; 2020; Derkach et al., 2021).

The viscoelastic behavior of the LF/βLG coacervates was not affected by the changes in temperature since G'' was always higher than G'. However, the values of the storage and the viscous modulus decreased with increasing temperatures from 5°C to 30°C. Concomitantly, the fraction of liquid to solid behavior increased with increasing temperature. The same tendency was observed for proteins/polysaccharide and proteins/polyelectrolytes systems and was attributed to the reinforcement of the molecular mobility and the weakness of the polymer−water hydrogen bonding network with increasing temperatures (Anvari et al., 2015; Dubin et al., 2008; Kayitmazer et al., 2007; Qiao et al., 2014; Suarez-Martinez et al., 2019). The application of the TTS theory using 15°C as reference temperature showed a good overlapping of the G'' and G' curves into a master curve. This master curve reflects that the coacervates relaxation process and energy of activation had the same temperature dependence. Moreover, since the coacervates obey to TTS, we can assume that, in the studied temperature range, the coacervates did not undergo any changes in their chemical structure nor in their morphology (Menczel & Prime, 2009). We thus find here for heteroprotein complex coacervates the behavior described for polyelectrolytes complex coacervates (Ali & Prabhu, 2018; Suarez-Martinez et al., 2019; Wang et al., 2019; Yang et al., 2019). However, TTS principle is widely under-studied for biopolymer based coacervates, e.g., proteins and polysaccharides and much less studied for heteroprotein coacervates, which made the comparison with our results quite difficult.

Similarly, to the temperature effect, the slight increase in ionic strength that drastically affect the formation step did not modify the liquid-like behavior of the final coacervates. Salt concentration increase led to an increase in both moduli in parallel with an increase of the loss tangent (tg(δ)). In addition to that, without added salt, the crossover modulus was measured at 628 rad/s, whereas no crossover modulus was observed for higher salt concentrations. In conclusion, the relaxation time decreased with increasing salt contents and the lifetime for interconnecting electrostatic interactions

between proteins decreases leading to a less stable structure. Different assumptions could explain the increase in dynamic moduli at larger salt contents:

- the salt mobile ions screened electrostatic repulsions instead of disturbing the electrostatic attractions between the two proteins so that interactions would be enhanced,
- the salt-bridges between the macromolecules enhanced the mechanical rigidity of the material,
- Reinforcement of hydrophobic interactions (Boral & Bohidar, 2010; P. Dubin et al., 1994; X. Wang et al., 2007).

5 Conclusion and future works

This project is an attempt to improve our understanding on the HPCC. Giving that HPCC is a relatively new field, several questions about the interactions between the proteins and the characteristics of the protein-based coacervates are still not quite understood.

In the present research study, we provided new insights and brought new elements on the high sensitivity of salt concentration on the LF/βLG HPCC process. These findings can be explored not only to better understand the specific interactions that governed the proteins complexation but also to facilitate the use of these coacervates in manufacturing new food products. We have determined the interesting effect of ionic strength on the HPCC from the molecular interactions and binding of the proteins to the formation and characterization of the final assembly of coacervates.

The first chapter of this work was conducted by combining experimental techniques and numerical simulations. We brought into focus the importance of the added salt concentration to the protein mixture, in fact, when a small amount is added the interactions between the proteins is promoted while a further increase decreased the interactions and suppressed the LLPS. These results should be taken into account when using the coacervates in food industry where salt is omnipresent. As mentioned in the literature, the LLPS is ensured by the formation of soluble droplets dispersed into a dilute phase. These droplets naturally coalesce and sediment to form a separate coacervate phase (P. Dubin et al., 1994). For the studied LF/βLG coacervates, even though, LLPS was abolished at ionic strength = 20 mM, ITC experiments and MC simulation proved that the interaction between proteins were still detected even for ionic strength around 100 mM. This led us to think that the first steps of the coacervation i.e. the interactions leading to the formation of primary units and soluble complexes is more resistant to ionic strength than the final steps i.e. the formation of a turbid micrometric droplets. This means that stronger electrostatic forces drive the initial steps of the HPCC. Further research using more sensitive technics should be conducted in order to identify the salt effect on the soluble complexes and its influence on the structure of the coacervates network. Preliminary study using Small-angle X-ray scattering “SAXS”

technique was carried out in order to investigate the influence of salt on the characteristics of the soluble complexes structure notably their size and shape. Up until now, only the effect of the salt on the LF/βLG coacervates formation process was investigated. A study on the reversible process i.e., the dissociation of the coacervates would be interesting to conduct. Previous works proved that high ionic strength can dissolve the coacervates network until reaching the initial individual molecules (Fares et al., 2018).

The second chapter of this work focused on the characterization of the structure of formed coacervates. We conducted a complete study of the viscoelastic properties and showed that in a range of 0 – 8 mM and a temperature of 5 - 40 °C, the coacervates exhibit a liquid-like dominant behavior and that the relaxation mechanism is independent of the temperature. In addition to that, an in-depth study of the viscous properties of the coacervates showed a reversible de-structuring of the coacervates at high shear rate. Furthermore, we highlighted the exceptionally high viscosity of the coacervates that can get higher at low temperature or with slight increase of the ionic strength. These results present a great opportunity for using coacervates as food texturizing agents that offer a great substitute for exogenous additives such as polysaccharides usually used as texturing agents. This will open new avenues into developing “clean label” functional food products. Besides replacing exogenous additives for texturizing food, coacervates can also be explored thanks to their high encapsulation yield for bioactives. For this reason, a study that aims to characterize the rheological properties of coacervates in the presence of bioactive molecules should be conducted as encapsulation can change the overall interactions between the protein and consequently the rheology of generated protein network. Also, experimental work using SAXS can be performed in order to determine the exact structure and the forming units of heteroprotein complex coacervates.

Table 5-1 summarizes the main results of this works and the potential future works.

Table 5-1 : highlights of the main results and the perspective of this work

Thesis chapters	Main results	Perspectives
Insights into ionic strength influence on the interaction between LF and βLG	➢ LF/βLG coacervation process is highly dependent on ionic strength. ➢ 20 mM of added NaCl is the critical value where no LLPS was detected. ➢ low salt concentration tuned the electrostatic interactions between the two proteins. ➢ During desalting, coacervation yield was not affected by protein mixing at high ionic strength. ➢ the strongest contribution in the total electrostatic energy was reported for Ion-ion interactions. ➢ The increase of the ionic strength progressively reduced the attraction between the proteins until the disappearance of almost all attraction at 100 mM. ➢ Two βLG dimers can bind into the LF surface on two different sites.	1. Study of the effect of high ionic strength in dissociation and dissolving of the LF/βLG coacervates 2. Small-Angle X-ray Scattering (SAXS) experiments will be used to confirm the simulation results. 3. Sampling the effect of ionic strength between LF and more βLG dimers

Rheological characterization of βLG/LF complex coacervates	➢ βLG/LF coacervates have dominate liquid-like behavior. ➢ βLG/LF coacervates showed an extremely high viscosity, 2500 times higher than that of individual proteins at the same concentration. ➢ A time dependent and reversible de-structuring of the assembly between the 2 proteins was observed. ➢ Decreasing the temperature led to an increase in both the viscosity and viscoelasticity of the coacervates. ➢ The relaxation mechanism of the coacervates is independent of the temperature. ➢ An increase in ionic strength led to a more viscous coacervates and a higher elastic modulus.	4. An in-depth study on the use of the ionic strength modulated βLG/LF coacervates as texturing agents in order to develop and promote "clean label" food products. 5. Study the influence of the presence of an encapsulated agent in the rheological properties of the coacervates. 6. Characterizing the effects of breaking/perturbing the hydrogen bonds on the rheological characterization of the coacervates.

6 References

Abraham, J., Sharika, T., Mishra, R. K., & Thomas, S. (2017). Rheological characteristics of nanomaterials and nanocomposites. In *Micro and Nano Fibrillar Composites (MFCs and NFCs) from Polymer Blends*, 327–350. Elsevier. https://doi.org/10.1016/B978-0-08-101991-7.00014-5

Adal, E., Sadeghpour, A., Connell, S., Rappolt, M., Ibanoglu, E., & Sarkar, A. (2017). Heteroprotein Complex Formation of Bovine Lactoferrin and Pea Protein Isolate: A Multiscale Structural Analysis. *Biomacromolecules*, *18*(2), 625–635. https://doi.org/10.1021/acs.biomac.6b01857

Ainis, W. N., Boire, A., Solé-Jamault, V., Nicolas, A., Bouhallab, S., & Ipsen, R. (2019). Contrasting Assemblies of Oppositely Charged Proteins. *Langmuir*, *35*(30), 9923–9933. https://doi.org/10.1021/acs.langmuir.9b01046

Alberti, S., Gladfelter, A., & Mittag, T. (2019). Considerations and Challenges in Studying Liquid-Liquid Phase Separation and Biomolecular Condensates. *Cell*, *176*(3), 419–434. https://doi.org/10.1016/j.cell.2018.12.035

Ali, S., & Prabhu, V. (2018). Relaxation Behavior by Time-Salt and Time-Temperature Superpositions of Polyelectrolyte Complexes from Coacervate to Precipitate. *Gels*, *4*(1), 11–23. https://doi.org/10.3390/gels4010011

Anal, A. K., & Singh, H. (2007). Recent advances in microencapsulation of probiotics for industrial applications and targeted delivery. *Trends in Food Science & Technology*, *18*(5), 240–251. https://doi.org/10.1016/j.tifs.2007.01.004

Anema, S. G., & de Kruif, C. G. (Kees). (2014). Complex coacervates of lactotransferrin and β-lactoglobulin. *Journal of Colloid and Interface Science*, *430*, 214–220. https://doi.org/10.1016/j.jcis.2014.05.036

Anema, S. G., & (Kees) de Kruif, C. G. (2012). Co-acervates of lactoferrin and caseins. *Soft Matter*, *8*(16), 4471-4478. https://doi.org/10.1039/c2sm00015f

Annan, N. T., Borza, A. D., & Hansen, L. T. (2008). Encapsulation in alginate-coated gelatin microspheres improves survival of the probiotic Bifidobacterium adolescentis 15703T during exposure to simulated gastro-intestinal conditions. *Food Research International*, *41*(2), 184–193. https://doi.org/10.1016/j.foodres.2007.11.001

Antonov, Y. A., & Goncalves, M. P. (1999). Phase separation in aqueous gelatin–k-carrageenan systems. *Food Hydrocolloids*, 13(6), 517-524.

Antonov, Y. A., Zhuravleva, I., Volodine, A., Moldenaers, P., & Cardinaels, R. (2017). Effect of the Helix–Coil Transition in Bovine Skin Gelatin on Its Associative Phase Separation with Lysozyme. *Langmuir*, *33*(47), 13530–13542. https://doi.org/10.1021/acs.langmuir.7b01477

Anvari, M., Pan, C.-H., Yoon, W.-B., & Chung, D. (2015). Characterization of fish gelatin–gum arabic complex coacervates as influenced by phase separation temperature. *International Journal of Biological Macromolecules*, *79*, 894–902. https://doi.org/10.1016/j.ijbiomac.2015.06.004

Archut, A., Klost, M., Drusch, S., & Kastner, H. (2023). Complex coacervation of pea protein and pectin: Contribution of different protein fractions to turbidity. *Food Hydrocolloids*, *134*, 108032. https://doi.org/10.1016/j.foodhyd.2022.108032

Arfin, N., Aswal, V. K., & Bohidar, H. B. (2014). Overcharging, thermal, viscoelastic and hydration properties of DNA–gelatin complex coacervates: Pharmaceutical and food industries. *RSC Adv.*, *4*(23), 11705–11713. https://doi.org/10.1039/C3RA46618C

Aryee, F. N. A., & Nickerson, M. T. (2012). Formation of electrostatic complexes involving mixtures of lentil protein isolates and gum Arabic polysaccharides. *Food Research International*, *48*(2), 520–527. https://doi.org/10.1016/j.foodres.2012.05.012

Awada, H. K., Hwang, M. P., & Wang, Y. (2016). Towards comprehensive cardiac repair and regeneration after myocardial infarction: Aspects to consider and proteins to deliver. *Biomaterials*, *82*, 94–112. https://doi.org/10.1016/j.biomaterials.2015.12.025

Banani, S. F., Lee, H. O., Hyman, A. A., & Rosen, M. K. (2017). Biomolecular condensates: Organizers of cellular biochemistry. *Nature Reviews Molecular Cell Biology*, *18*(5), 285–298. https://doi.org/10.1038/nrm.2017.7

Bartolini, A., Tempesti, P., Ghobadi, A. F., Berti, D., Smets, J., Aouad, Y. G., & Baglioni, P. (2019). Liquid-liquid phase separation of polymeric microdomains with tunable inner morphology: Mechanistic insights and applications. *Journal of Colloid and Interface Science*, *556*, 74–82. https://doi.org/10.1016/j.jcis.2019.08.015

Bastos, D. S., Barreto, B. N., Souza, H. K. S., Bastos, M., Rocha-Leão, M. H. M., Andrade, C. T., & Gonçalves, M. P. (2010). Characterization of a chitosan sample extracted from Brazilian shrimps and its application to obtain insoluble complexes with a commercial whey protein isolate. *Food Hydrocolloids*, *24*(8), 709–718. https://doi.org/10.1016/j.foodhyd.2010.03.008

Benkhedja, H., Canselier, J. P., Gourdon, C., & Haddou, B. (2017). Phenol and benzenoid alcohols separation from aqueous stream using cloud point extraction: Scaling-up of the process in a mixer-settler. *Journal of Water Process Engineering*, *18*, 202–212. https://doi.org/10.1016/j.jwpe.2017.06.016

Berret, J.-F. (2011). Controlling electrostatic co-assembly using ion-containing copolymers: From surfactants to nanoparticles. *Advances in Colloid and Interface Science*, *167*(1–2), 38–48. https://doi.org/10.1016/j.cis.2011.01.008

Bhatia, S. R., Khattak, S. F., & Roberts, S. C. (2005). Polyelectrolytes for cell encapsulation. *Current Opinion in Colloid & Interface Science*, *10*(1–2), 45–51. https://doi.org/10.1016/j.cocis.2005.05.004

Blocher, W. C., & Perry, S. L. (2017). Complex coacervate-based materials for biomedicine. *WIREs Nanomedicine and Nanobiotechnology*, *9*(4), 9:e1442. https://doi.org/10.1002/wnan.1442

Bohidar, H. B. (2015). *Fundamentals of polymer physics and molecular biophysics*. Cambridge University Press.

Bohidar, H., Dubin, P. L., Majhi, P. R., Tribet, C., & Jaeger, W. (2005). Effects of Protein−Polyelectrolyte Affinity and Polyelectrolyte Molecular Weight on Dynamic Properties of Bovine Serum Albumin−Poly(diallyldimethylammonium chloride) Coacervates. *Biomacromolecules*, *6*(3), 1573–1585. https://doi.org/10.1021/bm049174p

Boire, A., Bouchoux, A., Bouhallab, S., Chapeau, A.-L., Croguennec, T., Ferraro, V., Lechevalier, V., Menut, P., Pézennec, S., Renard, D., Santé-Lhoutellier, V., Laleg, K., Micard, V., Riaublanc, A., & Anton, M. (2018). Proteins for the future: A soft matter approach to link basic knowledge and innovative applications. *Innovative Food Science & Emerging Technologies*, *46*, 18–28. https://doi.org/10.1016/j.ifset.2017.06.012

Boral, S., & Bohidar, H. B. (2010). Effect of Ionic Strength on Surface-Selective Patch Binding-Induced Phase Separation and Coacervation in Similarly Charged Gelatin−Agar Molecular Systems. *The Journal of Physical Chemistry B*, *114*(37), 12027–12035. https://doi.org/10.1021/jp105431t

Bourbon, A. I., Pinheiro, A. C., Carneiro-da-Cunha, M. G., Pereira, R. N., Cerqueira, M. A., & Vicente, A. A. (2015). Development and characterization of lactoferrin-GMP nanohydrogels: Evaluation of pH, ionic strength and temperature effect. *Food Hydrocolloids*, *48*, 292–300. https://doi.org/10.1016/j.foodhyd.2015.02.026

Brangwynne, C. P., Eckmann, C. R., Courson, D. S., Rybarska, A., Hoege, C., Gharakhani, J., Jülicher, F., & Hyman, A. A. (2009). Germline P Granules Are Liquid Droplets That Localize by Controlled Dissolution/Condensation. *Science*, *324*(5935), 1729–1732. https://doi.org/10.1126/science.1172046

Bryant, C. (2000). Influence of xanthan gum on physical characteristics of heat-denatured whey protein solutions and gels. *Food Hydrocolloids*, *14*(4), 383–390. https://doi.org/10.1016/S0268-005X(00)00018-7

Bungenberg De Jong, H. G., & Kruyt, H. R. (1929). Coacervation (partial miscibility in colloid systems). In *Proceedings of the Royal Academy of Science at Amsterdam*, 32, 849–856.

Burgess, D. J. (1990). Practical analysis of complex coacervate systems. *Journal of Colloid and Interface Science*, *140*(1), 227–238. https://doi.org/10.1016/0021-9797(90)90338-O

Burgess, D. J., & Carless, J. E. (1984). *Microelectrophoretic Studies of Gelatin and Acacia for the Prediction of Complex Coacervation*, 98, 1-8.

Chai, C., Lee, J., & Huang, Q. (2014). The effect of ionic strength on the rheology of pH-induced bovine serum albumin/κ-carrageenan coacervates. *LWT - Food Science and Technology*, *59*(1), 356–360. https://doi.org/10.1016/j.lwt.2014.05.024

Chapeau, A.-L., Hamon, P., Rousseau, F., Croguennec, T., Poncelet, D., & Bouhallab, S. (2017). Scale-up production of vitamin loaded heteroprotein coacervates and their protective property. *Journal of Food Engineering*, *206*, 67–76. https://doi.org/10.1016/j.jfoodeng.2017.03.005

Chapeau, A.-L., Tavares, G. M., Hamon, P., Croguennec, T., Poncelet, D., & Bouhallab, S. (2016). Spontaneous co-assembly of lactoferrin and β-lactoglobulin as a promising biocarrier for vitamin B9. *Food Hydrocolloids*, *57*, 280–290. https://doi.org/10.1016/j.foodhyd.2016.02.003

Corredig, M. (2009). *Dairy-Derived Ingredients: Food and Nutraceutical Uses*.

Costalat, M., Alcouffe, P., David, L., & Delair, T. (2014). Controlling the complexation of polysaccharides into multi-functional colloidal assemblies for nanomedicine. *Journal of Colloid and Interface Science*, *430*, 147–156. https://doi.org/10.1016/j.jcis.2014.05.039

Costalat, M., David, L., & Delair, T. (2014). Reversible controlled assembly of chitosan and dextran sulfate: A new method for nanoparticle elaboration. *Carbohydrate Polymers*, *102*, 717–726. https://doi.org/10.1016/j.carbpol.2013.10.098

Croguennec, T., Tavares, G. M., & Bouhallab, S. (2017). Heteroprotein complex coacervation: A generic process. *Advances in Colloid and Interface Science*, *239*, 115–126. https://doi.org/10.1016/j.cis.2016.06.009

Cross, M. M. (1965). Rheology of non-newtonian fluids: A new flow equation for pseudoplastic systems. *Journal of Colloid Science*, *20*, 417–437.

Crowe, C. D., & Keating, C. D. (2018). Liquid–liquid phase separation in artificial cells. *Interface Focus*, *8*(5), 20428901. https://doi.org/10.1098/rsfs.2018.0032

Curk, T., Dobnikar, J., & Frenkel, D. (2016). Rational design of molecularly imprinted polymers. *Soft Matter*, *12*(1), 35–44. https://doi.org/10.1039/C5SM02144H

Damodaran, S., & Paraf, A. (1997). *Food Proteins and their Applications*.

Dardelle, G., & Erni, P. (2014). Three-phase interactions and interfacial transport phenomena in coacervate/oil/water systems. *Advances in Colloid and Interface Science*, *206*, 79–91. https://doi.org/10.1016/j.cis.2013.10.001

de Kruif, C. G., Weinbreck, F., & de Vries, R. (2004). Complex coacervation of proteins and anionic polysaccharides. *Current Opinion in Colloid & Interface Science*, *9*(5), 340–349. https://doi.org/10.1016/j.cocis.2004.09.006

Delboni, L. A., & Barroso da Silva, F. L. (2016). On the complexation of whey proteins. *Food Hydrocolloids*, *55*, 89–99. https://doi.org/10.1016/j.foodhyd.2015.11.010

Deng, N., & Huck, W. T. S. (2017). Microfluidic Formation of Monodisperse Coacervate Organelles in Liposomes. *Angewandte Chemie*, *129*(33), 9868–9872. https://doi.org/10.1002/ange.201703145

Derkach, S. R., Kolotova, D. S., Voron'ko, N. G., Obluchinskaya, E. D., & Malkin, A. Ya. (2021). Rheological Properties of Fish Gelatin Modified with Sodium Alginate. *Polymers*, *13*(5), 743–760. https://doi.org/10.3390/polym13050743

Desfougères, Y., Croguennec, T., Lechevalier, V., Bouhallab, S., & Nau, F. (2010). Charge and Size Drive Spontaneous Self-Assembly of Oppositely Charged Globular Proteins into Microspheres. *The Journal of Physical Chemistry B*, *114*(12), 4138–4144. https://doi.org/10.1021/jp9090427

Diarrassouba, F., Remondetto, G., Garrait, G., Alvarez, P., Beyssac, E., & Subirade, M. (2015). Self-assembly of β-lactoglobulin and egg white lysozyme as a potential carrier for nutraceuticals. *Food Chemistry*, *173*, 203–209. https://doi.org/10.1016/j.foodchem.2014.10.009

Dong, D., & Cui, B. (2019). Comparison of rheological properties of different protein/gum arabic complex coacervates. *Journal of Food Process Engineering*, *42*(6). e13196 https://doi.org/10.1111/jfpe.13196

Dong, D., Li, X., Hua, Y., Chen, Y., Kong, X., Zhang, C., & Wang, Q. (2015). Mutual titration of soy proteins and gum arabic and the complexing behavior studied by isothermal titration calorimetry, turbidity and ternary phase boundaries. *Food Hydrocolloids*, *46*, 28–36. https://doi.org/10.1016/j.foodhyd.2014.11.019

Drobot, B., Iglesias-Artola, J. M., Le Vay, K., Mayr, V., Kar, M., Kreysing, M., Mutschler, H., & Tang, T.-Y. D. (2018). Compartmentalised RNA catalysis in membrane-free coacervate protocells. *Nature Communications*, *9*(1), 3643. https://doi.org/10.1038/s41467-018-06072-w

D'Silva, L., Ozdowy, P., Krajewski, M., Rothweiler, U., Singh, M., & Holak, T. A. (2005). Monitoring the Effects of Antagonists on Protein−Protein Interactions with NMR Spectroscopy. *Journal of the American Chemical Society*, *127*(38), 13220–13226. https://doi.org/10.1021/ja052143x

Dubin, P., Bock, J., Davis, R., Schulz, D. N., & Thies, C. (Eds.). (1994). *Macromolecular Complexes in Chemistry and Biology*. Springer Berlin Heidelberg. https://doi.org/10.1007/978-3-642-78469-9

Dubin, P. L., Li, Y., & Jaeger, W. (2008). Mesophase Separation in Polyelectrolyte-Mixed Micelle Coacervates. *Langmuir*, *24*(9), 4544–4549. https://doi.org/10.1021/la702405d

Ducel, V., Richard, J., Popineau, Y., & Boury, F. (2005). Rheological Interfacial Properties of Plant Protein−Arabic Gum Coacervates at the Oil−Water Interface. *Biomacromolecules*, *6*(2), 790–796. https://doi.org/10.1021/bm0494601

Duvvuri, H., Wheeler, L. C., & Harms, M. J. (2018). *pytc*: Open-Source Python Software for Global Analyses of Isothermal Titration Calorimetry Data. *Biochemistry*, *57*(18), 2578–2583. https://doi.org/10.1021/acs.biochem.7b01264

Eleya, M. M. O., & Turgeon, S. L. (2000). The effects of pH on the rheology of b-lactoglobulin/k-carrageenan mixed gels. *Food Hydrocolloids*, 7.

Elgindy, N. A., & Elegakey, M. A. (1981). Carbopol-Gelatin Coacervation: Influence op Some Variables. *Drug Development and Industrial Pharmacy*, *7*(5), 587–603. https://doi.org/10.3109/03639048109057732

Fares, H. M., Ghoussoub, Y. E., Delgado, J. D., Fu, J., Urban, V. S., & Schlenoff, J. B. (2018). Scattering Neutrons along the Polyelectrolyte Complex/Coacervate Continuum. *Macromolecules*, *51*(13), 4945–4955. https://doi.org/10.1021/acs.macromol.8b00699

Flanagan, S. E., Malanowski, A. J., Kizilay, E., Seeman, D., Dubin, P. L., Donato-Capel, L., Bovetto, L., & Schmitt, C. (2015). Complex Equilibria, Speciation, and Heteroprotein Coacervation of

Lactoferrin and β-Lactoglobulin. *Langmuir*, *31*(5), 1776–1783. https://doi.org/10.1021/la504020e

Frankel, E. A., Bevilacqua, P. C., & Keating, C. D. (2016). Polyamine/Nucleotide Coacervates Provide Strong Compartmentalization of Mg^{2+}, Nucleotides, and RNA. *Langmuir*, *32*(8), 2041–2049. https://doi.org/10.1021/acs.langmuir.5b04462

Fresnais, J., Lavelle, C., & Berret, J.-F. (2009). Nanoparticle Aggregation Controlled by Desalting Kinetics. *The Journal of Physical Chemistry C*, *113*(37), 16371–16379. https://doi.org/10.1021/jp904665u

Gao, N., & Mann, S. (2023). Membranized Coacervate Microdroplets: From Versatile Protocell Models to Cytomimetic Materials. *Accounts of Chemical Research*, acs.accounts.2c00696. https://doi.org/10.1021/acs.accounts.2c00696

Ghosh, B., Bose, R., & Tang, T.-Y. D. (2021). Can coacervation unify disparate hypotheses in the origin of cellular life? *Current Opinion in Colloid & Interface Science*, *52*, 101415. https://doi.org/10.1016/j.cocis.2020.101415

Ghosh, R. (2002). Protein separation using membrane chromatography: Opportunities and challenges. *Journal of Chromatography A*, *952*(1–2), 13–27. https://doi.org/10.1016/S0021-9673(02)00057-2

Girard, M., Turgeon, S. L., & Gauthier, S. F. (2002). Interbiopolymer complexing between b-lactoglobulin and low- and high- methylated pectin measured by potentiometric titration and ultra®ltration. *Food Hydrocolloids*, 7.

Gokarn, Y. R., Fesinmeyer, R. M., Saluja, A., Razinkov, V., Chase, S. F., Laue, T. M., & Brems, D. N. (2011). Effective charge measurements reveal selective and preferential accumulation of anions, but not cations, at the protein surface in dilute salt solutions: Effective Charge Measurements Reveal Direct Anion-Protein Interactions. *Protein Science*, *20*(3), 580–587. https://doi.org/10.1002/pro.591

Hladílková, J., Callisen, T. H., & Lund, M. (2016). Lateral Protein–Protein Interactions at Hydrophobic and Charged Surfaces as a Function of pH and Salt Concentration. *The Journal of Physical Chemistry B*, *120*(13), 3303–3310. https://doi.org/10.1021/acs.jpcb.5b12225

Hospital, A., Goñi, J. R., Orozco, M., & Gelpí, J. L. (2015). Molecular dynamics simulations: Advances and applications. *Advances and Applications in Bioinformatics and Chemistry*. 8: 37–47.

Jachimska, B., Świątek, S., Loch, J. I., Lewiński, K., & Luxbacher, T. (2018). Adsorption effectiveness of β-lactoglobulin onto gold surface determined by quartz crystal microbalance. *Bioelectrochemistry*, *121*, 95–104. https://doi.org/10.1016/j.bioelechem.2018.01.010

Jho, Y., Yoo, H. Y., Lin, Y., Han, S., & Hwang, D. S. (2017). Molecular and structural basis of low interfacial energy of complex coacervates in water. *Advances in Colloid and Interface Science*, *239*, 61–73. https://doi.org/10.1016/j.cis.2016.07.003

Johnson, N. R., Ambe, T., & Wang, Y. (2014). Lysine-based polycation:heparin coacervate for controlled protein delivery. *Acta Biomaterialia*, *10*(1), 40–46. https://doi.org/10.1016/j.actbio.2013.09.012

Ka Zhang. (2012). Synthesis and release studies of microalgal oil-containing microcapsules prepared by complex coacervation (Ka Zhang, Hongman Zhang, Xuechao Hu, Shanshan Bao, & He Huang, Trans.). *Colloids and Surfaces*, *v. 89*, 61–66. PubAg. https://doi.org/10.1016/j.colsurfb.2011.08.023

Kaibara, K., Okazaki, T., Bohidar, H. B., & Dubin, P. L. (2000). PH-Induced Coacervation in Complexes of Bovine Serum Albumin and Cationic Polyelectrolytes. *Biomacromolecules*, *1*(1), 100–107. https://doi.org/10.1021/bm990006k

Kalantar, T. H., Tucker, C. J., Zalusky, A. S., Boomgaard, T. A., Wilson, B. E., Ladika, M., Jordan, S. L., Li, W. K., Zhang, X., & Goh, C. G. (2007). High throughput workflow for coacervate formation and characterization in shampoo system. *J Cosmet Sci*, 24, 375–383.

Kapelner, R. A., Yeong, V., & Obermeyer, A. C. (2021). Molecular determinants of protein-based coacervates. *Current Opinion in Colloid & Interface Science*, *52*, 101407. https://doi.org/10.1016/j.cocis.2020.101407

Kataoka, K., Harada, A., & Nagasaki, Y. (2001). Block copolymer micelles for drug delivery: Design, characterization and biological significance. *Advanced Drug Delivery Reviews*. 47(1):113-31. doi: 10.1016/s0169-409x(00)00124-1. PMID: 11251249.

Kaur, S., Weerasekare, G. M., & Stewart, R. J. (2011). Multiphase Adhesive Coacervates Inspired by the Sandcastle Worm. *ACS Applied Materials & Interfaces*, *3*(4), 941–944. https://doi.org/10.1021/am200082v

Kaushik, P., Dowling, K., McKnight, S., Barrow, Colin. J., & Adhikari, B. (2016). Microencapsulation of flaxseed oil in flaxseed protein and flaxseed gum complex coacervates. *Food Research International*, *86*, 1–8. https://doi.org/10.1016/j.foodres.2016.05.015

Kayitmazer, A. B. (2017). Thermodynamics of complex coacervation. *Advances in Colloid and Interface Science*, *239*, 169–177. https://doi.org/10.1016/j.cis.2016.07.006

Kayitmazer, A. B., Strand, S. P., Tribet, C., Jaeger, W., & Dubin, P. L. (2007). Effect of Polyelectrolyte Structure on Protein−Polyelectrolyte Coacervates: Coacervates of Bovine Serum Albumin with Poly(diallyldimethylammonium chloride) versus Chitosan. *Biomacromolecules*, *8*(11), 3568–3577. https://doi.org/10.1021/bm700645t

Kazmierski, M., Wicker, L., & Corredig, M. (2003). Interactions of (β-Lactoglobulin and High-methoxyl Pectins in Acidified Systems. *Journal of Food Science*, *68*(5), 1673–1679. https://doi.org/10.1111/j.1365-2621.2003.tb12312.x

Kelley, B. (2007). Very Large Scale Monoclonal Antibody Purification: The Case for Conventional Unit Operations. *Biotechnology Progress*, *23,995−1008*. https://doi.org/10.1021/bp070117s

Kelly, R., Gudo, E. S., Mitchell, J. R., & Harding, S. E. (1994). Some observations on the nature of heated mixtures of bovine serum albumin with an alginate and a pectin. *Carbohydrate Polymers*, *23*(2), 115–120. https://doi.org/10.1016/0144-8617(94)90035-3

Kizilay, E., Kayitmazer, A. B., & Dubin, P. L. (2011). Complexation and coacervation of polyelectrolytes with oppositely charged colloids. *Advances in Colloid and Interface Science*, *167*(1–2), 24–37. https://doi.org/10.1016/j.cis.2011.06.006

Kizilay, E., Seeman, D., Yan, Y., Du, X., Dubin, P. L., Donato-Capel, L., Bovetto, L., & Schmitt, C. (2014). Structure of bovine β-lactoglobulin–lactoferrin coacervates. *Soft Matter*, *10*(37), 7262. https://doi.org/10.1039/C4SM01333F

Knoerdel, A. R., Blocher McTigue, W. C., & Sing, C. E. (2021). Transfer Matrix Model of pH Effects in Polymeric Complex Coacervation. *The Journal of Physical Chemistry B*, *125*(31), 8965–8980. https://doi.org/10.1021/acs.jpcb.1c03065

Kurut, A., & Lund, M. (2013). Solution electrostatics beyond pH: A coarse grained approach to ion specific interactions between macromolecules. *Faraday Discuss.*, *160*, 271–278. https://doi.org/10.1039/C2FD20073B

Kurut, A., Persson, B. A., Åkesson, T., Forsman, J., & Lund, M. (2012). Anisotropic Interactions in Protein Mixtures: Self Assembly and Phase Behavior in Aqueous Solution. *The Journal of Physical Chemistry Letters*, *3*(6), 731–734. https://doi.org/10.1021/jz201680m

Kutscher, M., Cheow, W. S., Werner, V., Lorenz, U., Ohlsen, K., Meinel, L., Hadinoto, K., & Germershaus, O. (2015). Influence of salt type and ionic strength on self-assembly of dextran sulfate-ciprofloxacin nanoplexes. *International Journal of Pharmaceutics*, *486*(1–2), 21–29. https://doi.org/10.1016/j.ijpharm.2015.03.022

Laneuville, S. (2000). Effect of preparation conditions on the characteristics of whey protein—Xanthan gum complexes. *Food Hydrocolloids*, *14*(4), 305–314. https://doi.org/10.1016/S0268-005X(00)00003-5

Le Meins, J.-F., & Tassin, J.-F. (2001). Shear-Induced Phase Separation in an Associating Polymer Solution. *Macromolecules*, *34*(8), 2641–2647. https://doi.org/10.1021/ma001324a

Li, G.-Y., Chen, Q.-H., Su, C.-R., Wang, H., He, S., Liu, J., Nag, A., & Yuan, Y. (2021). Soy protein-polysaccharide complex coacervate under physical treatment: Effects of pH, ionic strength and polysaccharide type. *Innovative Food Science & Emerging Technologies*, *68*, 102612. https://doi.org/10.1016/j.ifset.2021.102612

Li, P., Banjade, S., Cheng, H.-C., Kim, S., Chen, B., Guo, L., Llaguno, M., Hollingsworth, J. V., King, D. S., Banani, S. F., Russo, P. S., Jiang, Q.-X., Nixon, B. T., & Rosen, M. K. (2012). Phase

transitions in the assembly of multivalent signalling proteins. *Nature*, *483*(7389), 336–340. https://doi.org/10.1038/nature10879

Liberatore, M. W., Wyatt, N. B., Henry, M., Dubin, P. L., & Foun, E. (2009). Shear-Induced Phase Separation in Polyelectrolyte/Mixed Micelle Coacervates. *Langmuir*, *25*(23), 13376–13383. https://doi.org/10.1021/la903260r

Liu, J., Shim, Y. Y., & Reaney, M. J. T. (2020). Ionic strength and hydrogen bonding effects on whey protein isolate–flaxseed gum coacervate rheology. *Food Science & Nutrition*, *8*(4), 2102–2111. https://doi.org/10.1002/fsn3.1504

Liu, R. C. W., Morishima, Y., & Winnik, F. M. (2002). Rheological Properties of Mixtures of Oppositely Charged Polyelectrolytes. A Study of the Interactions between a Cationic Cellulose Ether and a Hydrophobically Modified Poly[sodium 2-(acrylamido)-2-methylpropanesulfonate]. *Polymer Journal*, *34*(5), 340–346. https://doi.org/10.1295/polymj.34.340

Liu, S., Cao, Y.-L., Ghosh, S., Rousseau, D., Low, N. H., & Nickerson, M. T. (2010). Intermolecular Interactions during Complex Coacervation of Pea Protein Isolate and Gum Arabic. *Journal of Agricultural and Food Chemistry*, *58*(1), 552–556. https://doi.org/10.1021/jf902768v

Liu, S., Low, N. H., & Nickerson, M. T. (2009). Effect of pH, Salt, and Biopolymer Ratio on the Formation of Pea Protein Isolate−Gum Arabic Complexes. *Journal of Agricultural and Food Chemistry*, *57*(4), 1521–1526. https://doi.org/10.1021/jf802643n

Liu, Y., Momani, B., Winter, H. H., & L. Perry, S. (2017). Rheological Characterization of Liquid-to-Solid Transitions in Bulk Polyelectrolyte Complexes. *Soft Matter*, *13*(40), 7332–7340. https://doi.org/10.1039/C7SM01285C

Liu, Y., Winter, H. H., & Perry, S. L. (2017). Linear viscoelasticity of complex coacervates. *Advances in Colloid and Interface Science*, *239*, 46–60. https://doi.org/10.1016/j.cis.2016.08.010

Lund, M. (2016). Anisotropic protein–protein interactions due to ion binding. *Colloids and Surfaces B: Biointerfaces*, *137*, 17–21. https://doi.org/10.1016/j.colsurfb.2015.05.054

Maharana, S., Wang, J., Papadopoulos, D. K., Richter, D., Pozniakovsky, A., Poser, I., Bickle, M., Rizk, S., Guillén-Boixet, J., Franzmann, T. M., Jahnel, M., Marrone, L., Chang, Y.-T., Sterneckert,

J., Tomancak, P., Hyman, A. A., & Alberti, S. (2018). RNA buffers the phase separation behavior of prion-like RNA binding proteins. *Science*, *360*(6391), 918–921. https://doi.org/10.1126/science.aar7366

Marciel, A. B., Srivastava, S., & Tirrell, M. (2018). Structure and Rheology of Polyelectrolyte Complex Coacervates. *Soft Matter*, *14*, 2454–2464. https://doi.org/DOI: 10.1039/C7SM02041D

Marshall, K. (2004). Therapeutic Applications of Whey Protein. *Alternative Medicine Review*, *9*(2), 136-156.

McTigue, W. C. B., & Perry, S. L. (2020). *Protein Encapsulation Using Complex Coacervates: What Nature Has to Teach Us*, Small, 16, 1907671. https://doi.org/10.1002/smll.201907671

Menczel, J. D., & Prime, R. B. (Eds.). (2009). *Thermal analysis of polymers: Fundamentals and applications*. John Wiley.

Mi, X., Blocher McTigue, W. C., Joshi, P. U., Bunker, M. K., Heldt, C. L., & Perry, S. L. (2020). Thermostabilization of viruses *via* complex coacervation. *Biomaterials Science*, *8*(24), 7082–7092. https://doi.org/10.1039/D0BM01433H

Mjahed, H., Voegel, J.-C., Chassepot, A., Senger, B., Schaaf, P., Boulmedais, F., & Ball, V. (2010). Turbidity diagrams of polyanion/polycation complexes in solution as a potential tool to predict the occurrence of polyelectrolyte multilayer deposition. *Journal of Colloid and Interface Science*, *346*(1), 163–171. https://doi.org/10.1016/j.jcis.2010.02.042

Moulik, S. P., Rakshit, A. K., Pan, A., & Naskar, B. (2022). An Overview of Coacervates: The Special Disperse State of Amphiphilic and Polymeric Materials in Solution. *Colloids and Interfaces*, *6*(3), 45. https://doi.org/10.3390/colloids6030045

Muhoza, B., Qi, B., Harindintwali, J. D., Farag Koko, M. Y., Zhang, S., & Li, Y. (2022). Combined plant protein modification and complex coacervation as a sustainable strategy to produce coacervates encapsulating bioactives. *Food Hydrocolloids*, *124*, 107239. https://doi.org/10.1016/j.foodhyd.2021.107239

Neirynck, N., Van der Meeren, P., Bayarri Gorbe, S., Dierckx, S., & Dewettinck, K. (2004). Improved emulsion stabilizing properties of whey protein isolate by conjugation with pectins. *Food Hydrocolloids*, *18*(6), 949–957. https://doi.org/10.1016/j.foodhyd.2004.03.004

Nigen, M., Croguennec, T., & Bouhallab, S. (2009). Formation and stability of α-lactalbumin–lysozyme spherical particles: Involvement of electrostatic forces. *Food Hydrocolloids*, *23*(2), 510–518. https://doi.org/10.1016/j.foodhyd.2008.02.005

Nigen, M., Croguennec, T., Madec, M.-N., & Bouhallab, S. (2007). Apo α-lactalbumin and lysozyme are colocalized in their subsequently formed spherical supramolecular assembly: Properties of assembled α-lactalbumin and lysozyme. *FEBS Journal*, *274*(23), 6085–6093. https://doi.org/10.1111/j.1742-4658.2007.06130.x

Nigen, M., Gaillard, C., Croguennec, T., Madec, M.-N., & Bouhallab, S. (2010). Dynamic and supramolecular organisation of α-lactalbumin/lysozyme microspheres: A microscopic study. *Biophysical Chemistry*, *146*(1), 30–35. https://doi.org/10.1016/j.bpc.2009.10.001

Niu, F., Kou, M., Fan, J., Pan, W., Feng, Z.-J., Su, Y., Yang, Y., & Zhou, W. (2018). Structural characteristics and rheological properties of ovalbumin-gum arabic complex coacervates. *Food Chemistry*, *260*, 1–6. https://doi.org/10.1016/j.foodchem.2018.03.141

Oparin, A. (1924). The origin of life. *New York: Academic Press Translated by S Morgulis Macmillan 1953*.

Overbeek, J. T. G., & Voorn, M. J. (1957). Phase separation in polyelectrolyte solutions. Theory of complex coacervation. *Journal of Cellular and Comparative Physiology*, *49*(S1), 7–26. https://doi.org/10.1002/jcp.1030490404

Paquet, E., & Viktor, H. L. (2015). Molecular Dynamics, Monte Carlo Simulations, and Langevin Dynamics: A Computational Review. *BioMed Research International*, *2015*, 1–18. https://doi.org/10.1155/2015/183918

Pathak, J., Priyadarshini, E., Rawat, K., & Bohidar, H. B. (2017). Complex coacervation in charge complementary biopolymers: Electrostatic versus surface patch binding. *Advances in Colloid and Interface Science*, *250*, 40–53. https://doi.org/10.1016/j.cis.2017.10.006

Pathak, J., Rawat, K., Aswal, V. K., & Bohidar, H. B. (2014). Hierarchical Surface Charge Dependent Phase States of Gelatin− Bovine Serum Albumin Dispersions Close to Their Common pI. *J. Phys. Chem. B*, 118(38), 11161-71.

Pathak, J., Rawat, K., Aswal, V. K., & Bohidar, H. B. (2015). Interactions in globular proteins with polyampholyte: Coacervation route for protein separation. The Royal Society of Chemistry *Advances*, *5*(18), 13579–13589. https://doi.org/10.1039/C4RA13133A

Peixoto, P. D. S., Tavares, G. M., Croguennec, T., Nicolas, A., Hamon, P., Roiland, C., & Bouhallab, S. (2016). Structure and Dynamics of Heteroprotein Coacervates. *Langmuir*, *32*(31), 7821–7828. https://doi.org/10.1021/acs.langmuir.6b01015

Perry, S., Li, Y., Priftis, D., Leon, L., & Tirrell, M. (2014). The Effect of Salt on the Complex Coacervation of Vinyl Polyelectrolytes. *Polymers*, *6*(6), 1756–1772. https://doi.org/10.3390/polym6061756

Persson, B. A., & Lund, M. (2009). Association and electrostatic steering of α-lactalbumin–lysozyme heterodimers. *Physical Chemistry Chemical Physics*, *11*(39), 8879. https://doi.org/10.1039/b909179c

Peters, H. J. W., van Bommel, E. M. G., & Fokkens, J. G. (1992). Effect of gelatin properties in complex coacervation processes. *Drug Development and Industrial Pharmacy*, *18*(1), 123–134. https://doi.org/10.3109/03639049209043688

Plummer, R., Wilson, R. H., Calvert, H., Boddy, A. V., Griffin, M., Sludden, J., Tilby, M. J., Eatock, M., Pearson, D. G., Ottley, C. J., Matsumura, Y., Kataoka, K., & Nishiya, T. (2011). A Phase I clinical study of cisplatin-incorporated polymeric micelles (NC-6004) in patients with solid tumours. *British Journal of Cancer*, *104*(4), 593–598. https://doi.org/10.1038/bjc.2011.6

Polimeni, M. (2021). *Modelling Biomolecular Interactions of Protein Solutions: Combining Theories and Experiments*.

Priftis, D., Laugel, N., & Tirrell, M. (2012). Thermodynamic Characterization of Polypeptide Complex Coacervation. *Langmuir*, *28*(45), 15947–15957. https://doi.org/10.1021/la302729r

Priftis, D., Megley, K., Laugel, N., & Tirrell, M. (2013). Complex coacervation of poly(ethylene-imine)/polypeptide aqueous solutions: Thermodynamic and rheological characterization. *Journal of Colloid and Interface Science*, *398*, 39–50. https://doi.org/10.1016/j.jcis.2013.01.055

Qiao, C., Li, T., Zhang, L., Yang, X., & Xu, J. (2014). Rheology and viscosity scaling of gelatin/1-allyl-3-methylimidazolium chloride solution. *Korea-Australia Rheology Journal*, *26*(2), 169–175. https://doi.org/10.1007/s13367-014-0017-1

Raei, M., Rafe, A., & Shahidi, F. (2018). Rheological and structural characteristics of whey protein-pectin complex coacervates. *Journal of Food Engineering*, *228*, 25–31. https://doi.org/10.1016/j.jfoodeng.2018.02.007

Rios-Mera, J. D., Saldaña, E., Ramírez, Y., Auquiñivín, E. A., Alvim, I. D., & Contreras-Castillo, C. J. (2019). Encapsulation optimization and pH- and temperature-stability of the complex coacervation between soy protein isolate and inulin entrapping fish oil. *LWT- Food Science and Technology*, *116*, 108555. https://doi.org/10.1016/j.lwt.2019.108555

Salvatore, D. B., Duraffourg, N., Favier, A., Persson, B. A., Lund, M., Delage, M.-M., Silvers, R., Schwalbe, H., Croguennec, T., Bouhallab, S., & Forge, V. (2011). Investigation at Residue Level of the Early Steps during the Assembly of Two Proteins into Supramolecular Objects. *Biomacromolecules*, *12*(6), 2200–2210. https://doi.org/10.1021/bm200285e

Santos, M. B., de Carvalho, C. W. P., & Garcia-Rojas, E. E. (2018). Heteroprotein complex formation of bovine serum albumin and lysozyme: Structure and thermal stability. *Food Hydrocolloids*, *74*, 267–274. https://doi.org/10.1016/j.foodhyd.2017.08.016

Sato, H., & Nakajima, A. (1974). *Complex coacervation in sulfated polyvinyl alcohol-aminoaeetalyzed polyvinyl alcohol system If. Formationof coacervatedroplets*. 5. 944–948 https://doi.org/10.1007/BF01566615

Schmitt, C., Sanchez, C., Desobry-Banon, S., & Hardy, J. (1998). Structure and Technofunctional Properties of Protein-Polysaccharide Complexes: A Review. *Critical Reviews in Food Science and Nutrition*, *38*(8), 689–753. https://doi.org/10.1080/10408699891274354

Schmitt, C., Sanchez, C., Lamprecht, A., Renard, D., Lehr, C.-M., de Kruif, C. G., & Hardy, J. (2001). *Study of b-lactoglobulin/acacia gum complex coacervation by diffusing-wave spectroscopy and confocal scanning laser microscopy*, 299(2), 867-73.

Sing, C. E., & Perry, S. L. (2020). Recent Progress in the Science of Complex Coacervation. *Soft Matter*, *16*, 2885–2914. https://doi.org/10.1039/D0SM00001A

Singh, S. S., Aswal, V. K., & Bohidar, H. B. (2007). Structural studies of agar–gelatin complex coacervates by small angle neutron scattering, rheology and differential scanning calorimetry. *International Journal of Biological Macromolecules*, *41*(3), 301–307. https://doi.org/10.1016/j.ijbiomac.2007.03.009

Soussi Hachfi, R., Famelart, M.-H., Rousseau, F., Hamon, P., & Bouhallab, S. (2022). Rheological characterization of β-lactoglobulin/lactoferrin complex coacervates. *LWT- Food Science and Technology*, *163*, 113577. https://doi.org/10.1016/j.lwt.2022.113577

Stenqvist, B., Thuresson, A., Kurut, A., Vácha, R., & Lund, M. (2013). *Faunus* – a flexible framework for Monte Carlo simulation. *Molecular Simulation*, *39*(14–15), 1233-1239. https://doi.org/10.1080/08927022.2013.828207

Suarez-Martinez, P. C., Batys, P., & Sammalkorpi, M. (2019). *Time–Temperature and Time–Water Superposition Principles Applied to Poly(allylamine)/Poly(acrylic acid) Complexes*. Macromolecules, 52, 8, 3066–3074. https://doi.org/10.1021/acs.macromol.8b02512

Suresh, V., & Gopalakrishnan, R. (2021). Tutorial: Langevin Dynamics methods for aerosol particle trajectory simulations and collision rate constant modeling. *Journal of Aerosol Science*, *155*, 105746. https://doi.org/10.1016/j.jaerosci.2021.105746

Tainaka, K. (1967). Study of Complex Coacervation in Low Concentration by Virial Expansion Method. I. Salt Free Systems. *Biopolymers*, 37–59.

Tang, S., Wang, M., & Olsen, B. D. (2015). Anomalous Self-Diffusion and Sticky Rouse Dynamics in Associative Protein Hydrogels. *Journal of the American Chemical Society*, *137*(11), 3946–3957. https://doi.org/10.1021/jacs.5b00722

Tavares, G. M., Croguennec, T., Hamon, P., Carvalho, A. F., & Bouhallab, S. (2015). Selective coacervation between lactoferrin and the two isoforms of β-lactoglobulin. *Food Hydrocolloids*, *48*, 238–247. https://doi.org/10.1016/j.foodhyd.2015.02.027

Tavares, L., & Noreña, C. P. Z. (2020). Encapsulation of Ginger Essential Oil Using Complex Coacervation Method: Coacervate Formation, Rheological Property, and Physicochemical Characterization. *Food and Bioprocess Technology*, *13*(8), 1405–1420. https://doi.org/10.1007/s11947-020-02480-3

Tavares, L., & Zapata Noreña, C. P. (2019). Encapsulation of garlic extract using complex coacervation with whey protein isolate and chitosan as wall materials followed by spray drying. *Food Hydrocolloids*, *89*, 360–369. https://doi.org/10.1016/j.foodhyd.2018.10.052

Teo, A., Dimartino, S., Lee, S. J., Goh, K. K. T., Wen, J., Oey, I., Ko, S., & Kwak, H.-S. (2016). Interfacial structures of whey protein isolate (WPI) and lactoferrin on hydrophobic surfaces in a model system monitored by quartz crystal microbalance with dissipation (QCM-D) and their formation on nanoemulsions. *Food Hydrocolloids*, *56*, 150–160. https://doi.org/10.1016/j.foodhyd.2015.12.002

Tiebackx, F. W. (1911). Gleichzeitige Ausflockung zweier Kolloide. *Zeitschrift für Chemie und Industrie der Kolloide*, *8*(4), 198–201. https://doi.org/10.1007/BF01503532

Timilsena, Y. P., Adhikari, R., Barrow, C. J., & Adhikari, B. (2016). Microencapsulation of chia seed oil using chia seed protein isolate chia seed gum complex coacervates. *International Journal of Biological Macromolecules*, *91*, 347–357. https://doi.org/10.1016/j.ijbiomac.2016.05.058

Timilsena, Y. P., Akanbi, T. O., Khalid, N., Adhikari, B., & Barrow, C. J. (2019). Complex coacervation: Principles, mechanisms and applications in microencapsulation. *International Journal of Biological Macromolecules*, *121*, 1276–1286. https://doi.org/10.1016/j.ijbiomac.2018.10.144

Timilsena, Y. P., Wang, B., Adhikari, R., & Adhikari, B. (2016). Preparation and characterization of chia seed protein isolate–chia seed gum complex coacervates. *Food Hydrocolloids*, *52*, 554–563. https://doi.org/10.1016/j.foodhyd.2015.07.033

Timilsena, Y. P., Wang, B., Adhikari, R., & Adhikari, B. (2017). Advances in microencapsulation of polyunsaturated fatty acids (PUFAs)-rich plant oils using complex coacervation: A review. *Food Hydrocolloids*, *69*, 369–381. https://doi.org/10.1016/j.foodhyd.2017.03.007

Tiwari, A., Bindal, S., & Bohidar, H. B. (2009). Kinetics of Protein−Protein Complex Coacervation and Biphasic Release of Salbutamol Sulfate from Coacervate Matrix. *Biomacromolecules*, *10*(1), 184–189. https://doi.org/10.1021/bm801160s

Tomé Constantino, A. B., & Garcia-Rojas, E. E. (2022). Microencapsulation of betanin by complex coacervation of carboxymethylcellulose and amaranth protein isolate for application in edible gelatin films. *Food Hydrocolloids*, *133*, 107956. https://doi.org/10.1016/j.foodhyd.2022.107956

Trullàs, J., Giró, A., & Padró, J. A. (1989). Langevin dynamics simulation of ions in solution: Influence of the solvent structure. *The Journal of Chemical Physics*, *91*(1), 539–545. https://doi.org/10.1063/1.457490

van Gurp, M., & Palmen, J. (1998). *Time-temperature superposition for polymeric blends. Rheol. Bull. 67, 5-8.*

Van Snick, J. L., & Masson, P. L. (1976). The binding of human lactoferrin to mouse peritoneal cells. *Journal of Experimental Medicine*, *144*(6), 1568–1580. https://doi.org/10.1084/jem.144.6.1568

Veis, A. (2011). A review of the early development of the thermodynamics of the complex coacervation phase separation. *Advances in Colloid and Interface Science*, *167*(1–2), 2–11. https://doi.org/10.1016/j.cis.2011.01.007

Veis, A., Bodor, E., & Mussell, S. (1967). Molecular weight fractionation and the self-suppression of complex coacervation. *Biopolymers*, *5*(1), 37–59. https://doi.org/10.1002/bip.1967.360050106

Vitorazi, L., Ould-Moussa, N., Sekar, S., Fresnais, J., Loh, W., Chapel, J.-P., & Berret, J.-F. (2014). Evidence of a two-step process and pathway dependency in the thermodynamics of poly(diallyldimethylammonium chloride)/poly(sodium acrylate) complexation. *Soft Matter*, *10*(47), 9496–9505. https://doi.org/10.1039/C4SM01461H

Wang, B., Adhikari, B., & Barrow, C. J. (2014). Optimisation of the microencapsulation of tuna oil in gelatin–sodium hexametaphosphate using complex coacervation. *Food Chemistry*, *158*, 358–365. https://doi.org/10.1016/j.foodchem.2014.02.135

Wang, J., Sun, J., Sun, P., Yang, K., Dumas, E., & Gharsallaoui, A. (2022). Formation of lysozyme-caseinate heteroprotein complexes for encapsulation of lysozyme by spray-drying: Effect of mass ratio and temperature. *International Journal of Biological Macromolecules*, *215*, 312–320. https://doi.org/10.1016/j.ijbiomac.2022.06.123

Wang, J., Sun, S., Wu, B., Hou, L., Ding, P., Guo, X., Cohen Stuart, M. A., & Wang, J. (2019). Processable and Luminescent Supramolecular Hydrogels from Complex Coacervation of Polycations with Lanthanide Coordination Polyanions. *Macromolecules*, *52*(22), 8643–8650. https://doi.org/10.1021/acs.macromol.9b01568

Wang, W., Xu, Y., Li, A., Li, T., Liu, M., von Klitzing, R., Ober, C. K., Kayitmazer, A. B., Li, L., & Guo, X. (2015). Zinc induced polyelectrolyte coacervate bioadhesive and its transition to a self-healing hydrogel. *RSC Advances*, *5*(82), 66871–66878. https://doi.org/10.1039/C5RA11915D

Wang, X., Lee, J., Wang, Y.-W., & Huang, Q. (2007). Composition and Rheological Properties of β-Lactoglobulin/Pectin Coacervates: Effects of Salt Concentration and Initial Protein/Polysaccharide Ratio. *Biomacromolecules*, *8*(3), 992–997. https://doi.org/10.1021/bm060902d

Wang, X., Zhang, P., & Tian, L. (2021). Spatiotemporal organization of coacervate microdroplets. *Current Opinion in Colloid & Interface Science*, *52*, 101420. https://doi.org/10.1016/j.cocis.2021.101420

Wang, Y. -f., Gao, J. Y., & Dubin, P. L. (1996). Protein Separation via Polyelectrolyte Coacervation: Selectivity and Efficiency. *Biotechnology Progress*, *12*(3), 356–362. https://doi.org/10.1021/bp960013+

Wang, Y., Kimura, K., Dubin, P. L., & Jaeger, W. (2000). Polyelectrolyte−Micelle Coacervation: Effects of Micelle Surface Charge Density, Polymer Molecular Weight, and Polymer/Surfactant Ratio. *Macromolecules*, *33*(9), 3324–3331. https://doi.org/10.1021/ma991886y

Wang, Y., Kimura, K., Huang, Q., Dubin, P. L., & Jaeger, W. (1999). Effects of Salt on Polyelectrolyte−Micelle Coacervation. *Macromolecules*, *32*(21), 7128–7134. https://doi.org/10.1021/ma990972v

Weinbreck, F., de Vries, R., Schrooyen, P., & de Kruif, C. G. (2003). Complex Coacervation of Whey Proteins and Gum Arabic. *Biomacromolecules*, *4*(2), 293–303. https://doi.org/10.1021/bm025667n

Weinbreck, F., Nieuwenhuijse, H., Robijn, G. W., & de Kruif, C. G. (2004). Complexation of Whey Proteins with Carrageenan. *Journal of Agricultural and Food Chemistry*, *52*(11), 3550–3555. https://doi.org/10.1021/jf034969t

Weinbreck, F., Tromp, R. H., & de Kruif, C. G. (2004). Composition and Structure of Whey Protein/Gum Arabic Coacervates. *Biomacromolecules*, *5*(4), 1437–1445. https://doi.org/10.1021/bm049970v

Weinbreck, F., Wientjes, R. H. W., Nieuwenhuijse, H., Robijn, G. W., & de Kruif, C. G. (2004). Rheological properties of whey protein/gum arabic coacervates. *Journal of Rheology*, *48*(6), 1215–1228. https://doi.org/10.1122/1.1795191

Williams, M. L., Landel, R. F., & Ferry, J. D. (1955). The Temperature Dependence of Relaxation Mechanisms in Amorphous Polymers and Other Glass-forming Liquids. *Journal of the American Chemical Society*, *77*(14), 3701–3707. https://doi.org/10.1021/ja01619a008

Wu, J., Bratko, D., & Prausnitz, J. M. (1998). Interaction between like-charged colloidal spheres in electrolyte solutions. *Proceedings of the National Academy of Sciences*, *95*(26), 15169–15172. https://doi.org/10.1073/pnas.95.26.15169

Xia, J., Dubin, P. L., & Dautzenberg, H. (1993). Light scattering, electrophoresis, and turbidimetry studies of bovine serum albumin-poly(dimethyldiallylammonium chloride) complex. *Langmuir*, *9*(8), 2015–2019. https://doi.org/10.1021/la00032a020

Xiao, Z., Liu, W., Zhu, G., Zhou, R., & Niu, Y. (2014). A review of the preparation and application of flavour and essential oils microcapsules based on complex coacervation technology:

Microcapsules based on coacervation technology. *Journal of the Science of Food and Agriculture*, *94*(8), 1482–1494. https://doi.org/10.1002/jsfa.6491

Xiong, W. (2017). Complex coacervation of ovalbumin-carboxymethylcellulose assessed by isothermal titration calorimeter and rheology: Effect of ionic strength and charge density of polysaccharide. *Food Hydrocolloids*, 73, 41-50.

Xiong, W., Ren, C., Jin, W., Tian, J., Wang, Y., Shah, B. R., Li, J., & Li, B. (2016). Ovalbumin-chitosan complex coacervation: Phase behavior, thermodynamic and rheological properties. *Food Hydrocolloids*, *61*, 895–902. https://doi.org/10.1016/j.foodhyd.2016.07.018

Xiong, W., Ren, C., Tian, M., Yang, X., Li, J., & Li, B. (2017). Complex coacervation of ovalbumin-carboxymethylcellulose assessed by isothermal titration calorimeter and rheology: Effect of ionic strength and charge density of polysaccharide. *Food Hydrocolloids*, *73*, 41–50. https://doi.org/10.1016/j.foodhyd.2017.06.031

Xu, Y., Liu, M., Faisal, M., Si, Y., & Guo, Y. (2017). Selective protein complexation and coacervation by polyelectrolytes. *Advances in Colloid and Interface Science*, *239*, 158–167. https://doi.org/10.1016/j.cis.2016.06.004

Xu, Y., Mazzawi, M., Chen, K., Sun, L., & Dubin, P. L. (2011). Protein Purification by Polyelectrolyte Coacervation: Influence of Protein Charge Anisotropy on Selectivity. *Biomacromolecules*, *12*(5), 1512–1522. https://doi.org/10.1021/bm101465y

Yan, Y., Kizilay, E., Seeman, D., Flanagan, S., Dubin, P. L., Bovetto, L., Donato, L., & Schmitt, C. (2013). Heteroprotein Complex Coacervation: Bovine β-Lactoglobulin and Lactoferrin. *Langmuir*, *29*(50), 15614–15623. https://doi.org/10.1021/la4027464

Yang, M., Shi, J., & Schlenoff, J. B. (2019). Control of Dynamics in Polyelectrolyte Complexes by Temperature and Salt. *Macromolecules*, *52*(5), 1930–1941. https://doi.org/10.1021/acs.macromol.8b02577

Yewdall, N. A., André, A. A. M., Lu, T., & Spruijt, E. (2021). Coacervates as models of membraneless organelles. *Current Opinion in Colloid & Interface Science*, *52*, 101416. https://doi.org/10.1016/j.cocis.2020.101416

Zhang, C., Lillie, R., Cotter, J., & Vaughan, D. (2005). Lysozyme purification from tobacco extract by polyelectrolyte precipitation. *Journal of Chromatography A*, *1069*(1), 107–112. https://doi.org/10.1016/j.chroma.2004.10.018

Zhang, Q., Dong, H., Gao, J., Chen, L., & Vasanthan, T. (2020). Field pea protein isolate/chitosan complex coacervates: Formation and characterization. *Carbohydrate Polymers*, *250*, 116925. https://doi.org/10.1016/j.carbpol.2020.116925

Zhang, Q., Jeganathan, B., Dong, H., Chen, L., & Vasanthan, T. (2021). Effect of sodium chloride on the thermodynamic, rheological, and microstructural properties of field pea protein isolate/chitosan complex coacervates. *Food Chemistry*, *344*, 128569. https://doi.org/10.1016/j.foodchem.2020.128569

Zhang, Y., & Cremer, P. (2006). Interactions between macromolecules and ions: The Hofmeister series. *Current Opinion in Chemical Biology*, *10*(6), 658–663. https://doi.org/10.1016/j.cbpa.2006.09.020

Zhao, M., Huang, X., Zhang, H., Zhang, Y., Gänzle, M., Yang, N., Nishinari, K., & Fang, Y. (2020). Probiotic encapsulation in water-in-water emulsion via heteroprotein complex coacervation of type-A gelatin/sodium caseinate. *Food Hydrocolloids*, *105*, 105790. https://doi.org/10.1016/j.foodhyd.2020.105790

Zheng, J., Gao, Q., Ge, G., Sun, W., Van der Meeren, P., & Zhao, M. (2022). Encapsulation behavior of curcumin in heteroprotein complex coacervates and precipitates fabricated from β-conglycinin and lysozyme. *Food Hydrocolloids*, *133*, 107964. https://doi.org/10.1016/j.foodhyd.2022.107964

Zheng, J., Gao, Q., Ge, G., Wu, J., Tang, C., Zhao, M., & Sun, W. (2021). Heteroprotein Complex Coacervate Based on β-Conglycinin and Lysozyme: Dynamic Protein Exchange, Thermodynamic Mechanism, and Lysozyme Activity. *Journal of Agricultural and Food Chemistry*, *69*(28), 7948–7959. https://doi.org/10.1021/acs.jafc.1c02204

Zheng, J., Gao, Q., Ge, G., Wu, J., Tang, C., Zhao, M., & Sun, W. (2022). Sodium chloride-programmed phase transition of β-conglycinin/lysozyme electrostatic complexes from amorphous

precipitates to complex coacervates. *Food Hydrocolloids*, *124*, 107247. https://doi.org/10.1016/j.foodhyd.2021.107247

Zheng, J., Gao, Q., Tang, C., Ge, G., Zhao, M., & Sun, W. (2020). Heteroprotein complex formation of soy protein isolate and lactoferrin: Thermodynamic formation mechanism and morphologic structure. *Food Hydrocolloids*, *100*, 105415. https://doi.org/10.1016/j.foodhyd.2019.105415

Zheng, J., Tang, C., & Sun, W. (2020). Heteroprotein complex coacervation: Focus on experimental strategies to investigate structure formation as a function of intrinsic and external physicochemical parameters for food applications. *Advances in Colloid and Interface Science*, *284*, 102268. https://doi.org/10.1016/j.cis.2020.102268

Zhou, L., Shi, H., Li, Z., & He, C. (2020). Recent Advances in Complex Coacervation Design from Macromolecular Assemblies and Emerging Applications. *Macromolecular Rapid Communications*, *41*(21), 2000149. https://doi.org/10.1002/marc.202000149

Zhu, J., Li, H., Xu, Y., & Wang, D. (2019). Construction of Fucoxanthin Vector Based on Binding of Whey Protein Isolate and Its Subsequent Complex Coacervation with Lysozyme. *Journal of Agricultural and Food Chemistry*, *67*(10), 2980–2990. https://doi.org/10.1021/acs.jafc.8b06679

DOCTORAT ECOLOGIE
BRETAGNE GEOSCIENCES
LOIRE AGRONOMIE ALIMENTATION

L'INSTITUT agro Rennes Angers

Titre : Sensibilité à la force ionique de la coacervation complexe entre β-lactoglobuline et lactoferrine: des interactions protéine-protéine à la caractérisation des coacervats

Mots clés : Coacervation complexe, Force ionique, Rhéologie, β-Lactoglobuline, Lactoferrine.

Résumé : La coacervation complexe est une séparation de phase liquide-liquide qui conduit à la formation d'une phase concentrée (coacervats). Ces coacervats permettent entre autres applications l'encapsulation efficace de molécules bioactives. Des travaux précédents focalisés sur le cas spécifique de la coacervation hétéroprotéique entre la lactoferrine (LF) et la β-lactoglobuline (βLG), ont établi les conditions optimales de coacervation. L'objectif de ce projet de thèse était de déterminer l'influence de la force ionique sur le processus d'interactions et d'assemblage des protéines ainsi que sur l'état final des coacervats. Ce travail a montré que la coacervation complexe entre LF et βLG est hautement sensible à la force ionique. Au-delà de 20 mM, le processus de coacervation était aboli mais pas l'interaction au niveau moléculaire entre les protéines. La simulation par méthode de Monte Carlo a permis de montrer que l'énergie libre d'interaction a diminué avec l'augmentation de la force ionique du milieu. La caractérisation rhéologique a mis en évidence des propriétés exceptionnelle des coacervats avec notamment une viscosité 2500 fois supérieure à celle des protéines individuelles utilisées à une concentration protéique équivalente. Une diminution de la température ou une légère augmentation de la force ionique entraine une augmentation de la rigidité et la viscosité des coacervats. Ces résultats contribuent à mieux comprendre les interactions impliquées dans les solutions fortement concentrées en protéines en vue de leurs applications dans des matrices alimentaires comme substituts au additifs texturants.

Title : Ionic strength sensitivity of complex coacervation between β-lactoglobulin & lactoferrin: from protein-protein interactions to the characterization of the coacervates

Keywords : Complex coacervation, Ionic strength, Rheology, β-Lactoglobulin, Lactoferrin

Abstract: Complex coacervation is a liquid-liquid phase separation that leads to the formation of a highly concentrated phase or coacervates. The formed coacervates are proposed as carriers for bioactives thanks to their high encapsulation efficiency under defined optimal processing conditions. In this thesis, we investigated the specific case of heteroprotein complex coacervation of two globular milk proteins; lactoferrin (LF) and β-lactoglobulin (βLG) under specific physicochemical conditions. We aimed to determine how the ionic strength affects i- the LF/βLG complex coacervation process and ii- the rheological properties of formed coacervates. We showed that a low ionic strength, below 5 mM of added NaCl, promoted the coacervation process. Above 20 mM of added salt, the complex coacervation was abolished even if the interaction between the two proteins was still detected. Monte Carlo simulations demonstrated that the interaction free energy between the two proteins remarkably decreases with increasing ionic strength. In addition to that, a complete rheological characterization illustrated that coacervates exhibited a viscoelastic liquid-like behavior and showed exceptional viscosity, which was 2500 times higher than that found for individual proteins at equivalent total protein concentration. A decrease of the temperature or a small increase of the ionic strength enhanced the rigidity and the viscosity of the coacervates. These results allow better understanding of the involved interactions in concentrated protein solutions and open new avenues for the use of coacervates as texturizing agents in food matrices.